INAUGURAL - DISSERTATION

zur Erlangung der Doktorwürde der

Naturwissenschaftlich-Mathematischen Gesamtfakultät der

Ruprecht - Karls - Universität

Heidelberg

Vorgelegt von

Dipl.-Biol. Mark Bohlmann

aus Hamburg

Tag der mündlichen Prüfung:

Characterization of the SMC-hinge and MutL-homology domain (SMUDO) protein

Gutachter: Prof. Dr. Rainer Zawatzky

Dr. Thomas G. Hofmann

Meinen Eltern

Contents

1 Abstract

The recently discovered SMC-hinge and MutL-homology domain (SMUDO) protein was found to be a potential interaction partner of the stress induced homeodomain-interacting protein kinase 2 (HIPK2) which acts as a switching element in the DNA damage response. Upon severe DNA damage, HIPK2 induces apoptosis via p53-dependent as well as p53-independent pathways. SMUDO protein exhibits structural domains showing homology with the SMC and MutL protein families, both known for their involvement in DNA repair mechanisms.

The aim of this thesis was to characterize the SMUDO protein and to investigate its putative connection to HIPK2 as well as its possible functions in the context of the DNA damage response.

Early analysis by Northern blot, RT-PCR and Western blot revealed ubiquitous expression of SMUDO in human tissue samples as well as in diverse cell lines, suggesting functions that are not restricted to specific tissues.

Various DNA damage pathways have been studied to find indications for a role of SMUDO, where the focus was on those in which HIPK2 participates. Several kinds of DNA damage, such as double or single strand breaks as well as pyrimidine dimers, were generated by Adriamycin treatment or UV, stimuli which are known to activate HIPK2. However, SMUDO levels showed no alterations under these conditions, and SMUDO knockdown had no effect on levels of HIPK2, p53 phosphorylated at Ser46 or other DNA damage response transducers.

Pulldown experiments concerning HIPK2-SMUDO interaction support *in vitro* binding of the proteins, whereas *in vivo* interaction could not be confirmed by co-immunoprecipitation or immunofluorescence so far. This is probably due to SMUDO association to an insoluble fraction inside the nucleus, presumably chromatin. By FRAP technique, it could be shown that the SMC-hinge domain and the MutL domain of SMUDO influence the localization and mobility of the protein. The MutL domain seems to be responsible for a primarily nuclear localization of the protein and association with the insoluble nuclear fraction, while the SMC-hinge domain supports this association further limiting the mobility of SMUDO within the nucleus. Moreover, it could be demonstrated by co-immunoprecipitation that the SMC-hinge domain mediates SMUDO-SMUDO interaction.

Summarized, a SMUDO-HIPK2 interaction in the context of the DNA damage response seems to be unlikely. However, functional cooperation of the proteins might take place within other cellular processes such as epigenetic regulation.

2 Zusammenfassung

Das kürzlich entdeckte SMC-hinge and MutL domain (SMUDO) Protein wurde als potentieller Interaktionspartner der Stress-induzierten Homeodomain-interacting protein kinase 2 (HIPK2), welche eines der entscheidenden Elemente der DNS-Schadensantwort ist, identifiziert. Nach massiven DNS-Schäden induziert HIPK2 Apoptose über p53-abhängige sowie über p53-unabhängige Signalwege. Das SMUDO-Protein besitzt strukturelle Domänen, welche Homologien zu den SMC- und MutL-Proteinfamilien, die beide für ihre Beteiligung an DNS-Reparaturmechanismen bekannt sind, aufweisen.

Ziel dieser Arbeit war die Charakterisierung des SMUDO-Proteins und die Untersuchung sowohl seiner potentiellen Verbindung zu HIPK2 als auch seiner mögliche Rolle in der DNS-Schadensantwort.

Frühe Analysen durch Northern Blot, RT-PCR und Western Blot ergaben eine ubiquitäre Expression von SMUDO in humanen Gewebeproben sowie in diversen Zelllinien, was auf eine Funktion des Proteins hinweist, die nicht auf ein spezifisches Gewebe beschränkt ist.

Verschiedene DNS-Schadenssignalwege wurden untersucht, um Indizien für eine Funktion von SMUDO zu finden, wobei der Fokus auf Signalwegen lag, an denen HIPK2 teilhat. Unterschiedliche Arten von DNS-Schäden, wie Einzel- oder Doppelstrangbrüche sowie Pyrimidindimere, bekannte HIPK2-aktivierende Stimuli, wurden durch Adriamycin-Behandlung oder UV-Strahlung generiert. Jedoch zeigten die SMUDO-Proteinlevels keine Veränderung unter diesen Bedingungen. Auch hatte eine starke Reduzierung des SMUDO-Levels keinen Effekt auf die Levels von HIPK2, an Serin46 phosphorylierten p53 oder anderen Signaltransduktions-komponenten der DNS-Schadensantwort.

Pulldown-Experimente die sich auf HIPK2-SMUDO-Interaktion beziehen, untermauern *in vitro*-Bindung der Proteine, wohingegen *in vivo*-Interaktion bisher noch nicht durch Ko-Immunpräzipitation oder Immunfluoreszenzfärbung bestätigt werden konnte. Dies liegt vermutlich an der Assoziation von SMUDO mit einer unlöslichen Fraktion des Nukleus, wobei es sich wahrscheinlich um Chromatin handelt. Durch FRAP-Techniken konnte gezeigt werden, dass die SMC-hinge- und MutL-Domänen von SMUDO die Lokalisation und Mobilität des Proteins beeinflussen. Die MutL-Domäne scheint für die primär nukleäre Lokalisation sowie für die Assoziation mit der unlösliche Fraktion verantwortlich zu sein, während die SMC-hinge-Domäne diese Assoziation unterstützt und damit die Mobilität von SMUDO innerhalb des Nukleus weiter einschränkt.

Des Weiteren konnte demonstriert werden, dass die SMC-hinge-Domäne SMUDO-SMUDO-Interaktion vermittelt.

Zusammengefasst ist eine SMUDO-HIPK2-Interaktion im Kontext der DNS-Schadensantwort unwahrscheinlich. Jedoch könnte eine funktionelle Kooperation der Proteine innerhalb anderer zellulärer Prozesse, wie der epigenetischen Regulation, stattfinden.

3 Introduction

3.1 Cancer & DNA damage

Research revealed cancer to be a disease whose development is a multistep process in which a cell acquires several capabilities that allow it to become a population of malignant cells. During this process intracellular changes affect several signaling pathways like growth factor signaling, control of angiogenesis and regulation of apoptosis. Every single acquired capability constitutes an advantage in growth and therefore drives the Darwinian selection of the concerned cells. Common basis of these alterations are genetic aberrations, thus poor DNA changes present the initial event in carcinogenesis (Hanahan&Weinberg, 2000; Negrini et al, 2010).

DNA damage induced by environmental agents or produced spontaneously during (DNA) metabolism is a permanent threat for genome integrity. It has been estimated that up to 10^5 spontaneous DNA lesions per day can emerge in a single cell (Hoeijmakers, 2009). This includes DNA breaks and oxidized DNA bases generated by reactive oxygen species (ROS), a byproduct of normal cellular metabolism, misincorporation of dNTPs during DNA replication, deamination of DNA bases and other base modifications. Additionally environmental DNA damage is caused by chemical and physical sources such as diverse (waste) products of the chemical industry, chemotherapeutic agents, ultraviolet light (UV) from the sunlight and ionizing radiation (IR) from medical X-ray administration or cosmic radiation.

In healthy human cells complex enzymatic machinery continuously counteracts occurring DNA damage. This signal transduction pathway designated as DNA damage response (DDR) functions as a kinase cascade activated upon DNA damage but also in response to replicative stress (Gorgoulis et al, 2005; Kastan&Bartek, 2004). The DDR and its possible outcomes, DNA repair, cellular senescence and apoptosis, represent a biological barrier that reduces cellular transformation into a malignant state to an event of marginal probability (Bartkova et al, 2005). Of course, deficiency in components of the DDR itself can lead to accumulation of heritable mutations and therefore threatens genome maintenance.

Hence it could been shown that virtually all types of cancer exhibit dysfunctional key components of the DDR, which give a premalignant cell the means to acquire more capabilities and evolve into a malignant population (Hanahan&Weinberg, 2000). These proteins, for instance the ataxia telangiectasia mutated (ATM) protein or the transcription factor p53, are considered as tumor suppressors.

3.2 The DNA damage response

Once activated the DDR dictates the further cell fate dependent on the cellular context and the extent of damage (Bartek et al, 2007). Generally cells attempt to correct occurring mutations and to resume their natural life cycle. So they do upon mild DNA damage that induces cell cycle arrest to provide a window for cellular repair efforts. After severe DNA damage the repair machinery may be insufficient to master the plenty of injuries. In this case the DDR is able to drive a cell either into apoptosis, a controlled cell death, or senescence, a state in which further cell division is blocked but a cell is still allowed to fulfill its physiological function to some extent (Campisi&d'Adda di Fagagna, 2007; Ciccia&Elledge, 2010). Both options eliminate the premalignant cell from the pool of proliferating cells and prevent propagation of compromised genetic information. A network of tightly regulated sensors, transducers and effectors governs the DDR and ensures an appropriate response to the extent of damage.

The diversity of DNA lesions raised the need of adequate countermeasures and a set of distinct repair mechanisms has evolved from unicellular organisms to man to maintain genomic integrity and guarantee accurate transmission of genetic information across generations. In particular the human DNA damage repair machinery consists of at least five systems: Mismatch repair (MMR), base excision repair (BER), nucleotide excision repair (NER), nonhomologous end joining (NHEJ) and homologous recombination (HR) (David et al, 2007; Friedberg, 2001; Hoeijmakers, 2001; Jackson&Bartek, 2009). Among these, NHEJ is known to be one of the most error prone repair mechanisms, therefore its trigger, DNA double-strand breaks (DSBs), belongs to the most threatening types of DNA damage, which can be induced by physical exogenous agents like IR or endogenous agents such as ROS.

DDR kinase cascade is primarily mediated by the phosphatidylinositol 3-kinase-related kinases ATM, ataxia telangiectasia and Rad3-related (ATR) protein and DNA-dependent protein kinase (DNA-PK). ATM and DNA-PK are primarily activated upon DSBs whereas activation of ATR is triggered by replication protein A (RPA) coated single-stranded DNA

(ssDNA) that is a result of replication fork stalling but also occurs during DSB repair. Once induced, the kinases phosphorylate mediator proteins, which amplify the DDR by recruiting ATM and ATR substrates (Zhou&Elledge, 2000). Effector proteins can either be directly phosphorylated by ATM/ATR or by downstream kinases such as the checkpoint kinases 1 and 2 (CHK1, CHK2) or the homeodomain interacting kinase 2 (HIPK2) (Harper&Elledge, 2007; Hofmann et al, 2002).

Several sensors can detect DSBs, including the MRN-complex consisting of Mre11, Rad50 and Nbs1, that binds to the site of damage and recruits and activates ATM (Ciccia&Elledge, 2010). ATM then phosphorylates the histone H2A variant H2AX at serine 139 to form γH2AX, a binding platform for the mediator of checkpoint 1 (MDC1) and other repair factors. MDC1 and p53-binding protein1 (53BP1) facilitate the recruitment of additional MRN-ATM complexes which in turn boost the phosphorylation of H2AX. As a result of these positive feedback loop, γH2AX spreads up to 1-2 megabases around the DNA lesion and forms, together with other recruited proteins, so called γH2AX foci (van Attikum&Gasser, 2009). Moreover, ATM phosphorylates and activates the downstream kinase CHK2 in a MDC1 and 53BP1 dependent manner (Buscemi et al, 2004).

After getting activated, CHK2 diffuses in the nucleoplasm transmitting DDR signal throughout the nuclear space by phosphorylating its substrates such as cell-division cycle 25 (CDC25) phosphatases causing rapid cell-cycle arrest by its inhibition (Mailand et al, 2000). Phosphorylation of another target, transcription factor p53, leads to its stabilization and to increased transcription of p21, an inhibitor of cyclin-dependent kinases, and subsequently to stable cell-cycle arrest. Additional phosphorylation of p53 by downstream kinase HIPK2 stimulates p53 driven pro-apoptotic gene expression (Hofmann et al, 2002).

When single stranded (ss)DNA is exposed, for instance upon replication fork stalling, RPA binds to it and a sensor complex made of ATR and the ATR-interacting protein (ATRIP) associates with ssDNA/RPA (Cortez et al, 2001). ATR activity is amplified by topoisomerase-II-binding protein 1 (TOPBP1) and further boosted by the heterotrimeric 9-1-1 complex consisting of RAD9, RAD1 and HUS1 (Kumagai et al, 2006; Weiss et al, 2002). One of the main ATR targets is CHK1, which is also an inhibitor of CDC25. Overall it is estimated that ATR and ATM phosphorylate more than 700 substrates in response to DNA damage (Matsuoka et al, 2007).

3.3 HIPK2

Homeodomain interacting protein kinase 2 (HIPK2) is the best known member of a family of conserved Ser/Thr directed kinases and has been implicated in a range of cellular processes, such as regulation of apoptosis or pathways involved in development or differentiation (Bitomsky&Hofmann, 2009; Calzado et al, 2007). Three of the four family members, HIPK1-3, were originally identified as co-repressors of the homeodomain transcription factor NK3, and later on, the slightly more distant related HIPK4 was found due to sequence homology to the already known HIP-kinases (Arai et al, 2007; Kim et al, 1998). As a result of their high homology, the family members seem to be partially redundant in their functions. For instance, it could be shown that HIPK2 and HIPK1 singly deficient mice have no severe phenotype whereas HIPK1/HIKP2 double knockout mice die during embryogenesis (Isono et al, 2006).

HIPK2 is activated in response to genotoxic stress or by morphogenic signals and a plenty of substrates phosphorylated by HIPK2 at preferential serine or threonine residues followed by proline (SP/TP motifs) has been identified. Transcriptions factors like CtBP, c-Myb and CBP/p300 belong to the group of HIPK2 targets (Aikawa et al, 2006; Kanei-Ishii et al, 2004; Zhang et al, 2003). The most prominent target is the transcription factor and tumor suppressor p53. Upon severe DNA damage caused by environmental sources like UV and IR or by chemotherapeutics such as doxorubicin (adriamycin), HIKP2 is stabilized and phosphorylates p53 at Ser46, driving pro-apoptotic gene expression (D'Orazi et al, 2002; Dauth et al, 2007; Gresko et al, 2006; Hofmann et al, 2002). In addition, HIPK2 can promote apoptosis also in p53 independent manners. This includes activation of pro-apoptotic c-Jun NH(2)-terminal kinase (JNK) by affecting the TGF-beta pathway or stimulation of proteasomal degradation of anti-apoptotic transcriptional co-repressor C-terminal binding protein (CtBP) (Hofmann et al, 2003; Zhang et al, 2003).

In 2007 a study revealed HIPK2 to be a haploinsufficient tumor suppressor in the skin of a mice model probably acting by repressing cyclin D1 expression (Wei et al, 2007). The most recent support for the tumor suppressing function of HIPK2 is given by two publications, one shows that impaired HIPK2 expression in well-differentiated thyroid carcinomas (WDTCs) leads to overexpression of galectin-3 (Gal-3), an anti-apoptotic protein, and the second confirms the role of HIPK2 as haploinsufficient tumor suppressor, this time using a mouse lymphoma model (Lavra et al, 2011; Mao et al, 2011). Despite strong indications for a tumor suppressing function of HIPK2, there is still some discussion about this subject due to

controversial findings. On the one hand the pro-apoptotic function of HIPK2 trigged by DNA damage is known and its inactivation or down-regulation in several kinds of tumors has been demonstrated, on the other hand inactivation has been found only in a limited number of tumor types and moreover HIPK2 was shown to be overexpressed in some other cases (Al-Beiti&Lu, 2008; Bar et al, 2008; Deshmukh et al, 2008; Pierantoni et al, 2002; Pierantoni et al, 2007).

As mentioned before, besides its role in apoptosis regulation HIPK2 is involved in processes concerning development and differentiation. To give two examples: It phosphorylates and transactivates Pax6, a transcription factor that is essential for the development of eyes and other sensory organs, and also AML1 and p300, both important for hematopoiesis (Kim et al, 2006; Yoshida&Kitabayashi, 2008).

During the last years indications were given that HIPK2 might be involved in epigenetic processes. For example, HIPK2 was shown to phosphorylate and downregulate the methyl-binding transcription factor ZBTB4 which is known to repress p21 transcription (Weber et al, 2008; Yamada et al, 2009). Similar to this HIPK2 phosphorylates the methyl-CpG-binding protein 2 (MeCP2) promoting apoptosis induction in the brain (Bracaglia et al, 2009; Chahrour&Zoghbi, 2007).

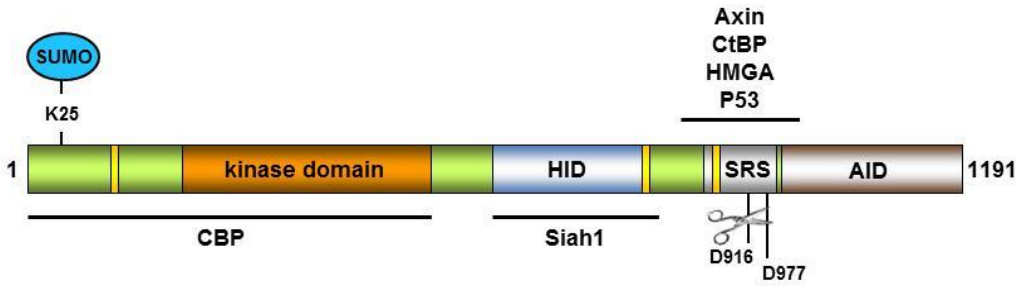

Figure 1: Schematic presentation of S/T protein kinase HIPK2. Functional domains and important residues are indicated, along with a selection of interaction partners. HID = homeoprotein interaction domain. SRS = speckle retension signal. AID = auto-inhibitory domain. D916, D977 = caspase cleavage sites. Yellow bars = nuclear localization signals (NLS). Illustration adapted and modified from Sombroek&Hofmann, 2009.

The overall protein structure of HIPK2 is characterized by an N-terminal kinase domain, a centrally located homeodomain interaction domain and an auto-inhibitory domain (AID) at the C-terminus, that plays a central role in regulation of HIPK2 activity since it is cleaved at Asp916 and Asp977 by caspase 6 upon DNA damage which leads to hyperactivation of kinase domain activity and thereby to amplification of the 53 response (Gresko et al, 2006). Alternatively, the AID can be masked by proteins such as Axin consequently preventing

auto-inhibition (Rui et al, 2004). Between the auto-inhibitory domain and the homeodomain interacting domain, a speckle-retention signal (SRS) is situated. Three nuclear localization signals (NLS) contained in the amino acid sequence of HIPK2 ensure a predominantly nuclear localization, while the SRS further promotes localization to nuclear bodies (NBs) (Kim et al, 1998). These NBs co-localize in part with domains of the epigenetic polycomb group (PcG) transcription repressors, a fact that supports the possibility of HIPK2 involvement in transcriptional regulation on epigenetic level (Roscic et al, 2006). HIPK2 can be covalently modified by attachment of small ubiquitin-like modifier (SUMO)-1 to lysine residue 25. Sumoylation leads to enhanced JNK activation by HIPK2 and further seems to augment its co-repressor function (Gresko et al, 2005; Hofmann et al, 2005; Roscic et al, 2006).

In unstressed cells HIPK2 has a high turnover due to constant degradation via the proteasomal system. Several ubiquitin E3 ligases, Siah1, Siah2, HDM2 and WSB-1 have been demonstrated to stimulate HIKP2 degradation (Calzado et al, 2009; Choi et al, 2008; Rinaldo et al, 2007a; Winter et al, 2008). Additional negative regulation is accomplished by proteins keeping away HIPK2 from potential targets. This is the case for the high-mobility group A1 (HMGA1) protein which binds HIPK2 and re-localizes the protein into the cytoplasm preventing p53 phosphorylation (Pierantoni et al, 2007).

3.4 The SMC protein family

The members of the structural maintenance of chromosomes (SMC) protein family constitute the core of multi-protein complexes that use energy from ATP hydrolysis to regulate the structural and functional organization of chromosomes. SMC proteins were initially identified in genetic screens in *Saccharomyces cervisiae* and it was shown that SMC defects destabilize chromosome segregation (Haering&Nasmyth, 2003). Over the following years many SMC proteins have been identified and studied in bacteria, yeast, nematodes and higher eukaryotes. At first two SMC complexes, cohesin and condensin, and their contribution in chromosome restructuring during mitosis were the matter of research (Hirano&Hirano, 2002; Matoba et al, 2005; Strunnikov et al, 1995). But since their initial description, a third complex, SMC5-SMC6, was discovered and SMC proteins have been implicated in a growing number of chromosomal activities such as recombination, DNA repair and epigenetic silencing of gene expression (Chuang et al, 1994; Haering et al, 2002; Lee&O'Connell, 2006; Losada&Hirano, 2005; Taylor et al, 2001).

Mammalian SMC proteins range in size from 110 to 170 kDa and they exhibit five common structural domains: A central hinge domain, two nucleotide-binding domains at the termini, and two coiled-coil regions separating the other domains. During maturation the proteins fold back through antiparallel coiled-coil interactions forming a ATPase head domain at one end and a hinge domain at the other (Melby et al, 1998). SMC hinge domains mediate the formation of V-shaped (condensin) or ring-like (cohesin, SMC5-SMC6) SMC heterodimers which act as the core component of multi-protein complexes, each containing several regulatory non-SMC subunits that bind to the ATP head domains thereby able to close the arms of the dimers (Hirano&Hirano, 2002). In particular SMC1-SMC2 act as the core of cohesin that is essential for sister-chromatid cohesion (Haering&Nasmyth, 2003) and SMC2-SMC4 functions as the core unit of condensin which is important for chromosome assembly and segregation (Hirano, 2005). SMC5-SMC6 heterodimers constitute the core of a yet unnamed complex (so far called SMC5-SMC6 complex) that has been shown to be involved in DNA repair and checkpoint responses (Lehmann, 2005).

Besides their functions in chromosomal metabolism, checkpoint signaling and DNA repair which had been in the focus of SMC protein studies over the decades, involvement in epigenetic mechanisms was indicated by several studies. For instance, it was shown that a complex closely related to condensin acts as a critical regulator of dosage compensation in *C. elegans* (Chuang et al, 1994; Jans et al, 2009). Furthermore, interactions of condensin subfractions with epigenetic factors like DNA methyltransferases were revealed (Geiman et al, 2004).

Two nucleotide-binding motifs, called Walker and Walker B motifs, are located at the N-terminus and C-terminus of SMC proteins, respectively (Fig. 2, panel B). Additionally a conserved C motif, that is also found in the family of ATP-binding cassette (ABC) ATPases, is contained in the C-terminus. ATP binding to the pockets made by the Walker motifs of one SMC subunit stimulates head-head engagement in a way that the bound ATP makes contact with the C motif of the second SMC subunit forming a nucleotide-sandwich dimer. Subsequent ATP hydrolysis triggers disengagement of the head domains and release of ADP completes the SMC-ATPase cycle (Lammens et al, 2004), which is therefore thought to play a critical role in SMC-DNA interaction.

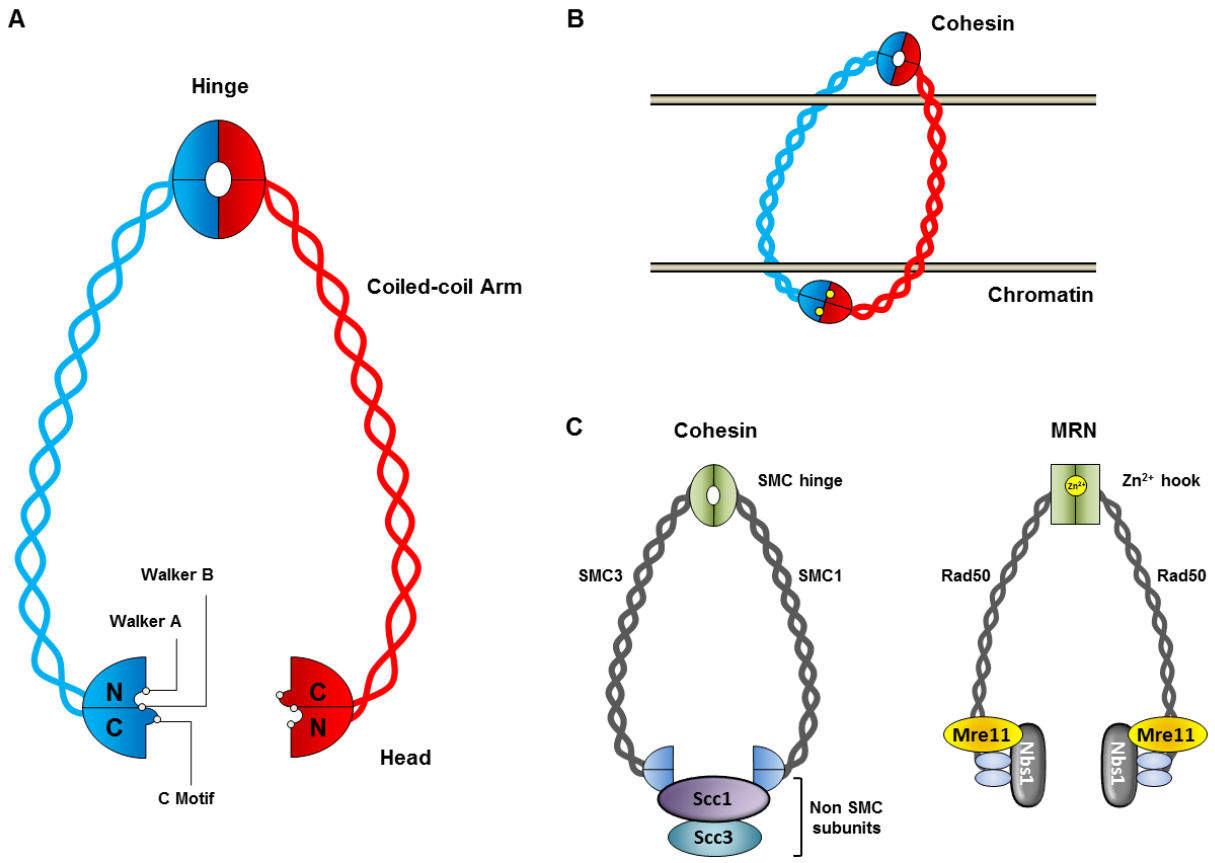

Figure 2: Architecture of SMC dimers and potential action of cohesin. (A) Sketch of the basic architecture of SMC dimers, the core component of SMC protein complexes. The SMC subunits fold back by antiparallel coiled-coil interaction to form a flexible arm, an ATP-binding head at one end and a hinge domain at the other. Hinge domains mediate dimerization and give rise to a V-shaped structure. **(B)** The ring model in which cohesin embraces two sister chromatids. Yellow dots indicate bound ATP. Images adapted and modified from Hirano et al., 2006. **(C)** The structure of the cohesin complex includes the non SMC subunits sister chromatid cohesion protein 1 and 3 (Scc1, Scc3). Containing a zinc hook instead of a hinge domain the SMC related Rad50 protein provides the core of the MRN complex which detects DNA damage and activates DNA damage checkpoint via ATM.

Hinge and head domains of SMC proteins are separated by coiled-coil domains that are responsible for stable backfolding of the maturing protein. They also constitute a prominent feature of the SMC complexes: Their length. Each coiled-coil arm is approximately 50 nm long, a distance that is equivalent to that of 150 bp of double-stranded DNA. Considering the possibilities of closing the SMC complex structure by hinge-hinge interaction, head-head engagement triggered by ATP binding or head-head contact mediated by non-SMC subunits, respectively, an elongated ring structure with a noticeable circumference comes up. Due to this architecture, it has been early supposed that SMC complexes accomplish their functions by encircling one or more DNA strands (Haering et al, 2002).

In contrast to the head-head engagement that is controlled by ATP binding and hydrolysis, the hinge-hinge interaction was shown to be very strong and independent of ATP.

Furthermore there is no hint so far that any cations are required for hinge-mediated SMC dimerization, as it is the case in the zinc-hook domain of the SMC related Rad50 protein (Hopfner et al, 2002). Studies of BsSMC, a SMC homodimer in *Bacillus subtilis*, and mammalian SMC1 and SMC3 showed that a couple of conserved glycine residues are crucial for a stable hinge-hinge interaction of these proteins (Chiu et al, 2004; Hirano et al, 2001). Over the years it has been revealed that the SMC hinge domain is not only a dimerization domain, but also a vital factor of the dynamic interaction between SMC proteins and DNA (Hirano&Hirano, 2002).

BsSMC has two positively charged basic patches (BP1 and BP2) made up of lysine residues located near the glycine dimerization interface in the hinge domains. It has been shown that BP2 is necessary for initial DNA binding. Binding then stimulates ATP hydrolysis and disengagement of the head domains which leads to conformational change in the hinge domains allowing BP1 to go into a more stable attachment to the DNA. As a result the arms of the complex encompass the DNA strand and subsequent ATP binding further stabilizes SMC-DNA interaction by causing new head-head engagement and enclosing of DNA strands (Hirano&Hirano, 2006).

Their structure allows the SMC complexes to undergo intermolecular interactions. Electron microscopy studies confirmed open and closed V-shaped and ring-like structures, but also revealed rosette-like configurations in which 4-8 SMC dimers bind to each other through their head domains (Matoba et al, 2005; Melby et al, 1998). Whether these structures are functional or only artifacts is still unclear, but they display the various potential intermolecular SMC complex interactions. Thus further hypothetical formations are for instance a filament-like arrangement that consists of opened SMC heterodimers connected via the head domains or double rings composed of two dimers, again linked by the head domains. Besides such types of conformations, which would likely require ATP, other formations, independent of ATP but depending on interactions of coiled-coil regions, might be possible (Hirano, 2006).

In mammalian cells existing DSBs are either repaired by NHEJ or by HR, where HR is the considerably more reliable mechanism since homologous regions of the sister chromatids, related sequences in the genome or homologous chromosomes are used as template to repair affected DNA. Spatial proximity of homologous regions is a requirement for this process, thus HR is favored during late S and G2 phase, when two sister chromatids are available and close to each other. First indications for a role of cohesin in DNA repair were

given by studies which showed that the absence of cohesin leads to impaired DSB repair in yeast and vertebrate cells (Sjogren&Nasmyth, 2001; Sonoda et al, 2001). Furthermore, it was show that after laser-induced DNA damage cohesin accumulates at the site of damage in mammalian cells (Kim et al, 2002). In yeast cohesin recruitment to DSBs depends on H2AX phosphorylation by the damage checkpoint kinases Mec1 and Tel1, orthologs of mammalian ATM and ATR, respectively (Unal et al, 2004). At least in mammalian cells ATM also directly phosphorylates SMC1 and this protein modification of cohesin seems to be important for its function in DNA repair, but not its role in cohesion (Kim et al, 2002; Kitagawa et al, 2004). Cohesin primary contribution to DSB repair is probably the establishment of a new link between the injured chromatid and its intact sister chromatid to allow HR (Strom et al, 2004).

While the physiological function of SMC5-SMC6 is not fully clarified yet, many studies have implicated an involvement of this third SMC complex in DNA damage repair. As early as the gene encoding for SMC6 was described for the first time, the connection to DNA damage response was made since the gene was found in screen for radiosensitive mutants in *S.pombe* (Lehmann et al, 1995). Like cohesin, SMC5-SMC6 accumulates at DSB sites and promotes sister chromatid recombination and observations suggest a model in which the complex actually recruits cohesin to the breaks sites (De Piccoli et al, 2006; Potts et al, 2006). Moreover, a role of SMC5-SMC6 in maintaining G2 arrest is likely, because it was demonstrated that *S.pombe smc6* mutant cells are able to establish G2 checkpoint after IR, but they escape arrest before DNA repair is completed and subsequent unrepaired DNA cumulates until lethal levels are reached and cells die (Harvey et al, 2004; Lehmann, 2005).

3.5 MutL proteins and their functions

Correction of mismatched and unmatched bases emerging from imperfect DNA replication is carried out by mismatch repair (MMR). The system has been recognized as critical for genomic stability, humans and mice inheriting defects in MMR components are susceptible to tumor formation. For instance, over 90% of cases of hereditary nonpolyposis colorectal cancer (HNPCC) show malfunction in MMR (Peltomaki, 2005). MMR is conserved from bacteria to men and has been intensively studied in *E.coli*, but also in yeast and human (Iyer et al, 2006).

Since the correction of mismatched or unmatched base pairs requires the proper template, nucleotide removal has to be specific to the newly synthesized DNA strand. In *E.coli*

discrimination depends on delayed methylation of the daughter strand while in eukaryotes the repair presumably starts from strand breaks such the 3' or 5' ends of Okazaki fragments in the lagging strand, or the 3' end in the leading strand (Lacks et al, 1982; Yang, 2007).

The MMR process in *E.coli* can be summarized as followed: MutS (mutator S) protein recognizes Nucleotides which fail to make a Watson-Crick pair in the DNA duplex and binds to the site of concern. MutL (mutator L) protein is recruited to the MutS-mismatch complex and couples the error recognition to incision of the new daughter stand, subsequent nucleotide removal and *de novo* strand synthesis. For incision MutL recruits MutH (mutator H) and, together with MutS, it activates the endonuclease which nicks the unmethylated strand of hemimethylated GATC sequences. Then UvrD helicase displaces the error-containing strand segment and the gap is filled in by DNA Pol III and finally sealed by DNA ligase. The first two steps are again MutL mediated by direct interaction with UvrD as well as with DNA Pol III (Polosina&Cupples, 2010a). In human MMR the MutL and MutS orthologs MutL-α and MutS-α and –β, respectively, act in concert with the exonuclease ExoI, since there is no MutH homolog existing, and other downstream repair-associated proteins many of which have not been identified for far. However, many of the known factors interact with MutL-α including ExoI, PCNA, RCF and Polη (Li, 2008). Because of its numerous known interactions and regulatory control of MMR proteins MutL is often designated to be the coordinator of the MMR pathway.

For almost a decade after its first isolation and characterization in 1989 the MutL protein was thought to have no enzymatic activity. Because its activities can be only measured indirectly by its impact on interaction partners, all efforts to uncover simple biochemical activities of the protein have been unsuccessful until ATP binding capacity and a weak ATPase activity could be demonstrated simultaneously to determination of its crystal structure (Ban&Yang, 1998; Grilley et al, 1989).

E.coli MutL functions as a homodimer of two MutL monomers whereas the human MutL-α is a heterodimer consisting of two paralogous proteins, MLH1 and PMS2. Stable dimers are formed by the C-terminal domain of the MutL monomers in *E.coli* and human, which is separated from the conserved N-terminal domain by a random coil (~90 AA in *E.coli*, ~300 AA in human). N-terminal domains as well as C-terminal domains have been demonstrated to interact directly with DNA. In addition, N-terminal ATPase domains of MutL dimers can bind and hydrolyze ATP causing conformational alterations of the protein. While no ATP bound (apo-state), the N-terminal domains make no contact with each other. Following ATP

binding the N-terminal domains dimerize and the overall structure of the dimer adopt a more compact form (condensed state). ATP hydrolysis brings the dimer back into the less condensed state and subsequent ADP release causes dissociation of the N-terminal domains (Yang, 2000). Although the direct mechanistic and biochemical impact of the MutL ATPase cycle is still not fully understood, its importance is revealed by MutL mutants deficient in ATP binding and/or hydrolysis that are defective in MMR (Spampinato&Modrich, 2000).

Besides their functions in MMR the MutL proteins have been shown to participate in several other DNA repair pathways such as very short patch repair (VSP) in *E.coli*, base excision repair (BER) and nucleotide excision repair (NER), and also in non-DNA repair pathways like cell-cycle signaling where MutL orthologs seem to initiate cell-cycle delay and further apoptosis via ATR in a manner independent of MMR capacities (Cannavo et al, 2007; Cejka et al, 2003; Polosina&Cupples, 2010a). Growing evidence of MutL protein family involvement in a number of different pathways definitely show that MMR is not their only function and give rise to the idea that MMR may not even be their primary function but rather one component of their assigned tasks.

3.6 SMUDO homologs

To date, only two studies exist which deal with SMUDO-like proteins in particular. In 2008 a study was published that described a previously uncharacterized mouse gene whose product is an ortholog to the SMUDO protein, the subject of this thesis (Blewitt et al, 2008). Some years before the same group had performed an N-ethyl-N-nitrosourea (ENU) mutagenesis screen in mice to identify genes that are involved in epigenetic reprogramming (Blewitt et al, 2005). Several mutant phenotypes named MommeD1-6 (modifier of murine metastable epiallels) were produced and examined. The MommeD1phenotype showed a semidominant effect on transgene variegation, homozygous female-specific mid-gestation lethality and hypomethylation of the X-linked gene Hprt1 indicating a defect in X inactivation, a mechanism important for dosage compensation in mammalian female cells (Ng et al, 2007).

The *MommeD1* mutation was mapped to a gene which is located on mouse chromosome 17 and exhibits a stop codon in exon 23 of 48 in total. Due to its homology to genes encoding for SMC proteins the gene was named *SmcHD1* (structural maintenance of chromosomes hinge domain containing 1). Blewitt et al. characterized the *SmcHD1* gene and its product using a mouse model carrying an *SmcHD1* allele terminated by a gene trap, which featured the same

characteristics as the *MommeD1* phenotype, thus confirming that the mutation in the *SmcHD1*gene is indeed causative of the MommeD1 phenotype (Blewitt et al, 2008).

Several experiments concerning transcriptional activation of an X-linked transgene suggested that there is a defect in embryos undergoing random X inactivation and also in extraembryonic lineages undergoing imprinted X inactivation, such as placental tissue. *SmcHD1*$^{\text{MommeD1/MommeD1}}$ females died during embryogenesis and a decrease in size of trophoblast giant cells, which support the embryo during development, was found.

RNA fluorescent *in situ* hybridization (FISH) was used to verify regular expression of *Xist* transcript expression, the only event that is known to be essential for initiation of X inactivation. Localization of Eed, a core component of the polycomb repressive complex 2 (PRC2) which targets genomic regions to be silenced during X inactivation by modifications like histone methylation, appeared normal. Furthermore, association of histone H3 trimethylated on lysine 27 (H3K27me3), a marker for X inactivation, also seemed to be unaffected. These results indicated a normal initiation of X inactivation in homozygous mutant mice.

Analysis of DNA methylation of 16 CpG islands subject to X inactivation at stage E10.5 revealed hypomethylation in all cases in homozygous female compared to control animals, but no general hypomethylation was detected in chromosomal areas independent of X inactivation. Some of the genes tested were found to be up regulated. Additionally co-localization of SmcHD1 and H3K27me3 marks could be shown in *SmcHD1*$^{+/+}$ females.

Together the results demonstrated a specific requirement for SmcHD1 in methylation of CpG islands during X inactivation, which is a prerequisite of gene silencing and maintenance of X inactivation.

At the same time Kanno et al. presented a study concerning a protein which is involve RNA-directed DNA methylation (RdDM) in *Arabidobsis thaliana* and features a characteristic SMC-hinge domain (Kanno et al, 2008). It had been shown before that in plants small RNAs directed against enhancer regions can trigger *de novo* cytosine methylation and subsequent transcriptional silencing (Huettel et al, 2007). In their study Kanno et al. searched for components of the RdDM system by targeting an enhancer upstream a GFP reporter gene. They noticed DNA methylation not only at the promoter side as expected, but also beyond that, and the process included secondary siRNAs.

In a screen for mutants defective for enhancer methylation and further investigations they identified a gene (*DMS3*; *DEFECTIVE IN MERISTEM SILENCING 3*) whose product exhibits a domain similar to the hinge domain region of SMC proteins. According to their findings Kanno et al. proposed that the protein could potentially link nucleic acids during RNAi-mediated epigenetic modifications in a way that it holds together siRNA and target DNA.

Considering both studies, one function of SMUDO protein might be participation in DNA methylation or epigenetic regulation in general. Nevertheless, its characteristic structure and other hints presented in this thesis suggested a potential role in DNA damage response.

3.7 Task of this thesis

SMUDO is a recently discovered and sparsely characterized protein. Its structural features link it to the SMC and MutL protein families which are involved in several DNA repair mechanisms such as mismatch repair and homologous recombination (Losada&Hirano, 2005; Polosina&Cupples, 2010b). Furthermore, experimental evidence indicated a function in a pathway that includes HIPK2 (see results, sections 5.1 and 5.3), a serine/threonine directed kinase activated upon genotoxic stress (Sombroek&Hofmann, 2009).

The aims of this thesis were to characterize fundamentally SMUDO protein and to search for indications for its functions, with focus on DNA damage response.

4 Materials and Methods

4.1 General

All commercially available chemicals were of analytic grade and used without further purification. If not otherwise stated standard reagents and solvents were purchased from Gerbu (Gaiberg, Germany), Sigma Aldrich (St. Louis, USA), Merck (Darmstadt, Germany), Roth (Karlsruhe, Germany), Biozol (Eching, Germany), AppliChem (Darmstadt, Germany) and Roche Diagnostics (Mannheim, Germany).

The cell culture media and solutions were obtained from Invitrogen (Carlsbad, USA) and PAA Laboratories (Pasching, Austria). Further material is listed in section 4.8.

4.2 Methods in microbiology

4.2.1Transformation of chemical competent cells

For transformation of chemically competent bacteria, *Escherichia coli* DH5-α, TOP10, BL21 and SCS110 host strains from Invitrogen were used. For 50 µl of cell suspension were thawed on ice and mixed with 0.1-1.0 µg plasmid DNA or following ligation reactions with the complete aliquot. Suspensions of all bacteria strains except of SCS110 were incubated on ice for 5 min and head-shocked for 45 sec at 42°C. Aliquots were chilled on ice and diluted in 1 ml 1xLB medium. *Escherichia coli* SCS110 cell were mixed with DNA and diluted with H_2O to a volume of 80 µl. 20 µl KCM buffer was added and the suspension incubated on ice for 20 min and thereafter on RT for 10 min before it was diluted in 1 ml 1xLB medium.

Afterwards, all cell suspensions were incubated at 37°C for 1 h with moderate agitation. Aliquots were spread onto pre-warmed LB agar-plates containing kanamycin, ampicillin or spectinomycin as selection marker. Plates were incubated o/n at 37°C.

4.2.2 Preparation of bacterial cultures

For plasmid preparation or production of recombinant fusion proteins either 5 or 300 ml 1xLB medium containing the appropriate selection marker were inoculated with a single clone and incubated o/n at 37°C and 180 rpm. For storage, 0.5 ml suspension of transformed

bacteria were mixed with 0.5 ml 60% (v/v) clycerol in a cryoconservation vial and transferred to a -80°C freezer.

4.2.3 Screening of recombinants for fusion protein expression

For expression of recombinant protein in *E.coli* in BL21, glutathione-S-transferase (GST) fusion constructs were established and proteins were purified by affinity chromatography using glutathione-sepharose. Expression was under control of the *lac* promoter and therefore induced by isopropyl-β-D-thiogalactopyranoside (IPTG). To screen for fusion protein expression, 5 ml o/n cultures were prepared. Two times 500 µl of each cell suspension were diluted in 500 µl 1xLB medium supplemented with ampicillin and incubated o/n at 37°C and 180 rpm. 4 h prior harvesting, one culture of each clone was induced with 1 mM IPTG. Cultures were then centrifuged for 5 min at 5,000 rpm (Pico 17, Thermo Fischer Scientific) and resuspended in 200 µl SDS sample buffer. After heating at 95°C for 5 min, samples were loaded onto a SDS-polyacrylamide gel and protein expression was analyzed by Coomassie blue staining and comparison of induced and non-induced cultures.

4.2.4 Production of recombinant fusion proteins

For production of GST or polyhistidine fusion proteins, 100 ml o/n cultures of transformed *E.coli* BL21 were used to inoculate 400 ml pre-warmed 1 x LB medium supplemented with the appropriate antibiotic. Cultures were incubated at 37°C for 1 hour before IPTG was added to a final concentration of 0.1 to 1 mM. Cells were harvested after incubation at 30°C for 4 to 12 hours by centrifugation at 5,000 rpm and 4°C for 10 min, pellets were stored o/n at 80°C or directly used for purification as described later on (section 4.7.8).

4.3 Methods in cell biology

4.3.1 Cell culture

Work with mammalian cell was carried out under sterile conditions in appropriated flow hoods.

All used immortalized cell lines were obtained from ATCC (Manassa, USA) whereas all primary cell lines were received from the Coriell Institute repository (Camden, USA).

Immortalized cells were cultured in Dulbecco's modified Eagle's medium (DMEM) supplemented with heat-inactivated 10 % FCS (vol/vol), 2 mM L-glutamine, 50 U/ml penicillin/streptomycin, 1 mM sodium pyruvate and 10 mM Hepes at 37°C in a humidified atmosphere containing 5 % CO_2. Medium for primary cells was additionally supplemented with non-essential amino acids (NEAA) and with 15 % FCS instead of 10 %. Every second to third day adherent cells were subcultered when they had reached confluency of 80-90 % on 10 cm cell culture dishes. Growth medium was removed and cell layers washed with PBS before 2 ml of 0.25 % Trypsin-EDTA solution were added to detach cells. After short incubation growth medium was added and cell suspension collected by pipetting. Aliquots of desired size were transferred to new culture dishes.

4.3.2 Cryoconservation

For conservation cells were trypsinized when had reached 80-90 % confluency, resuspend and centrifuged at 1200 rpm and RT for 5 min (Varifuge RF, Heraeus Sepatech). Then cells were resuspended in supplemented growth medium containing 10 % DMSO and transferred into cryovials, which were cooled down on ice for a couple of minutes before stored at -80°C for 2-5 days. Finally the vials were transferred into a liquid nitrogen storage tank. Contrary the thawing of cryo-stored cells was carried out quickly. The vials were warmed at 37°C and cell suspension centrifuged at 1200 rpm and RT for 5 min. Cells were resuspended in pre warmed growth medium and plated onto cell culture dishes. After one day the medium was replaced by new.

4.3.3 Transient transfection of eukaryotic cells

Calcium phosphate transfection

Calcium phosphate transfection was used for over expression experiments and as well as for production of lentivirus in 293T cells. One day prior transfection 2.5-3 x 10^6 cells were seeded onto 10 cm culture dishes. For transfection plasmid DNA was diluted in H_2O to an overall volume of 450 µl, 500 µl 2 x HBS buffer and thereafter 50 µl 2.5 M $CaCl_2$ were added. Aliquots were mixed vigorously and incubated for 5 min at RT. The Calciumphosphate-DNA-precipitates were mixed again and put on cultured cell in a dropwise manner. Cells were

harvested 12-48 h after transfection. For production of lentivirus cells were washed with PBS 4 h after transfection and growth medium was renewed. Virus containing supernatant was harvested 36-48 h after transfection.

Polyethylenimine transfection

Another method used to transfect 293T cells is polyethylenimine (PEI) transfection. Cells were transfected on 10 cm dishes at 80-90 % confluence and PEI was used at ratio of 3 µl per µg plasmid DNA. For transfection PEI was diluted 1 ml Optimem (Invitrogen), plasmid DNA was added and aliquots were mixed vigorously. After incubation for 15 min at RT aliquots were given to cells by pipetting. Cells were harvested 12-48 h after transfection.

FuGENE6 transfection

To transfect U2OS cells for fluorescence experiments FuGENE6 (Roche) reagent was used. Cover slips had been placed in 24-well plates and cells were seeded on it. Cells were transfected when confluence of about 80 % was reached. FuGENE6 reagent was diluted with Optimem and aliquots were mixed by vortexing for 1 sec. Afterwards plasmid DNA was added and aliquots were mixed again prior incubation for 15-30 min. A ratio of 3 µl FuGENE6 to 1 µg DNA was used and the total volume of the transfection complex was 100 µl per 24-well. 24-wells were pre-filled with 1 ml of growth medium and transfection complex was added after incubation. About 24 hours after transfection cells were used for fluorescence experiments. For live cell imaging live cell chambers were used instead of 24-well plates.

HiPerFect siRNA transfection

HiPerFect reagent (Qiagen) was used for transient siRNA transfect of mammalian cells. 6-well were used as containers for this approach. Per 6-well a number of 2×10^5 of previously trypsinized cells was diluted in 1.8 ml growth medium. 100 µl Optimem were supplemented with 12 µl HiPerFect and 10 µl 20 µM siRNA, mixed and incubated for 5 min at RT. Subsequently aliquots were mixed with the prepared cell suspension and seeded onto the 6-wells. The final siRNA concentration was 100 nM. Cells were harvested after 24 h to 48 h.

4.3.4 Lentiviral transduction of eukaryotic cell

For production of lentiviral vectors 293T cells (10 cm dish) were transfected with 20µ a pG-lenti vector which is based on the murine leukemia virus (MLV) and carries the transgene of interest and a GFP-reporter gene. Additional vectors encoding several packaging proteins and support factors were co-transfected along with the pG-lenti vector. In detail this were 5 µg of pRSVrev vector, 5 µg pVSVg vector and 10 µg of pMDLg vector. 4 h after transfection growth medium was renewed. Transfection efficiency was checked under a fluorescence microscope. Virus containing medium was collected 48 h after transfection, centrifuged at 1.200 rpm for 5 min and supernatant filtered using a PVDF-membrane filter with a diameter of 0.45 µm. Target cells were seeded on 6-wells and used for transduction at confluence of 60-80 %. For this purpose growth medium was removed from 6-wells and replaced by 2 ml of virus containing medium supplemented with polybrene (final concentration: 8 µg per ml). Virus was spun down onto cells at 2.000 rpm and RT for 90 min. After 4 h cells could be subcultured to favored volumes and transduction efficiency was checked using a fluorescence microscope.

4.3.5 Treatment of eukaryotic cells

UV-irradiation

To damage cells by UV-irradiation medium was removed and opened culture dishes were placed into a UV Stratalinker 1800. Disired UVC dosages were applied and new growth medium was quickly given to cells. Dependent on the experinent cell were harvested 5 min to 48 h after UV-irradiation.

Doxorubicin (Adriamycin) treatment

The chemotherapeutic drug Doxorubicin (a.k.a. Adriamycin) was used to induce DNA double-strand breaks. To do this growth medium was supplemented with Adriamycin at concentrations from 4-10 µM.

Fluorouracil treatment

Fluorouracil (5-FU) was used to induce G/T mismatch repair. The drug was added to growth medium to final concentration of 5 to 55 µM. After 14 h of incubation medium was

renewed and cells were incubated under growth conditions to reach confluence appropriate to perform colony formation assays.

4.3.6 Colony Formation Assay

To assay cells viability upon various treatments colony formation assays were made. At first a defined number of cells were seeded on several cell culture dishes of the same size. When adherent cells were treated in an experimental dependent manner, they were subsequently incubated under growth conditions until requested confluence was reached. Medium was removed and cells were fixed and stained at the same time by incubation with crystal violet solution for 10 min. Cells were washed with water for three times to remove remaining staining solution before were air dried. Number of cells was dependent of the cell type and the size of the culture dishes used for the concerning experiment. Typically, 10^6 HCT116 cells were seeded on one well of a 6-well plate.

4.4 Methods in molecular biology

4.4.1 Plasmid preparation

For isolation of plasmid DNA at analytical scale, 2 ml of o/n cultures were centrifuged at 4,500 rpm, RT for 5 min (Pico 17, Thermo Fischer Scientific). Afterwards plasmid DNA was isolate by using the QIAprep Spin Miniprep kit, which is based on the methods of alkaline lysis and anion-exchange chromatography, according to the manufacturer's protocol. For isolation of larger amounts of plasmid DNA, 300 ml of o/n culture were centrifuged at 5,000 rpm and 4°C for 10 min (GS3, Sorvall Instruments). Plasmid DNA was isolated by using Qiagen Plasmid Maxi Kit. Quantity and purity of isolated DNA were determinate by using a micro-volume spectrophotometer from NanoDrop Technologies to measure absorption at 260 nm and 280 nm.

4.4.2 Agarose gel electrophoresis

For analysis or preparation DNA fragments were separated in 0,7-1,5 % (w/v, in 1 x TAE buffer) agarose gels containing ethidium bromoide (EtBr) at 5-10 V/cm. DNA fragments were visualized via simulating fluorescence of intercalated EtBr by UV radiation.

4.4.3 DNA digestion and molecular cloning

DNA digestion

For a typical digestion reaction of DNA 0.2-2 µg of Plasmid DNA were incubated with 1-10 units (U) of the appropriate restriction enzyme under producer defined conditions. The total volume was 20 µl and incubation time 10-60 min. Resulting DNA fragments were separated by agarose gel electrophoresis (see 4.4.2) and required fragments cut out of the gel. DNA was purified from agarose gel by means of QIAquick Extraction Kit (Qiagen).

Dephosphorylation

To remove 5´-phosphates of DNA, 0.2-1 µg DNA was incubated with 1 U of calf intestine phosphatase (CIP) in appropriate buffer (total volume: 30µl) for 30 min at 37°C. CIP was inactivated by heating aliquots at 74°C for 10 min.

Ligation

To ligate DNA fragments into a plasmid vector, 50-500 ng of the digested and dephosphorylated vector were incubated with the 3 to 5-fold molar amount of insert DNA fragment and 1 U T4-DNA ligase in appropriate buffer containing ATP. The total volume was 20 µl and incubation time was 1h at 37° or alternatively o/n at 16°C. Subsequently DNA was used to transform bacteria. Cloning of PCR products was performed by using the TOPO-TA cloning kit and the Zero-Blunt TOPO PCR cloning kit according to the manufacturer suggested procedure.

4.4.4 RNA isolation

Isolation of RNA out of human cells was performed using the RNeasy Mini Kits from Qiagen following manufacture's protocol.

4.4.5 Reverse transcription

The enzyme reverse transcriptase was used to generate DNA complementary to RNA templates (cDNA). 2 µg RNA were diluted in water to a volume of 14 µl and pre-incubated with 1 µg random primer for 10 min at 56°C. Per reaction 4.5 µl reaction mix containing 1 µl

dNTS (100 mM), 2 µl 10 x buffer, 0.5 µl RNase Out (40 U/µl) and 1 µl AMV reverse transcriptase were added. Aliquots were incubated at 42°C for 40 min and 2 min at 95°C.

4.4.6 DNA amplification by polymerase chain reaction (PCR)

The technique of polymerase chain reaction (PCR) was used to amplify DNA segments. For each segment a pair of specific oligonucleotide primers, one 5´-forward primer and one 3-reverse primer, were designed and used. 100 ng of DNA template were mixed with 10 pmol of each primer, 0.08 mM dNTP mix, 2,5 U Taq DNA polymerase or 1 µl Pfu DNA polymerase, respectively, and diluted in corresponding buffer containing 1,5 mM $MgCl_2$ to an overall volume of 50µl. Reaction protocol was started with an initial denaturation step at 95°C for 5 min and continued with 20-30 amplification cycles, each consisting of 30 s of denaturation at 95 °C, 30 s annealing at 58°C and 3 min elongation at 72°C. Finally reaction was terminated by onetime heating to 72°C for 5 min and the PCR products were purified using the PCR Purification Kit from Qiagen following manufacturer's protocol. In case of PCR was performed subsequent reverse transcription control primers (β-actin forward, β-actin reverse) were added to the reaction mixture.

4.4.7 Generation of expression constructs

SMUDO full-length construct was previously cloned from cDNA libraries (DKFZ) by Ilka Dauth using PCR and subcloning of PCR products into pCDNA3 vector. By further subcloning via BamHI, XbaI restriction sites various tagged SMUDO full-length expression constructs were created (GFP-SMUDO, Myc-SMUDO, Flag-SMUDO). Due to the size of the SMUDO open reading frame (ORF) of about 6 kb cloning procedure pointed out to be difficult and several times cloning had to made in two steps, which included a third restriction site that was dependent on the destination vector used. SMUDO constructs lacking the MutL or the SMC region, respectively, were produced by PCR and subcloning into pEGFP-C1, pCMV-3Tag1A and pCMV-Tag3B vectors. Several GST-tagged SMUDO fragment expression constructs were produced by subcloning fragments of the SMUDO ORF out of pCR4-TOPO and pCR-Blunt vectors into pGEX-4T1 vector. Lentiviral knock constructs were produced by cloning siRNA sequences into pGLenti vectors.

4.4.8 Northern blot analysis

For production of a SMUDO Northern blot probe a part of SMUDO's nucleotide sequence was digested with HindIII and NheI. The generated fragment was 1724 bp in size (SMUDO bp 2194-3917). Labeling of the probe was done by using the Fermentas Label Plus DNA labeling kit, where the instructions of the manufacturer have been followed. The probe was applied to a membrane pre-hybridized with human tissue specific RNA (Frstchoice™ Humanblot1 from Ambion). The instructions of the manufacturer have been followed. ULTRAhyb hybridization solution and Northern Max low stringency wash solution from Ambion were used for the procedure.

4.4.9 Yeast two-hybrid screening

The yeast two-hybrid screens were performed at PanBioNet Company.

4.4.10 DNA sequencing

DNA sequencing was performed at GATC Biotech AG (Konstanz, Germany) or at the Genomic and Proteomics Core Facility of the DKFZ.

4.5 Microscopy

4.5.1 Immunofluorescence microscopy

To visualize endogenous proteins for microscopy they were indirectly stained with fluorescent dyes using adequate antibodies. Cover slips were placed in 24-wells and U2OS cells were seeded on it. For pre-extraction of loose intracellular material cell were washed with PBS and afterwards with cytoskeletal buffer (CSK buffer) before incubated with CSK buffer supplemented with 0.5 % Triton X-100 for 2 min at RT. Cell were washed again with pure CSK buffer and PBS. For fixation cells were incubated in PBS containing 4 % paraformaldehyde (PFA) for 20 min, RT. Residues of PFA were removed by washing cover slips two times with PBS. Without previous pre-extraction cells had to be permeabilized by incubation in PBS supplemented with 0.5 % Triton X-100 for 5 min at RT. Primary antibodies directed against the endogenous proteins were diluted in PBS and per cover slip a 70 µl drop was placed on Parafilm. Cover slips were put onto drops with the side covered with cells directed to the antibody dilution. For each primary antibody used the dilution

factor was individually adjusted. Incubation was carried out over night at 4°C while cover slips were stored in a non-transparent container. To avoid evaporation of antibody dilution humidity inside the container was increased by placing wet tissues inside. Next, cover slips were washed five times with PBS, each time for at least 5 min, and dilution of secondary dye-coupled antibodies directed against the primary antibodies was prepared. The typical dilution factor for secondary antibodies was 1:450 and solution was additionally supplemented with Hoechst 33258 dye to label DNA. Incubation of the cells for 45 min was followed by five times washing with PBS and embedding of cover slips into Mowiol on an object slide. Mowiol was hardened by air drying o/n and sealed with nail enamel.

For microscopy studies of overexpressed fluorescent fusion proteins expression plasmid of the protein of interest was transfected into cells by one of the transfection methods described earlier. Pictures have been taken with an Olympus IX81 confocal microscope. For conventional fluorescent pictures the microscope pinhole diameter was greater than 150 nm, while it was 80-100 nm for confocal pictures. Olympus FluorView software was used for microscope control.

4.5.2 Fluorescence recovery after photobleaching (FRAP)

The technique of Fluorescence recovery after photobleaching (FRAP) was used to quantify diffusion of GFP tagged SMUDO protein trough the nuclear membrane of mammalian cells. Cells were seeded in live cell chambers which have a base made of silica glass to allow laser application. Cells were transfected with expression plasmid and 24 h after transfection standard growth medium was exchanged by medium lacking phenol red, since this pH indicator interferes with fluorescent assays. For picture documentation and fluorescent bleaching an Olympus IX81 confocal microscope and attached laser emitters have been used. Olympus FluorView software was used for microscope and laser control. For compartment bleaches 30 frames with an interval of 20 seconds have been taken. The scan time was 3.2 seconds per frame. Bleaching was applied by a 488 nm laser at 100% emission for 6 frames. One frame was taken before bleaching. The timespan for a complete procedure was 9 minutes and 50 seconds. For point bleaches 30 frames have been taken at a free run (fast as possible). The scan time was 1.6seconds per frame. Bleaching was applied by a 488 nm laser at 100% emission for 2 frames at the tornado mode (downwards spiral of laser focus). One frame was taken before bleaching. The timespan for a complete procedure was 50 seconds.

4.6 Bioinformatics

For software analysis of nucleotide and protein sequences the BLAST server (http://blast.ncbi.nlm.nih.gov/Blast.cgi) and the correlated NCBI Conserved Domains tool (http://www.ncbi.nlm.nih.gov/Structure/cdd/wrpsb.cgi) were used. In addition, free software available at the ExPASy tool server (http://expasy.org/tools) was used. In detail, the NetES 1.1 server (http://www.cbs.dtu.dk/services/NetNES/) was used to predict nuclear localization signals, the PredictNLS software was used to predict nuclear localization signals (http://www.cubic.columbia.edu.cgi.var.nair.resonline.pl), Compute pI/Mw software was used to calculate the molecular weight of SMUDO protein and SUMOsp prediction software was used to find potential SUMOylation sites inside SMUDO's amino acid sequence. Sequence alignments were carried out at the CLUSTALW server (http://www.genome.jp/tools/clustalw/).

4.7 Methods in protein biochemistry

4.7.1 Preparation of total cell lysates

Cell transfected with expression plasmid and / or treated with agents as well as untransfected and untreated control cells were lysed in various types of buffers for different applications. For biochemical analysis of cellular protein total cell lysates were prepared using NP-40 / 1 % SDS or Triton X-100 lysis buffer, respectively. Adherent cells were washed twice with ice-cold PBS and scraped off cell culture dishes using rubber policemen. Detached cell were taken up in PBS and collected by centrifugation at 13,000 rpm, 4°C, for 5 min, resupension in about 300 µl PBS, followed by transfer into 1,5 ml micro tubes and once again centrifugation for 5 min at 13,000 rpm and 4°C. 100-400 µl of lysis buffer were given on cells and suspension was chilled on ice for 5 min before sonicated (output 2, NP-40 / 1 % SDS buffer: 3 x 10 sec, Triton X-100 buffer: 2 x 8 sec) while kept on ice. Lysates were then centrifuged at 13,000 rpm and 4°C for at least 30 min to separate soluble lysates from insoluble cellular remains. If necessary, 3 µl of the lysates were taken for determination of protein concentration. Lysates were mixed with 5 x SDS sample buffer, that contains β-mercaptoethanol to reduce disulfide bonds, and heated at 95°C for 5 min to denature and stabilize proteins. Lysates were directly used for SDS-PAGE or placed at -20°C for storage. For immunoprecipitation cells were lysed in NP-40 / 1 % SDS buffer and handled as described below (4.7.9).

4.7.2 Determination of protein concentration and purity

To allow equal loading of SDS-PAGE gels and equal settings for endogenous immunoprecipitations, protein concentration of lysates was determined by using the BCA Protein Assay Kit (Thermo Fisher Scientific) following the manufacturer's instructions and measuring absorbance at 570 nm in a plate reader (Labsystems Multiskan Ms). Reference curves were regenerated by measuring absorbance of BSA protein standard solutions. Purity and concentration of proteins isolated out of bacteria was checked by SDS-PAGE gel and subsequent Comassie staining. Again BSA standard solutions were used as reference.

4.7.3 Subcellular fractionation

This method was used to obtain separated protein extracts from nuclei and cytoplasmic compartments of mammalian cells. For one sample two to three 10 cm dishes of confluent adherent cells were harvested as described above, resuspended in a suitable volume of PBS and the third part was taken to make total cell lysates for control using NP-40 / 1 % SDS buffer. The remaining cells were further handled for fractionation. After pelletizing by centrifugation they were taken up in 100 µl cellular fractionation buffer A, that was supplemented with protein inhibitors, and held on ice for 12 min. To break cellular membranes, 6.25 µl of 10 % NP-40 solution was added and aliquots were immediately mixed by vortexing for 10 sec. Subsequently lysates were centrifuged for 1 min at 13,000 rpm, 4°C, and supernatant was transferred into a new 1.5 ml micro tube (cytoplasmic fraction), at that clear separation from pellet was critical. Remaining pellet was washed on time with PBS, resuspended in 100 µl NP-40 / 1 % SDS, sonicated and centrifuged at 13,000 rpm and 4°C for at least 30 min. Supernatant was transferred to a new 1,5 ml micro tubes (nuclear fraction). Both, cytoplasmic and nuclear fraction were mixed with 5 x SDS sample buffer and headed at 95°C for 5 min. For analysis the control lysates as well as equal amounts of cytoplasmic lysates and nuclear lysates were loaded on SDS-PAGE gel.

4.7.4 SDS-polyacrylamide gel electrophoresis

Sodium dodecyl sulfate (SDS) polyacrylamide gel electrophoresis under denaturing conditions was used to separate proteins according to their electrophoretic mobility. For this lysates were prepared as described before (see 4.7.1) and desired protein amount or a distinct volume was loaded on 4-20 % PAGEr Gold Precast gel (Lonza). Electrophoresis

procedure was accomplished in apparatuses purchased from Bio Rad Laboratories (Hercules, USA).

4.7.5 Coomassie blue staining

To stain GST-fusion proteins in SDS-gels, they were incubated in Coomassie Brilliant Blue (CBB) R250 staining solution. SDS-gel covering solution was heated in a microwave oven for about 1 min to immobilize and stain proteins. Staining solution was removed and gels were rinsed with waster to dispose excess stain. Afterwards gels were incubated in destaining solution, which was renewed 1-2 times, until background was reduced to acceptable level and protein bands were clearly visible.

4.7.6 Drying of SDS-polyacrylamide gels

For long term storage, gel could be dried and sealed into plastic foil. For this purpose gels were placed on wet Whatman filter paper, covered with plastic foil and dried for 1-2 h at 80°C in a vacuum gel dryer (Bio Rad).

4.7.7 Western blot (Immunoblotting)

Proteins were blotted from a SDS-gel onto a PVDF membrane (Hybond-P) using wet electrophoretic transfer method. To do this PVDF membrane was activated in pure methanol for 10 sec and equilibrated in wet blot buffer besides SDS-gels, Whatman paper and fiber pads. SDS-gel was placed on the membrane and both parts were covered with Whatman paper and fiber pads. The gel/membrane sandwich was assembled in a holder cassette and placed into a transfer apparatus (Bio Rad). Protein transfer was carried out at 380 mA and 4°C for 1 h and 20 min. After that transfer efficiency was checked by Poncau S staining. Subsequently membrane was washed with deionized water and incubated in 5 % fat-free milk powder in TBS-T buffer for at least one 1 h to block free unspecific binding sites. Primary antibody was diluted in 5 % BSA or 5 % fat-free milk/TBS-T buffer, respectively, and membranes were incubated with constant agitation either at RT for 2-4 h or o/n at 4°C. To remove excess primary antibody membrane was washed 3 x 10 min with TBS-T. Horseradish peroxidase (HRP) coupled secondary antibody was diluted 1:20,000 in 5 % fat-free milk/TBS-T buffer and membrane was incubated for 30-60 min at RT with

agitation. Again membrane was washed for at least 3 x 10 min with TBS-T, placed in an X-ray cassette and moistened with a 1:1 mixture of the SuperSignal West Dura Extended Duration Substrate solutions (Thermo Scientific). Proteins were indirectly detected by exposition of X-ray film to the peroxidase generated chemiluminescence.

4.7.8 Purification of recombinant proteins

Bacteria cultures were harvested by centrifugation or thawed on ice, if had been stored at -80°C. Pellet was taken up in ice-cold PBS and cells were held on ice during all following step. Fist, cells were broken by sonication (3 x 15 sec, output 3) and Triton X-100 was added to a final concentration of 1 %. After 10 min cell extracts were sonicated again (3 X 15 sec, output 3). Unbroken cells and cellular remains were separated by centrifugation at 13,000 rpm and 4°C for 30 min (Sorvall ultracentrifuge, SS34 rotor). Glutathione Sepharose™ 4 Fast Flow was added to supernatant and aliquot were incubated for at least 2 h on a rotator. Speharose was washed 3 x with PBS. For experiments either sepharose-coupled proteins were used or proteins were eluted from sepharose prior performance by using reduced glutathione (final conc. 8 mM). Elution was carried in 1.5 ml micro tubes on a rotator for 1 h. After short centrifugation (2 min at 3,000 rpm, 4°C) supernatant was transferred into a new 1.5 ml micro tube. Finally the solution containing the protein was dialyzed o/n against a 1,000-fold volume of dialysis buffer. Proteins were directly used for experiment or stored at 4°C.

For purification of histidine-fusion proteins bacteria were harvested suitable time after induction of protein expression and resuspended in HEMGN buffer. Cells were broken by sonication and aliquots were supplemented with NP-40 (final conc. 0.1 %) and chilled on ice for 10 min before sonicated again. Unbroken cells and cellular remains were separated by centrifugation at 13,000 rpm and 4°C for 30 min. Ni-NTA agarose (Qiagen), KCl (final conc.: 0.2 M) and imidazole (final conc.: 10 mM) were added to supernatant and aliquots were incubated on a rotator at 4°C for 2 h. Afterwards agarose was washed 3 x with HEMGN buffer, 0.2 M, 10 mM imidazole. For elution agarose was transferred to a new 1.5 ml micro tube histidine elution buffer was added and suspension was incubated on a rotator for 1h. After centrifugation (2 min at 3,000 rpm, 4°C) supernatant was transferred into another 1.5 ml tube and the solution containing the protein was dialyzed o/n against a 1,000-fold volume of HEMGN buffer. Proteins were directly used for experiment or stored at -80°C after shock freezing.

4.7.9 Immunoprecipitation and Co-Immunoprecipitation

To perform immunoprecipitation assays, total cell lysates were prepared as described in section 4.7.1. Lysates were pre-cleared by adding 25 µl protein A/G Plus Sepharose beads (Santa Cruz, USA) and incubation on a rotator for 1 h at 4°C, to do this the volume of each aliquot had been previously adjusted to 750 µl with lysis buffer to ensure proper mixing. Solid phase was separated by centrifugation for 2 min at 3,000 rpm, 4°C, and discarded. Supernatants were incubated with 5-10 µg of specific antibody on a rotator for 4-14 h at 4°C. Subsequently 25-30 µl protein A/G Plus Sepharose beads were added and lysates were incubated again for 1 h to bind antibodies to beads. Sepharose beads were washed 3 times by adding each time 750 µl lysis buffer, gently mixing and short centrifugation (3,000 rpm,4°C, 2min). Then lysis buffer was removed and beads were resuspended in 1 x SDS sample buffer and heated at 95°C for 5 min before analyzed on SDS-PAGE gel and Western blot. For storage samples were kept at -20°C. For Immunoprecipitaion of overexpressed Flag-tagged proteins, Flag M2 agarose beads were used following the manufacturer's protocol.

4.7.10 *In vitro* Translation of ^{35}S-labeled Proteins

Radioactive labeling of proteins with L- ^{35}S-methionine for pulldown experiments was accomplished by using the TNT Coupled Reticulolysate Lysate system (Progema).

Reticulolysates were aliquoted on ice in total volumes of 50 µl and mixed with 2µg plasmid DNA containing a T7 or T3 promoter and corresponding RNA polymerase. After incubation for 90 minutes at 30°C samples were directly used for pulldown experiments or stored at -80°C.

4.7.11 GST pulldown assay

To examine protein *in vitro* interaction, GST pulldown assays have been performed. For experiments recombinant GST-HIPK2ΔC fusion protein and *in vitro* generated and ^{35}S-labeled SMUDOΔN were incubated in 750 µl PBS supplemented with 0.1 % NP40, 1 mM

sodium orthovanadate, protease inhibitor cocktail and gluthation sepharose at 4°C for 1.5 hours on an orbital shaker. Sepharose was washed 3 times with 750µl interaction buffer, resuspended in 1xSDS sample buffer and analyzed by SDS-PAGE. For one pulldown

experiment 3-5µg of GST fusion proteins and 10µl of *in vitro* translated proteins were used. Proteins were stained with coomassie and radioactive signal were amplified by incubation in amplifier solution (Amplify Solution, Amersham) for 15 min. Finally radioactive signals were detected on an X-ray film.

4.7.12 *In vitro* phosphorylation experiments

To test phosphorylation of SMUDO by HIPK2 *in vitro* phosphorylation experiments were performed. For this purpose Flag-tagged HIPK2 was overexpressed in 293T cells and subsequently precipitated or His- tagged HIPK fusion protein was purified from *E.coli*.

GST-SMUDO fragments were generated and precipitated as described before (4.7.8). Proteins were incubated in a total volume of 30 µl Ser/Thr kinase buffer supplemented with 40µM [γ-S]-ATP and 5 µCi [γ-^{32}P]-ATP for 30 min at 30°C. Typically, 1-5 µg of substrates (SMUDO fragments) and 0.5-1 µg of rHis-HIPK2 were applied. Reaction was stopped by adding 7.5ml 5 x SDS sample buffer and boiling at 95°C for 5 min. Samples were separated by SDS-PAGE. After gel fixation and staining with coomassie, gels were dried and analyzed with X-ray films.

4.8 Materials

4.8.1 Materials and Kits

Material	Manufacturer
1.5 ml reaction tubes	Sarstedt AG
10 cm cell culture dishes	Greiner & TPP AG
15 ml reaction tubes	Greiner
2 ml reaction tubes	Sarstedt AG
50 ml reaction tubes	Falcon
6 cm cell culture dishes	Greiner & TPP AG
6-well plates	Nunc GmbH
96-well plates	Falcon
Firstchoice Humanblot 1	Ambion
Complete protease inhibitor cocktail	Roche
Cryo vials	Roth
Fugene	Roche
Glutathion-Sepharose	Amersham Biosciences
HiPerFect	Qiagen
Lipofectamine™ 2000	Invitrogen
Mg/ATP slolution	Boston Biochem
Nickel-NTA-Agarose	Qiagen
PCR tubes	Nerbe
Pierce ECL-Kits	Thermo Fischer Scientific
Pierce® BCA Protein Assay Kit	Thermo Fischer Scientific
Protein A/G Plus Sepharose	Santa Cruz
PVDF-membrane „Hybond™-P”	GE Healthcare
QIAGEN® Plasmid Maxi Kit	Qiagen

Material	Manufacturer
QIAprep® Spin Miniprep Kit	Qiagen
QIAquick® Gel Extraction Kit	Qiagen
TNT® Coupled Reticulocyte Lysate System	Promega
TOPO® TA Cloning® Kit	Invitrogen
X-ray films „Fuji Super FX“	FUJIFILM
Zero Blunt® TOPO® PCR Cloning Kit	Invitrogen

4.8.2 Chemicals

Reagent	Manufacturer
β-Glycerophosphate	AppliChem
[γ-^{32}P]-ATP	Perkin-Elmer
[γ-S]-ATP	Roche Diagnostics
5-Fluorouracil	Sigma Aldrich
Adriamycin (doxorubicin)	Merck Biosciences
Ammoniumperoxysulfate (APS)	Sigma Aldrich
Ampicillin	Gerbu
ATP	US Biological
BSA	Servia
Coomassie brilliant blue G250	BioRad
Dithiothreitol	US Biological
Glutathion	Sigma Aldrich
Imidazole	Sigma Aldrich
IPTG	Roth
Kanamycin	Gerbu
L-^{35}S-Methionin	Perkin-Elmer

Reagent	Manufacturer
MG-132	US Biological
Phenylmethanesulphonyl fluoride (PMSF)	Sigma Aldrich
Sodium orthovanadate	Sigma Aldrich

Standard chemicals were purchased from Sigma Aldrich, Roche Diagnostics, Roth, Gerbu, Biozol and Merck.

4.8.3 Proteins and enzymes

Protein/Enzyme	Manufacturer
ApaI	New England BioLabs
BamHI	New England BioLabs
BglII	New England BioLabs
BmpI	New England BioLabs
BspEI	New England BioLabs
BssSI	New England BioLabs
Calf intestinal phosphatase (CIAP)	New England BioLabs
DpnI	New England BioLabs
DrdI	New England BioLabs
EagI	New England BioLabs
EcoRI	New England BioLabs
HindIII	New England BioLabs
Kpn!	New England BioLabs
MBP, dephosphorylated	Millipore (Upstate®)
NaeI	New England BioLabs
NcoI	New England BioLabs
NheI	New England BioLabs

Protein/Enzyme	Manufacturer
NotI	New England BioLabs
NspI	New England BioLabs
Pfu DNS Polymerase	Fermentas
PstI	New England BioLabs
SacII	New England BioLabs
T 4 ligase	New England BioLabs
Taq DNS Polymerase	Invitrogen
Trypsin/EDTA	Invitrogen (GIBCO®)
XcmI	New England BioLabs
XhoI	New England BioLabs
XmaI	New England BioLabs

4.8.4 Markers

Marker	Manufacturer
PageRuler™ Plus Prestained Protein Ladder	Fermentas
Prestained Protein Molecular Weight Marker	Fermentas
GeneRuler™ 1kb DNA Ladder	Fermentas

4.8.5 Buffers, Solutions and Media

Buffers and Solutions

Buffer	Ingredient	Concentration
TAE buffer (50x)	Tris-acetate, pH 8.0	2 M
	EDTA	50 mM

Buffer	Ingredient	Concentration
DNA sample buffer (6x)	Formamide	85% (v/v)
	EDTA, pH 8.0	10 mM
	Bromphenol blue	1 mg/ml
	Xylen cyanol	1 mg/ml
PBS	Na_2HPO_4/KH_2PO_4, pH 7.4	12 mM
	NaCl	137 mM
	KCl	2.7 mM
TBS (20x)	Tris-HCL, pH 7.5	500 mM
	NaCl	1.5 M
TBST	1x TBS buffer	
	Tween 20	0.1% (v/v)
SDS sample buffer (5x)	Tris-HCL, pH 6.8	62.5 mM
	Glycerol	40% (v/v)
	ß-Mercaptoethanol	5% (v/v)
	SDS	2% (w/v)
	Bromphenol blue	0.5% (w/v)
SDS stacking gel	Tris-HCL, pH 6.8	125 mM
	Acrylamid-bisacrylamid (37.5:1)	5% (v/v)
	SDS	0.1% (w/v)
	APS	0.04% (v/v)
	TEMED	0.075% (v/v)

Buffer	Ingredient	Concentration
SDS resolving gel	Tris-HCL, pH 8.8	350 mM
	Acrylamid-bisacrylamid (37.5:1)	6-12.5%
	SDS	0.1% (w/v)
	APS	0.04% (v/v)
	TEMED	0.075% (v/v)
SDS-Laufpuffer (10x)	Tris-Base, pH 8.3	250 mM
	Glycin	1.92 M
	SDS	1% (w/v)
Ponceau S staining solution	Ponceau S	0.5% (w/v)
	Acetic acid	1% (v/v)
Coomassie staining solution	Coomassie-Brilliantblau R 250	0.5% (w/v)
	Methanol	45% (v/v)
	Acetic acid	10% (v/v)
Coomassie destain solution	Methanol	45% (v/v)
	Acetic acid	10% (v/v)
Transfer buffer	Tris	25 mM
	Glycin	190 mM
	Methanol	10% (v/v)
HEMGN buffer	Hepes-KOH, pH 8.0	25 mM
	KCl	100 mM
	$MgCl_2$	12.5 mM
	Glycerol	10 %
	EDTA	0.1 mM

Buffer	Ingredient	Concentration
Histidine elutionpuffer	HEMGN buffer	
	KCl	0.2 M
	Imidazole	250 mM
GST elution buffer	Hepes, pH 7.5	30 mM
	NaCl	150 mM
	GSH	8 mM
	Dithiothreitol	2 mM
GST dialysis buffer	Hepes, pH 7.5	30 mM
	NaCl	150 mM
Ubiquitinierungspuffer	Tris, pH 7.4	50 mM
	$MgCl_2$	5 mM
	Dithiothreitol	2 mM
Kinase buffer	Hepes, pH 7.4	20 mM
	NaCl	150 mM
	β-Glycerophosphate	25 mM
	$MgCl_2$	20 mM
	NaF	10 mM
	Dithiothreitol	2 mM
	Na_3VO_4	1 mM
HBS-Puffer (2x)	HEPES, pH 7.05	42 mM
	Na_2HPO_4	1.4 mM
	NaCl	274 mM
	KCl	10 mM
	Dextrose (D(+)-Glucose)	12 mM

Buffer	Ingredient	Concentration
Fractionation buffer A	HEPES, pH 7.9	10 mM
	KCl	10 mM
	EDTA	0.1 mM
	EGTA	0.1 mM
NP40 buffer*	Tris-HCl, pH 7.4	20 mM
	NaCl	150-250 mM
	NaF	25 mM
	Glycerol	10 % (v/v)
	EDTA	5 mM
	NP40	1 % (v/v)
Totex buffer*	HEPES-KOH, pH 7.9	20 mM
	NaCl	350 mM
	Glycerol	20% (v/v)
	NP40	1% (v/v)
	$MgCl_2$	1 mM
	EDTA	0.6 mM
1% SDS lysis buffer*	Tris-HCl, pH 7.4	20 mM
	NaCl	150-250 mM
	NaF	25 mM
	EDTA	5 mM
	NP40	1% (v/v)
	SDS	1% (v/v)

Buffer	Ingredient	Concentration
0.1% SDS lysis buffer*	Tris-HCl, pH 7.4	20 mM
	NaCl	150-250 mM
	NaF	25 mM
	EDTA	5 mM
	NP40	1% (v/v)
	SDS	0.1% (v/v)

*Lysis buffers were supplemented with 1mM sodium orthovanadate, 0.1 mM PMSF, 10μM MG-132 and Complete protease inhibitor cocktail before used.

Growth media

Medium	Ingredient	Concentration
DMEM	Dulbecco's Modified Eagle Medium (GIBCO®)	
	Fetal calf serum (FCS)	10% (v/v)
	HEPES	10 mM
	L-Glutamine	2 mM
	Sodium pyruvate	1 mM
	Penicillin	50 U/ml
	Streptomycin	50 µg/ml
	(Non-essential amino acids)	1% (v/v)
Opti-MEM	Serum reduced medium (GIBCO®)	
LB medium	Yeast extract	0.5% (w/v)
	Tryptone	1% (w/v)
	NaCl	1% (w/v)

4.8.6 Eukaryotic cell lines

Cell line	Distributor
HEK293T	ATCC
H1299	ATCC
MCF7	ATCC
HCT116	ATCC
U2OS	ATCC
HCT116	ATCC
GM03491	ATCC
HT1080	ATCC
Hep3B	Coriell Repositories

4.8.7 Bacterial strains

E. coli	Genotype	Distributor
TOP10	F^- *mcr*A Δ(*mrr-hsd*RMS-*mcr*BC) Φ80*lac*ZΔM15 Δ*lac*X74 *rec*A1 *ara*D139 Δ(*ara-leu*)7697 *gal*U *gal*K *rps*L (Str^R) *end*A1 *nup*G	Invitrogen
BL21	B F^- *dcm omp*T *hsd*S($r_{B-}m_{B-}$) galλ	Invitrogen

4.8.9 cDNA clones

Designation	Reference
DKFZ686O0631	DKFZ
RZPD434k063	DKFZ

4.8.10 Expression vectors

Vector backbone	Tag	Insert
pCDNA3-Flag	1 x Flag	HIPK2
pCMV-Tag3B (mod.)	1 x Myc	SMUDO, SMUDOΔMutL,
pCMV-3Tag1A	3 x Flag	SMUDO, SMUDOΔSMC
pDEST-HA	1 x HA	SMUDO
pEGFP-C1	eGFP	SMUDO, SMUDOΔMutL, SMUDOΔSMC
pGTB9-GW	GAL4 DNA binding domain	SMUDO
pGEX-4T	GST	SMUDOaa1-391, SMUDOaa252-735, SMUDOaa728-1311, SMUDOaa1291-1998
pGLenti (pLentiLox3.7)	-	shSM1, shSM3
pSUPER	-	shSM1, shSM3

4.8.11 Synthetic oligonucleotides

Primers for PCR

Designation	Sequence (5' → 3')
Moc-Klon-1-For	GGATCCATGGCAGCGGCGGACGGC
Moc-Klon-1-KpnI-Rev	AGATCTGGTTGACAATCTTAGTAGGTACCTTC
Moc-Klon-1b-For	GGATCCATGATAAGCAAACCTGCAGATTC
Moc-Klon-1-Rev	TCTAGATCCTGGAAGCTTTTGCATTGCTTC
Moc-Klon-2-For	GGATCCATGCAAAAGCTTCCAGGAACAAG
Moc-Klon-2-Rev	TCTAGAGGCATGAGCTTTAAATTGCTAG
Moc-Klon-3-For	GGATCCATGCCAGCACCGGTACAACATG
Moc-Klon-3-Rev	TCTAGATCACCTATTTTGTCTTGTAGCTTC
Moc-RT-2-For	CAACCAGAACACATACAGTACTTG
Moc-RT-2-Rev	CTCTAGCTGCTTTCTCAAGTATG
Actin-RT-For	CCTCGCCTTTGCCGATCC
Actin-RT-Rev	GGATCTTCATGAGGTAGTCAGTC
SMUDO-429-Rev	CGATCGAAATGGCAAAGGATTTCC
SMUDO-646-For	CGATCGTCAGGATATGTTCGTCCAGTACC
SMUDO-1203-Rev	CGTCTGCATGTCGTCTTGTATTT
SMUDO-4451-For	TGCCTAATCAACCTGTGAAGTTAG
SMUDO-4998-Rev	CCGCGGGGCCTCTTTTAATCTTGCTTCTT
SMUDO-5464-For	CCGCGGCATTGTGAAACAGTATTTGGTATGC
SMUDO-5997-Rev	TCTAGATCACCTATTTTGTCTTGTAGCTTCTC

The listed oligonucleotide primers were purchased from Invitrogen Company.

siRNAs for RNA interference

Designation	Target sequence (5' → 3')
siSMUDO1	CGTATTTTGTCTACTCTTT
siSMUDO2	TGTTGTTCATCCTTTCTTT
siSMUDO3	CAAATACCTAGAACTCGAT
siMutL	AATGATGAAACACAAGGAAAA
siLuci	AACGTACGCGGAATACTTCGA

RNA oligonucleotides were purchased from Qiagen Company.

4.8.12 SMUDO Northern blot probe

Sequence of the SMUDO Northern blot probe in 5'-3' orientation (SMUDO bp 2194-3917):

```
aagcttccaggaacaagccatggagggtcaaagaaactcctggttgagctcaaagttattttacattcttcaagtggaaataa
agagattatttcgcatattagtcaacatggaggaaaatggccttactggtttaaaaaaatggaaaatattcagaagttgggga
attataccttgaaattacaagttgtgttgaatgaaagtaatgcagacacttatgcaggaagaccactaccatctaaagcaatt
aagttttctgttaaagagggtaagccagagaaattttcatttggtcttctggatcttccttttcgtgttggagttccatttaa
tatccctctggagtttcaggatgaatttggtcataccagtcaactagtaactgatattcagccagttcttgaagcaagtggtt
tatctttacattatgaagaaataaccaaaggaccaaattgtgtaattcgaggtgttacagccaagggccctgtaaactcttgt
caaggcaagaattataatctgaaggttactctgcctggcttaaaagaagactcacagattttgaaaattagattactacctgg
tcaccctcgtcgactgaaagtgaaacctgattctgaaattttagttatagaaaatggaacagctttcccatttcaggtggaag
ttttagatgaatcagacaacataacagcacaaccaaaattgattgttcattgtaagttttcaggtgctccaaaccttccagtc
tatgttgtagattgcagtagttctggaaccagtattttaacaggatctgcaattcaagttcagaatattaaaaaagaccagac
gcttaaagcaagaattgaaatacctagttgtaaagatgtggcacctgtggagaagactattaagttgcttcccagtagccatg
ttgcaagactacaaatattcagtgtagaaggacaaaaggcaattcagatcaaacatcaggatgaggttaattggatagcgggt
gatattatgcataatcttatttttcaaatgtatgatgaaggagaaagagaaatcaatataacatcagctttagcagaaaaaat
taaagttaattggactcctgagattaacaaagaacacttgctacagggtctgcttcctgatgtgcaagtaccaacatctgtaa
aagatatgcgctattgccaggtttcattccaagatgatcatgtgtctttggaaagtgcgtttacagtaagaccacttcctgat
gaacctaaacatttaaaatgtgaaatgaaaggaggaaaaacagtacagatgggccaagagcttcaaggagaagtagttataat
aattacagatcagtacggaaatcagattcaagcattttcaccaagttctttatcttctttgtcaattgctggggttggacttg
atagctcaaatttgaaaacaacctttcaggaaaacacacagagtataagtgtaagaggcatcaaatttattccaggtcctcct
ggaaataaggatctttgttttacttggcgtgagttttctgactttattcgagtgcaactaatttctggacctcctgctaaact
tctccttatagactggccagaactaaaggagtccattccagtgattaatggaagagatttacagaaccctattattgttcaac
tttgtgatcagtgggataatccagcaccggtacaacatgttaaaataagtcttacaaaagctag
```

4.8.13 Synthetic Peptides

Designation	Sequence (N→C)
SMUDO 16mer (aa319-335)	NH2-TFSCNKIKDNDKEDGC-COOH
SMUDO 17mer (aa854-871)	NH2-KCNDSLRHSPKVETTDC-COOH

Synthetic peptides were produced at Eurogentic and used for generation of anti-SMUDO antibodies.

4.8.14 Antibodies

Primary antibodies

Designation	Species	Manufacturer
Aktin	Mouse	Sigma
ATM (2C1)	Mouse	Abcam
ATR (AB-2)	Rabbit	Calbiochem
Chk1	Rabbit	Cell Signaling
Chk2	Rabbit	Cell Signaling
Flag (M2)	Mouse	Sigma
GFP	Rabbit	Santa Cruz
GST (Z-5)	Rabbit	Santa Cruz
HA (12CA5)	Mouse	Roche
HA (3F10)	Rat	Roche
HIPK2#88	Rabbit	Eurogentec
Myc (9E10)	Mouse	Santa Cruz
p53 (DO-1)	Mouse	Santa Cruz
p53 (FL-393)	Rabbit	Santa Cruz
PARP1	Mouse	Santa Cruz
pS46 (p53)	Rabbit	Cell Signaling
SMC1	Rabbit	Bethyl Laboratories
SMC2 (BL548)	Rabbit	Laboratories
SMC5 (BL1118)	Rabbit	Laboratories
SmcHD1	Rabbit	Abcam
SMUDO16A	Rabbit	Eurogentec
SMUDO16B	Rabbit	Eurogentec
SMUDO16C	Rabbit	Eurogentec

Designation	Species	Manufacturer
SMUDO16D	Rabbit	Eurogentec
SMUDO17A	Rabbit	Eurogentec
SMUDO17B	Rabbit	Eurogentec
SMUDO17C	Rabbit	Eurogentec
SMUDO17D	Rabbit	Eurogentec
γH2-AX	Rabbit	Cell Signaling

Secondary antibodies, peroxidase-coupled

Designation	Species	Manufacturer
Rat	Goat	Dianova
Mouse	Goat	Dianova
Rabbit	Goat	Dianova

4.8.15 Devices

Type of device	Manufacturer
Incubation shaker „Minitron“	Infors GmbH
CO_2-incubator „CB 210“	Binder
Clean bench „Gelaire BSB 4A“	Flow Laboratories
Ultracentrifuge „RC5C“	Sorvall Instruments (DuPont)
Cooling centrifuge „Varifuge RF“	Heraeus Sepatech
Table centrifuge „Pico 17“	Thermo Fischer Scientific
Table centrifuge „Biofuge® fresco“	Heraeus
Thermomixer „comfort“	Eppendorf
Thermocycler „MyCycler“	Bio-Rad Laboratories
Power supply „PowerPac“	Bio-Rad Laboratories

Type of device	Manufacturer
Mini-PROTEAN® 3 System	Bio-Rad Laboratories
Mini Trans-Blot® System	Bio-Rad Laboratories
Gel dryer „Gel Dryer Model 583“	Bio-Rad Laboratories
pH-Meter „765 Calimatic“	Knick
Microscope	Olympus IX Confocal Micros.
Photometer „Ultrospec 3000 *pro*“	Amersham Biosciences
Pipette „Pipetman® Pipette Kit“	Gilson
Pipette „Matrix CellMate® II“	Thermo Fischer Scientific
Sonifier „Sonifier® S-250A“	Branson
UV Stratalinker 1800	Stratagene
ELISA-Reader „Multiscan MS“	Labsystems
Inverting shaker „UltraRocker“	Bio-Rad Laboratories
Film developer „Curix 60“	AGFA HealthCare
Agarose gel chambers	CTI GmbH
Rotaion mixer „Test Tube Rotator“ (34528)	Buddeberg GmbH
Balance „CP2202S-OCE“	Sartorius
Fine scale balance „TE124S-OCE“	Sartorius
Water bath „Julabo UC“	Julabo
Magnetic stirrer „IKAMAG® RCT“	IKA® Werke
Neubauer chamber	Marienfeld

5 Results

5.1 A new potential interaction partner of HIPK2

With the aim to gain novel insights into HIPK2 functions, a yeast two-hybrid screen in which the N-terminal part of HIPK2 containing the kinase domain was the bait has been performed and revealed a new potential interaction partner of the kinase. In this screen two independent fragments of a so far uncharacterized protein were fished and subsequent a full-length clone encoding for the concerned protein was cloned from cDNA libraries by coworker Ilka Dauth. The encoded protein is 1998 amino acids in size and has been termed SMC-hinge and MutL-homology domain (SMUDO) protein due to prominent structural homology to these factors, which were described in detail in the introduction (3.4, 3.5) (Losada&Hirano, 2005; Polosina&Cupples, 2010b). Overlapping of the two fished SMUDO fragments suggest that this region (118 aa) is part of a domain mediating interaction with HIPK2 (Fig. 3).

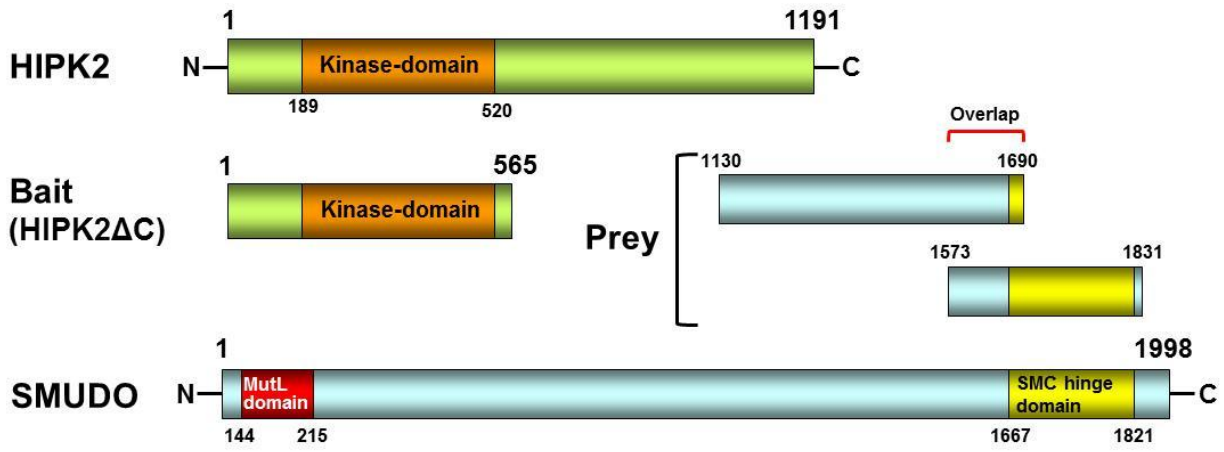

Figure 3: Schematic overview on HIPK2 kinase and SMUDO protein. Fragments of these proteins which were used in the yeast-2-hybrid as bait or fished as prey screen, respectively, are shown. Numbers indicate consecutive amino acids. MutL domain (71 AA) of the SMC-hinge and MutL-homology domain (SMUDO) protein is marked by a red box, the SMC-hinge domain (154 AA) by a yellow one.

Several open source software (ExPASy tools) were used to analyze the protein on the basis of its AA sequence A molecular weight of about 223 kDa was calculated for the SMUDO protein. Two conventional nuclear export signals (NES) and one nuclear localization signal

(NLS) were predicted inside the AA sequence. Beside this, a number of potential phosphorylation target motifs for HIPK2 (TP/SP sites) and also for ATM and ATR (SQ/TQ) were found. Additionally a couple of high potential SUMOylation sites were predicted by analysis software (Fig. 4A).

A

Properties and results of software analysis	
Number of amino acids	1998
Calculated molecular weight	~230 kDa
Potential HIPK2 phosphorylation motifs (TP/SP)	11
Potential ATM/ATR phosphorylation motifs (SQ/TQ)	11
Nuclear export signals	2
Nuclear localization signals	1
Predicted high potential SUMOylation motifs	13

B

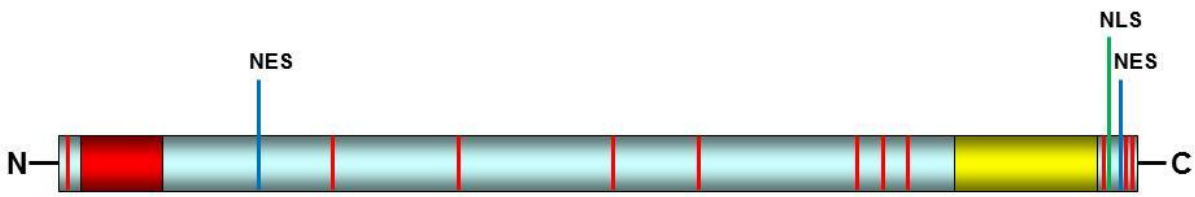

Figure 4: Properties of SMUDO protein and results of software analysis based on its aa sequence. (A) Table listing result of software analysis. Exclusively open source software accessible via the ExPASy tools server was used for analysis and predictions. **(B)** Scheme of SMUDO protein indicating positions of potential HIPK2 phosphorylation sites (red lines), nuclear export signal (green line) and nuclear export signals (blue lines) inside the aa sequence. Red box: MutL domain. Yellow box: SMC-hinge domain.

Hereafter it was decided to investigate the newly found protein more in detail, since its discovery as a potential HIPK2 interaction partner and its structural features, which refer to SMC and MutL protein classes which are involved in homologous recombination, mismatch repair and other DNA damage repair mechanisms, created a promising and attractive starting situation to get novel insight into the functions of HIPK2 and the mechanisms of DNA damage response in general (Losada&Hirano, 2005; Polosina&Cupples, 2010b).

5.2 SMUDO mRNA is ubiquitously expressed in human tissues

To check whether SMUDO is regularly expressed in human cells, reverse transcription polymerase chain reaction (RT-PCR) was applied to detect SMUDO mRNA. For this RNA was prepared out of human cell lines derived from different tissues. SMUDO mRNA expression could be detected in all tested cell lines (Fig. 5A).

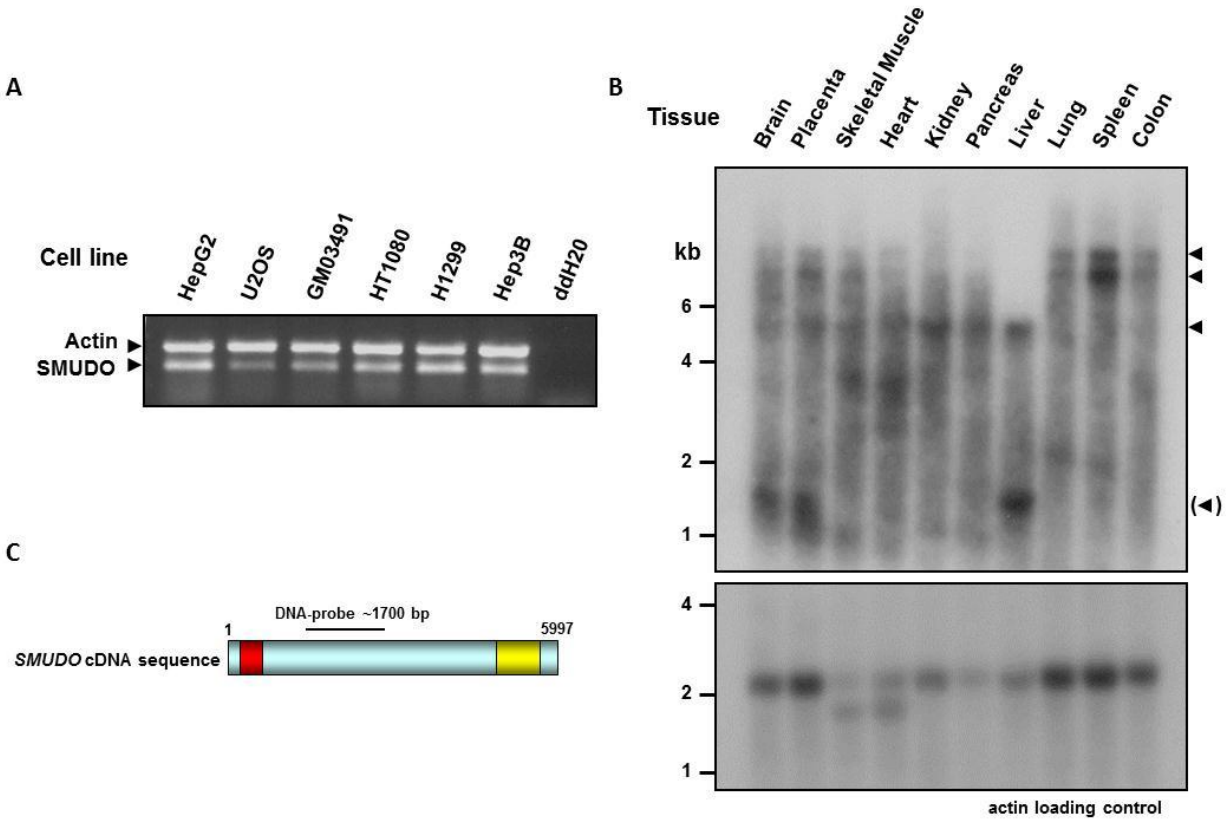

Figure 5: SMUDO mRNA expression. (A) RT-PCR using human cell lines of several different origins. HepG2, Hep3B←liver carcinoma; U2OS←osteosarcoma; GM03419←primary fibroblasts; H1299←lung carcinoma. Actin mRNA was used as loading control. **(B)** Northern blot analysis of several human tissues. At least three different isoforms of SMUDO mRNA are indicated by arrows, one additional and very small potential isoform is indicated by an arrow set in brackets. Actin mRNA was used as loading control. **(C)** Sketch pointing out binding position of the DNA-probe used for northern blot. Experiments performed by Ilka Dauth.

At least three different isoforms of SMUDO mRNA could be detected and in every single examined human tissue sample at the minimum one isoform was found. These results prove a ubiquitous expression of mRNA in diverse human tissues and strongly suggest the presence of SMUDO protein in those tissues.

After Blewitt et al. had reported on the SMUDO mouse paralog SmcHD1, expression of three isoforms of the human protein has been stated on the UniProtKB protein knowledgebase (Blewitt et al, 2008). The new information about the paralog in mice has been connected with preexisting and also with new data from different sources such as large scale screenings to identify the protein isoforms and to match them with the human SMUDO/SMCHD1 (www.uniprot.org; accession: A6NHR9). The longest isoform consists of 2005 amino acids and exhibits seven additional amino acids at the C-terminus compared to the SMUDO construct used in this study. This isoform has been classed as the canonical one. The two smaller isoforms display splice variants with a length of 1917 and 762 amino acids, respectively, and have not been validated on the protein level so far. Overall, the data fit to the results of the Northern blot experiment shown above (Fig. 5B), which revealed three SMUDO mRNA isoforms (excluding the very small potential isoform), where two isoforms are similar in size and one is markedly smaller.

5.3 HIPK2-SMUDO interaction

Since SMUDO was found in a yeast-2-hybrid screen as a possible interaction partner of HIPK2, attempts were made to investigate HIPK2-SMUDO interaction. To examine interaction *in vitro*, GST pull-down experiments were performed. For this purpose an expression vector suitable for *in vitro* translation and coding for a C-terminal fragment of SMUDO protein (SMUDOΔN) was produced. Radioactive labeled SMUDOΔN was generated by *in vitro* translation and a prokaryotic expression vector was used for preparation of GST-tagged HIPK2 fragment (GST-HIPK2ΔC) matching the part of HIPK2 that was used for the initial yeast-2-hybrid screen (see section 5.1).

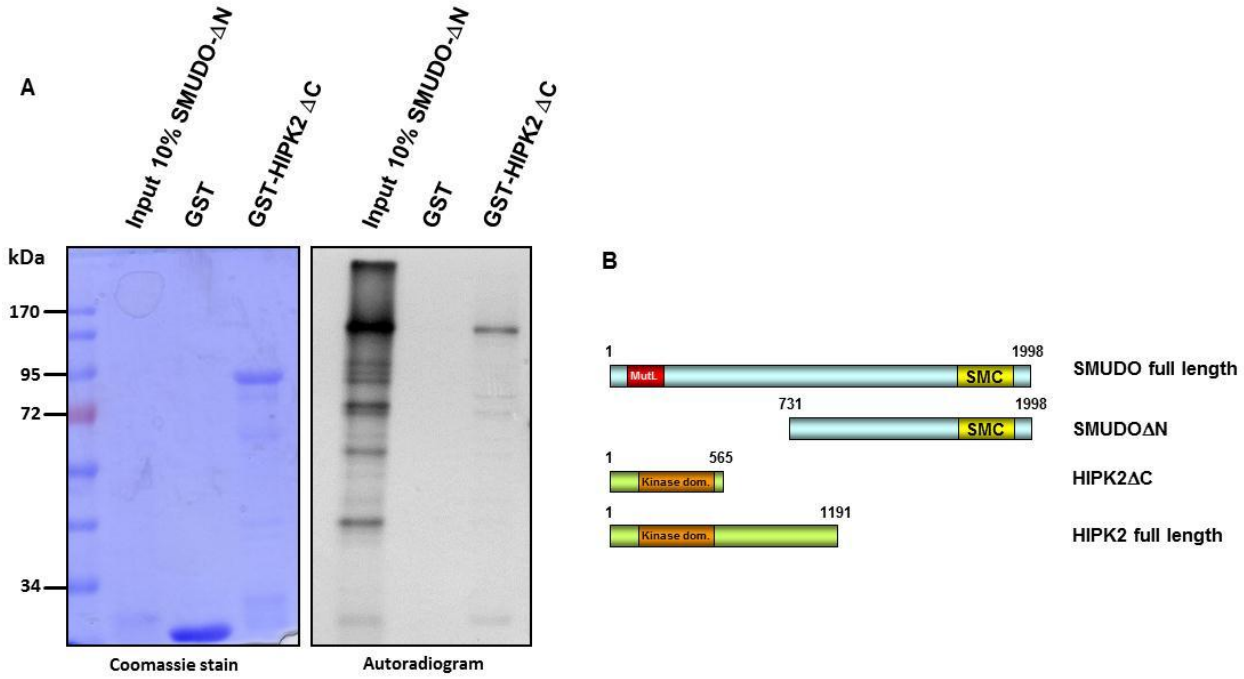

Figure 6: SMUDO-HIPK2 *in vitro* interaction. (A) GST pull-down experiment. Signal in GST-HIPK2ΔC lane of the autoradiogram displays interaction of SMUDOΔN and the used GST-tagged fragment of HIPK2. Coomassie stain was used to check protein loading and GST protein as negative control for the pull-down. Experiment by Ilka Dauth. **(B)** Sketch indicating the parts of HIPK2 and SMUDO used for the pull-down experiment.

GST protein was used as negative control and protein loading was checked by coomassie staining. On the autoradiogram a weak but clear signal was detectable (6A, last lane) confirming interaction between the used fragments of SMUDO and HIPK2 under *in vitro* conditions.

Once *in vitro* interaction of HIPK2 and SMUDO was demonstrated experiments were made to prove *in vivo* interaction of the proteins. Neither co-immunoprecipitation experiments with endogenous or overexpressed proteins, respectively, nor immunofluorescence studies have been successful to do so. More SMUDO interaction studies are described in section 5.9.

5.4 Generation of SMUDO specific antibodies

For further studies on the SMUDO protein, suitable tools for protein detection were needed. No commercial anti-SMUDO antibodies had been available at the time, thus polyclonal antibodies were generated in rabbit.

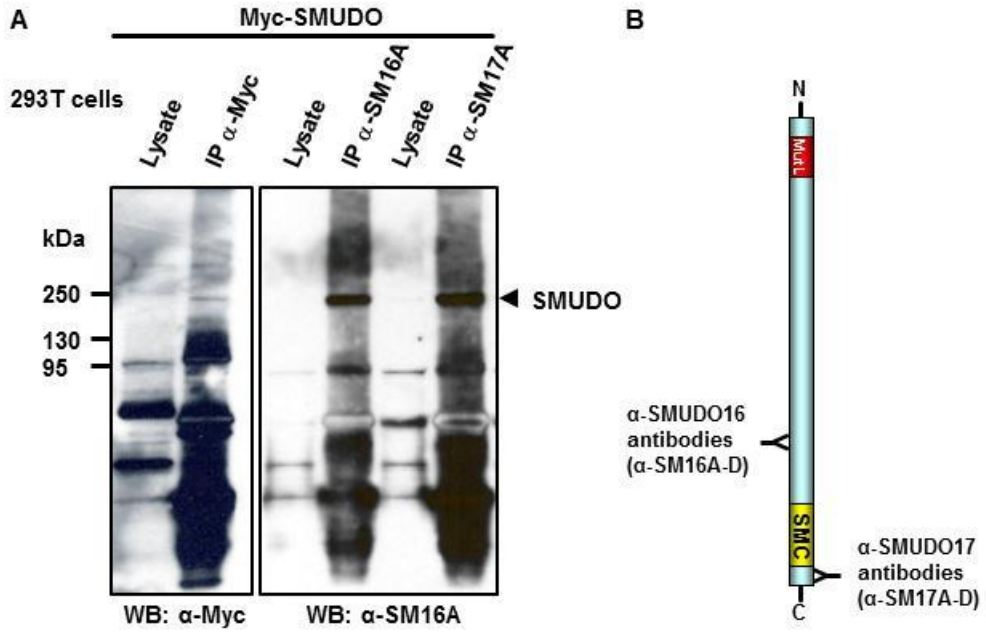

Figure 7: SMUDO specific antibodies detect overexpressed SMUDO protein. (A) Myc-SMUDO was overexpressed in HEK293T cells. Lysates were prepared and SMUDO was precipitated by means indicated antibodies. SMUDO protein was finally detected via Western blot system. Functionality of anti-SMUDO antibodies is exemplarily shown for αSM16A (IP+WB) and αSM17A (IP). About 1 mg lysate was used for each IP. 5% (~50 µg) lysate controls gave only very weak SMUDO signal. **(B)** Schematic view indicating the positions of the epitopes inside the SMUDO aa sequence the antibodies bind to. Four polyclonal antibodies directed against a synthesized 17-mer were named anti-SMUDO17A-D (α-SM17A-D), another four directed against a 16-mer were named anti-SMUDO16 (α-SM16A-D).

For this two different oligopeptides corresponding to segments of the amino acid sequence of SMUDO protein were synthesized and applied to the animals in order to stimulate

generation of antibodies directed against SMUDO. Blood serum was taken from the animals and antibodies were purified for usage. One 16-mer peptide and one 17-mer peptide were used for the procedure, thus four generated antibodies directed against the 16 amino acid peptide were named anti-SMUDO16A-D (α-SM16A-D) and, in the same way, four antibodies directed to the 17 oligopeptide were labeled anti-SMUDO17A-D (α-SM17A-D).

Then, antibodies were tested for biochemical applications. First, capability of the antibodies to precipitate SMUDO overexpressed in mammalian cells and to detect the protein in a Western blot system was checked (Fig. 7A).

Furthermore, the antibodies were tested for immunoprecipitation of endogenous SMUDO protein out of lysates of several mammalian cell lines. Control HEK293T cells were transfected with Myc-SMUDO expression vector.

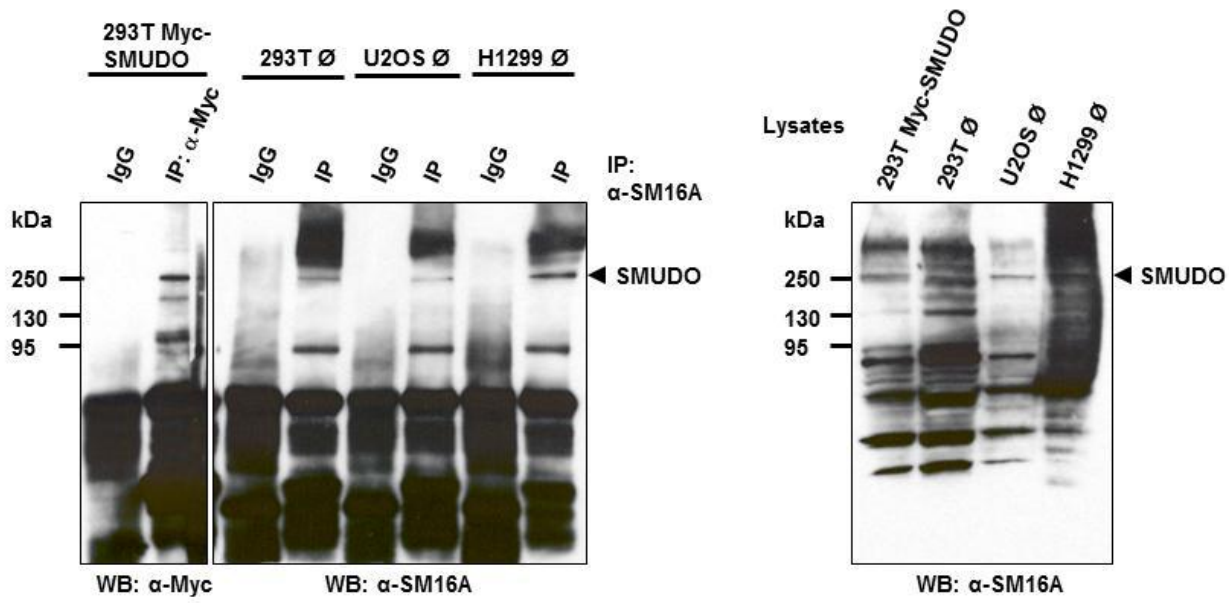

Figure 8: Antibodies detect endogenous SMUDO protein. Each time 1 mg cellular lysate of HEK293T, U2OS or H1299 cells was applied for endogenous IP using anti-SMUDO antibodies. HEK293T cells overexpressing Myc-SMUDO were used as positive control. To check specificity of antibody binding, normal rabbit IgGs were used. 10% (100 µg) lysate controls were applied.

Finding of SMUDO signal in IP lanes as well as in lysate controls (Fig. 8) demonstrated ability of the generated SMUDO-directed antibodies to bind the protein in a specific manner and their use for immunoprecipitation approaches and protein detection via immunoblot. Furthermore it confirmed the data from RNA expression experiments which had indicated SMUDO protein expression in several different cell lines (section 5.2).

5.5 Establishing of a SMUDO knockdown system

One of the aims of this study was to get a hint at SMUDO protein function by suppressing its functions and monitoring a possible phenotype in cultured cell lines. For this purpose and for further experiments the establishment of a working knockdown system was required. Thus, RNA interference (RNAi) was used to downregulate SMUDO protein expression in a post-transcriptional manner. SMUDO cDNA sequence was searched for sequences suitable for siRNA targeting and several siRNAs were synthesized at Qiagen. Different human cell lines were transfected with siRNA and after 24 and 48 hours RNA was prepared out of the cell lysates. Semiquantitative RT-PCR was done and SMUDO mRNA levels were compared with a luciferase siRNA control (Fig. 9A). As loading control actin mRNA was used.

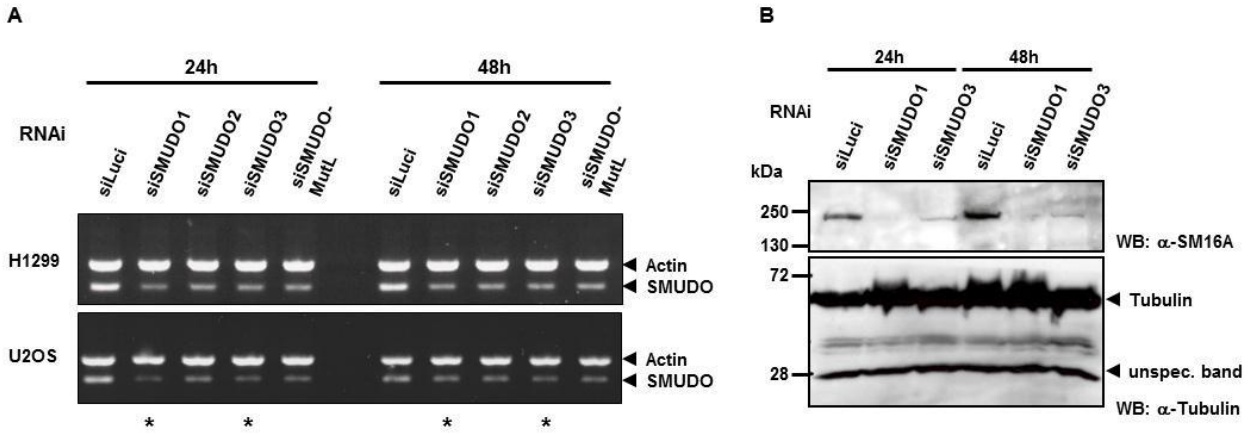

Figure 9: siRNA mediated SMUDO knockdown. (A) RT-PCR after SMUDO siRNA transfection of HEK293T. Several SMUDO siRNAs were tested. siRNA directed against luciferase mRNA was used as knockdown control and actin mRNA as loading control. Asterisks mark most efficient siRNAs. **(B)** Western blot analysis of SMUDO protein level upon siRNA transfection of HEK293T cells. Tubulin (and unspecific band) was used as loading control.

All tested SMUDO siRNA proved effective and two were selected for testing knockdown efficiency at protein level. As shown in Fig. 9, panel B, level of SMUDO protein was significantly decreased upon SMUDO siRNA transfection of HEK293T cells. The decrease of the SMUDO protein level was approximately about 70-90% after 24 hours and still stable after 48 hours. Since knockdown by transient siRNA transfection worked well, the next step was to establish cellular systems exhibiting persistent SMUDO knockdown for long term experiments. SMUDO siRNA sequences were cloned into lentiviral shRNA expression vectors

(pGLenti constructs) which were used for virus production and subsequent transduction of several target cell lines.

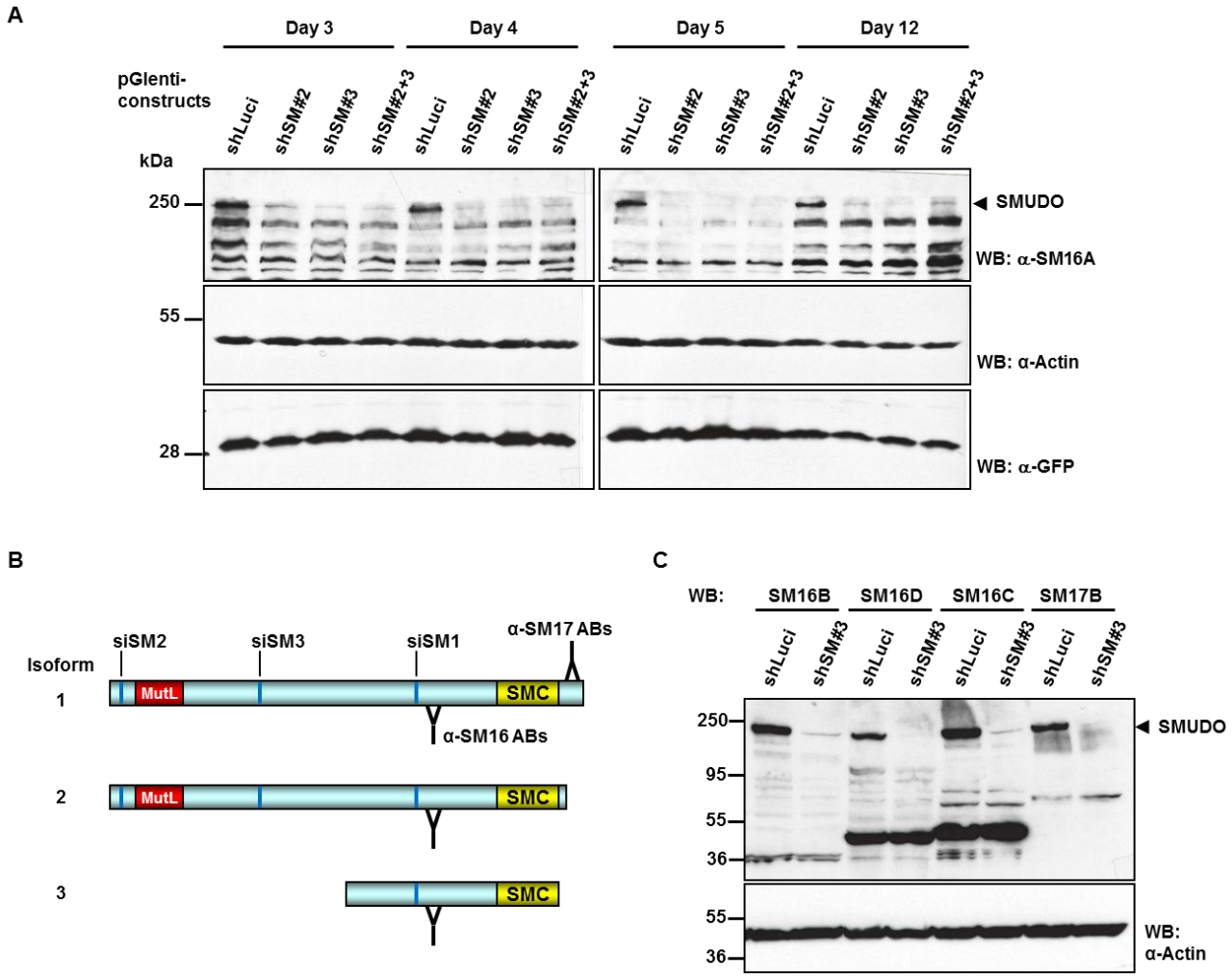

Figure 10. Lentiviral SMUDO knockdown and siRNA target sites. (A) Western blot analysis of HCT116 cell lysates after transduction with lentiviral SMUDO shRNA constructs. A lentiviral construct carrying luciferase shRNA sequence was used as knockdown control. Actin was used as loading control. Lentiviral constructs express GFP, which was used as control of transduction efficiency. **(B)** Sketch indicating the siRNA target sites within mRNA as well as antibody binding sites in the amino acid sequence of the three predicted SMUDO isoforms. siRNAs: siSMUDO1-3 (siSM1-3). **(C)** Background bands of three anti-SMUDO16 antibodies and one anti-SMUDO17 antibody in comparison. Apparently none of these antibodies detects the second or the third potential isoform of SMUDO. Prominent bands either are not affected by SMUDO knockdown or they are not recognized by antibodies which should detect another isoform, respectively. Lysate out of HCT116 cells was used for this Western blot approach.

Cells transduced with described constructs showed an efficient reduction of SMUDO protein level for several weeks without additional selection and also displayed GFP expression suggesting stable integration of shRNA expressing constructs into host cell genomes (Fig.

10A). This system was established in HCT116 cells as well as in U2OS cells and provided a tool for experiments based on SMUDO protein knockdown.

As shown in Figure 10B, the used siRNAs siSMUDO2 and siSMUDO3 target sequences within the mRNAs of SMUDO isoform one and two. The third siRNA, siSMUDO1 targets all three isoforms. Primarily, siSMUDO3 was used in experiments, since its efficiency was best in most cases. In addition, the α-SMUDO17 antibodies bind only to the first protein isoform (canonical full-length isoform), whereas the α-SMUDO16 antibodies recognize each of the three. Consequently, shSMUDO3 should affect the two bigger isoforms which are similar in size and knockdown of the second isoform should be detectable with the batch of α-SMUDO16 antibodies. However, a band that runs beneath the primary SMUDO band and disappears subsequent to SMUDO knockdown could not be detected (Fig. 10A, C). The same was true for smaller bands which could have represented the third isoform.

5.6 SMUDO in the context of the DNA damage response

SMUDO protein shares characteristics with SMC proteins and also with MutL proteins, two protein families that have been shown to be involved in DNA damage repair (Cortes-Ledesma et al, 2007; Polosina&Cupples, 2010a). Additionally, within this study, SMUDO was found to be an interaction partner of HIPK2 *in vitro* and potentially *in vivo*, where HIPK2 plays a role in governing DDR (Calzado et al, 2007; D'Orazi et al, 2002; Dauth et al, 2007; Hofmann et al, 2002). Together these clues prompted the author to investigate a possible role of SMUDO in cells response to DNA damage. The previously established SMUDO knockdown systems were used to look at changes in markers for DDR after genotoxic stress was applied. For this, either UV light or Adriamycin (doxorubicin) were utilized to cause DNA damage and provoke a cellular response.

In view of the demonstrated SMUDO-HIPK2 *in vitro* interaction, p53 phosphorylation at Serine 46 (p53Ser46-P) as indicator for HIPK2 activity as well as HIPK2 levels were the most likely candidates to examine. p53 protein level was used as a general indicator for DNA damage.

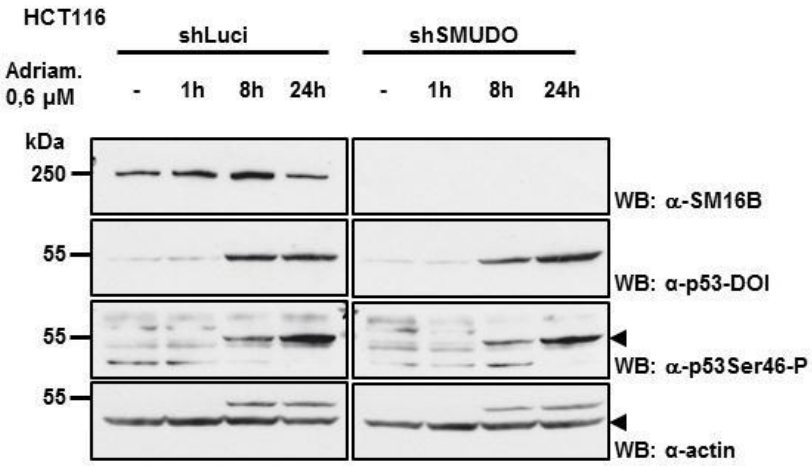

Figure 11: DDR in HCT116 SMUDO knockdown cells upon Adriamycin treatment. Adriamycin was applied to HCT116-shSMUDO cells and control cells. Cells were harvested at indicated time points and lysates were prepared and used for Western blot analysis.

In total, the experiments demonstrated that a knockdown of SMUDO protein has no obvious influence on HIPK2 activity (Fig. 11). Comparison of p53Ser46-P levels of control cells and SMUDO knockdown cells showed no significant or reproducible change. The same

observation was made for HIPK2 levels under steady state conditions as well as upon DNA damage caused by UV (Fig. 12B) or Adriamycin (not shown).

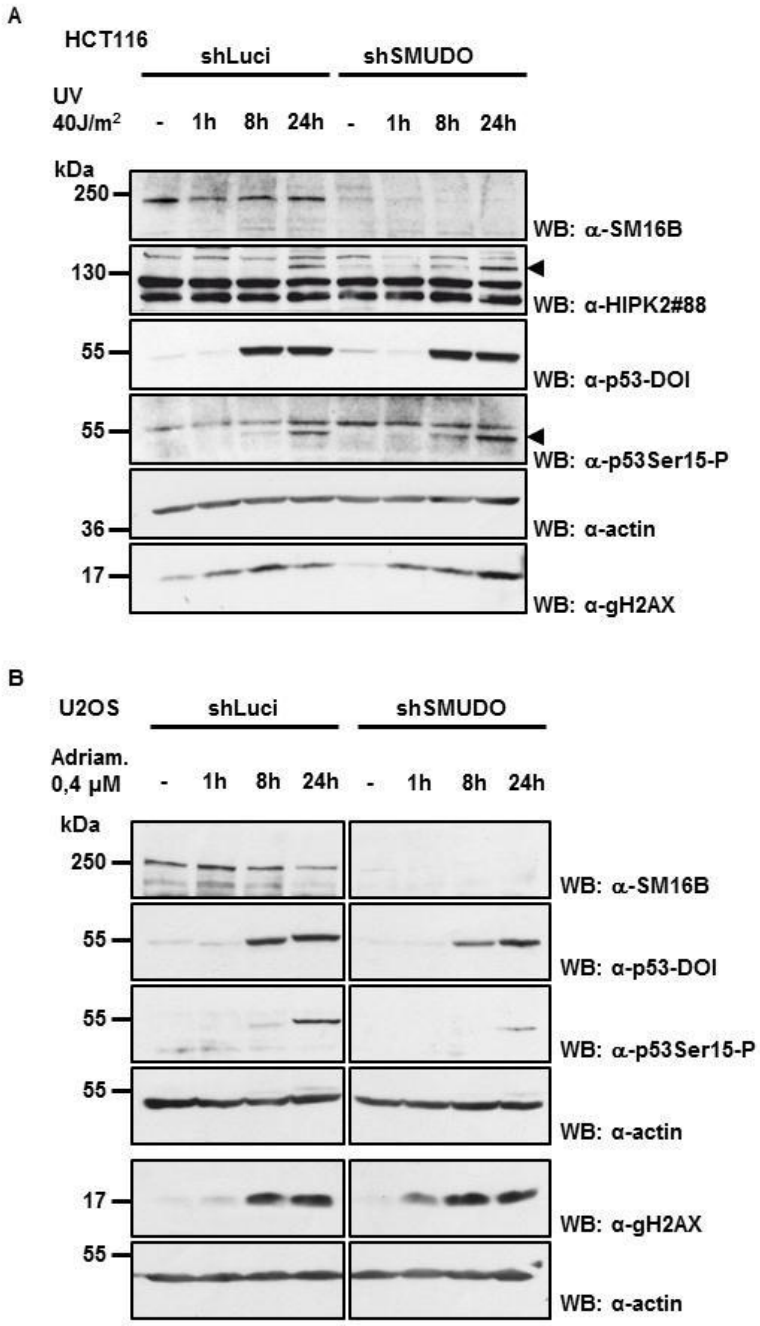

Figure 12: DDR in HCT116 SMUDO knockdown cells. (A). DDR in HCT116 SMUDO knockdown cells upon UV. HCT116-shSMUDO cells and control cells have been irradiated with UV-C at 40J/m². Cells were harvested at indicated time points and lysates were prepared and applied for Western blot analysis. **(B)** DDR in U2OS SMUDO knockdown cells upon Adriamycin treatment. Adriamycin was applied to U2OS-shSMUDO cells and control cells. Cells were harvested at indicated time points and lysates were prepared and used for Western blot analysis.

Since no effect on HIPK2 was found, additional other markers well known for their function in DNA damage response were chosen to check influence of SMUDO knockdown on DDR pathways not directly connected to HIPK2. Histone H2AX phosphorylated at Ser139 (γ-H2AX) displayed formation of DNA repair foci and phosphorylation of p53 at Ser15 reflected activity of Chk1, a central downstream kinase in the DDR.

In some experiments alterations were noticed in p53-Ser15-P, γ-H2AX (Fig. 12A) or even in SMUDO levels (Fig. 11) but those were not reproducible and in other experiments of the same setting no changes or even contrary changes happened (Fig. 12B, 12A). This was true for both HCT116 and U2OS cells. Thus those alterations were considered to be changes raised by as yet unidentified factors like small differences in cell density or passage.

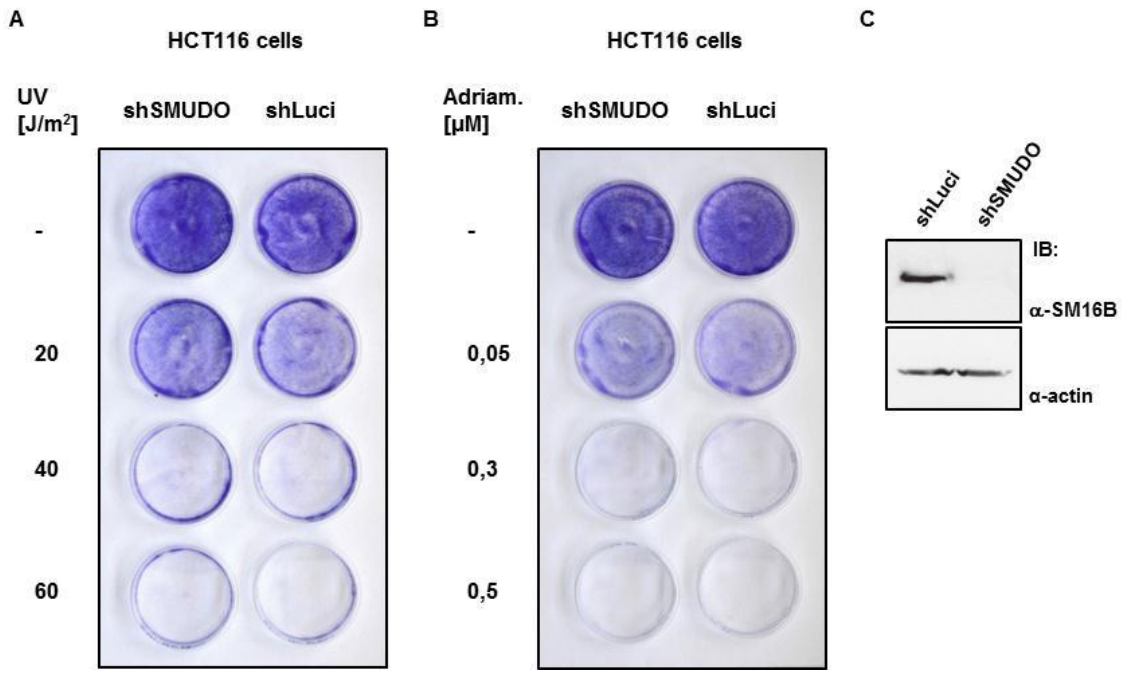

Figure 13: Colony formation of HCT116 SMUDO knockdown cells upon DNA damage. Cells were plated onto 6cm dishes and one day after plating DNA damage has been applied by UV **(A)** or Adriamycin **(B)** at indicated dosages. Five days later living cells were stained with Crystal violet. **(C)** Western blot analysis of cells used in **(A)** and **(B)** demonstrating knockdown of SMUDO protein.

The results indicate that knockdown of SMUDO has no significant effect on DDR pathways examined in these experiments. To see whether a SMUDO knockdown influences overall cell survival for reasons not evident from these experiments, colony formation assays were additionally performed. Assays were performed in HCT116 (Fig.13) as well as in U2OS cells

(not shown) and revealed no alteration in cell survival after SMUDO protein knockdown indicating that the protein is not required for the cellular response to the applied DNA damage.

5.7 Knockdown of SMUDO does not influence the overall activity of TDG

At the same time described experiments for SMUDO characterizations have been carried out, another attempt was made to obtain information suggesting potential SMUDO functions. For this a second yeast-2-hybrid screen, in which an N-terminal part of SMUDO was the bait, has been performed. In the screen three times fusion hybrids of the thymine DNA glycosylase (TDG) came up as a potential interaction partner of SMUDO.

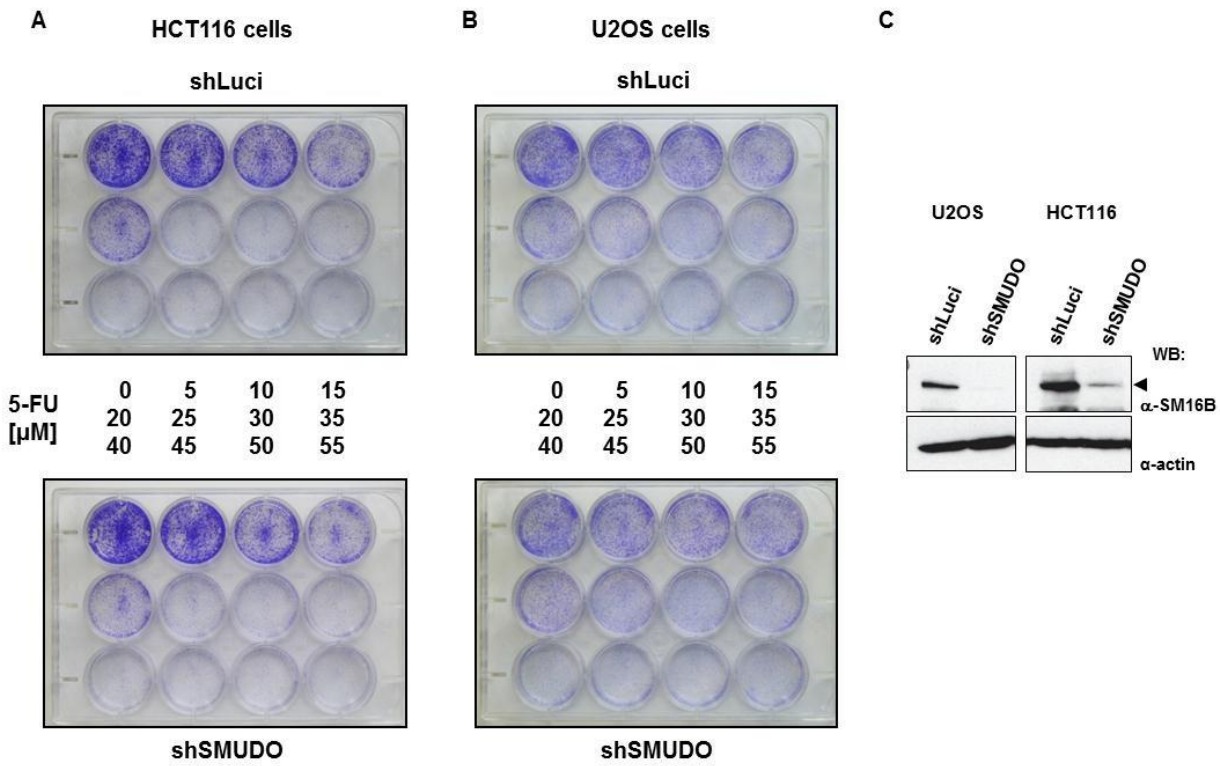

Figure 14: Colony formation of shSMUDO-cells upon 5-FU treatment. HCT116 shSMUDO-cells **(A)** and U2OS shSMUDO-cells **(B)** as well as control cells were seeded on 6-well plates one day prior application of 5-fluorouracil at indicated dosages. After five days cells were stained with crystal violet. **(C)** Western blots showing knockdown of SMUDO protein in cells used for the colony formation experiments.

TDG is a G/T mismatch DNA glycosylase in mammals that removes thymine parts of G/T mismatches by hydrolyzing the bond between the thymine nucleobase and the sugar-phosphate backbone of DNA. It also possesses a lower activity for C/T and T/T mismatches. Furthermore TDG also acts as a uracil DNA glycosylase (UDG), which removes uracil species misincorporated into DNA or generated by deamination, and has been demonstrated to mediate cytotoxicity of 5-fluorouracil (5-FU), a pyrimidine analogue whose metabolites are incorporated into DNA and RNA (Cortazar et al, 2007; Kunz et al, 2009). Mouse and human cells deficient in TDG display a high resistance to 5-FU exposure compared to wild type cells, whereas heterozygous cells show an intermediate sensitivity (Kunz et al, 2009). This context was used in the following colony formation experiment.

After involvement of SMUDO in DDR could not be determined in previous assays using UV or Adriamycin to apply DNA damage, experiments were performed to check possible influence of SMUDO protein on the UDG activity of TDG. As shown in Figure 14, SMUDO knockdown seems to have no effect on TDGs cytotoxicity mediating UDG activity, since cell viability was not altered in SMUDO knockdown cells. Whether one of TDGs other activities is affected is not apparent from this experiment, but it demonstrated that SMUDO knockdown does not influence TDGs overall activity.

5.8 SMUDO fragments are not phosphorylated *in vitro* by HIPK2

With HIPK2 being an S/T directed kinase and demonstrated *in vitro* interaction of SMUDO and HIPK2 fragments (section 5.3), SMUDO might be a phosphorylation target of HIPK2 (Sombroek&Hofmann, 2009). To investigate this possibility, *in vitro* phosphorylation assays have been performed. The SMUDO amino acid sequence contains eleven SP/TP sites which are the phosphorylation motifs of HIPK2. For the experiments, GST-tagged fragments of SMUDO protein as well as a His-HIPK2-Flag construct have been expressed in *E.coli* and purified. HIPK2 and each single SMUDO protein fragment were then used for a phosphorylation reaction which included [γ-^{32}P]-ATP.

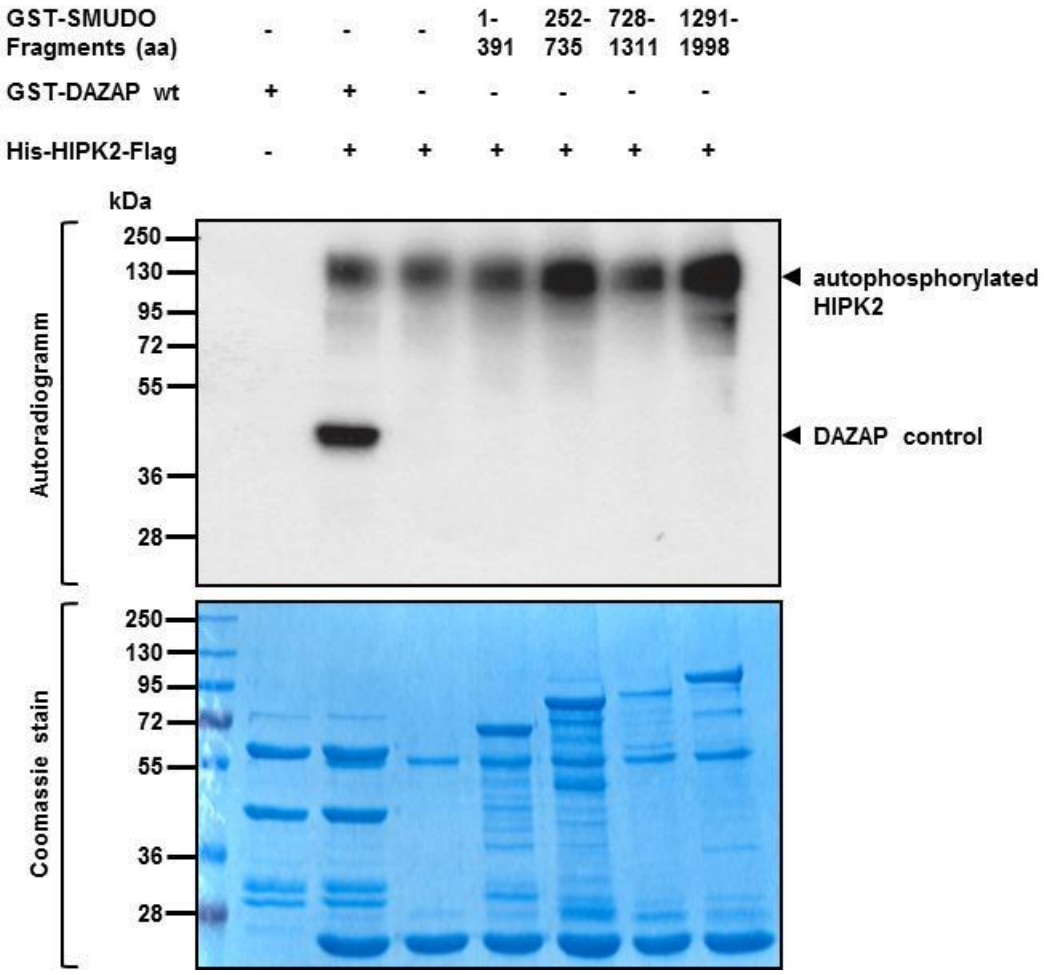

Figure 15: *In vitro* phosphorylation assay. Recombinant GST-tagged SMUDO fragments, DAZAP wt and His-HIPK2-Flag were used for an *in vitro* kinase reaction. Radioactive labeled ATP, [γ-^{32}P]-ATP, was used to mark phosphorylated proteins. GST-DAZAP wt was used as positive control.

On the autoradiogram HIPK2 showed typical autophosphorylation signals at the height of the full-length protein at about 130 kDa (Fig. 15) and the positive control (GST-DAZAP wt) also indicated proper working kinase HIPK2 activity. However, SMUDO fragments displayed no phosphorylation signals, not even the aa1291-1998 fragment, which contains six SP/TP sites. The emerging band below 95 kDa in the last lane of Fig. 15, which could have been mistaken for a signal of phosphorylated SMUDO fragment, was revealed to be a result of HIPK autophosphorylation and a signal shadow caused by SMUDO protein fragment and was also seen in other experiments of the series.

According to the results of this experiment HIPK2 does not phosphorylate any of SMUDOs SP/TP sites under given *in vitro* conditions. Whether there could be phosphorylation under different *in vitro* conditions or *in vivo* will be discussed later.

5.9 The SMC-hinge domain mediates SMUDO autointeraction

Since SMC proteins are known to form dimers via the SMC-hinge domain and SMUDO possessing such a domain, it was a consequent step to check SMUDO's potential to make up homodimers (Losada&Hirano, 2005).

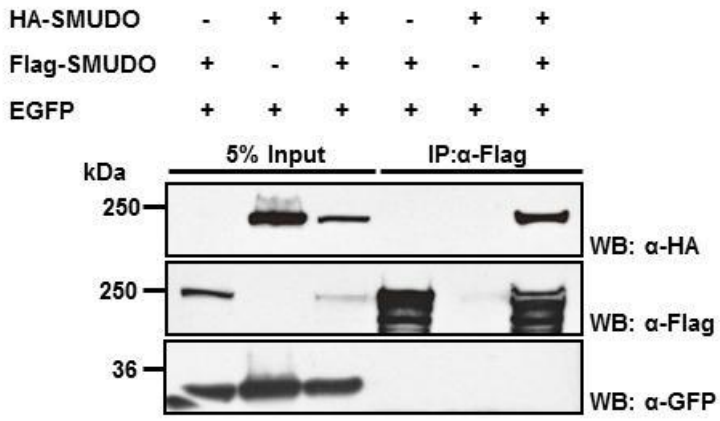

Figure 16: SMUDO auto-interaction. HA-SMUDO and Flag-SMUDO have been overexpressed in HEK293T cells. Co-immunoprecipitation has been performed using anti-Flag antibodies. HA-SMUDO signal was detectable in Flag-SMUDO/HA-SMUDO co-expressing cells (last lane). GFP was used as transfection control.

As shown in Figure 16 (last lane), HA-tagged SMUDO could be precipitated in presence of a Flag-tagged SMUDO construct in an anti-Flag immunoprecipitation. After SMUDO auto-

interaction could be demonstrated using tagged full-length constructs, the next step was to use MutL- and SMC-deletion constructs of SMUDO to verify the role of the SMC hinge domain in mediating binding and to look at a possible contribution of the MutL domain.

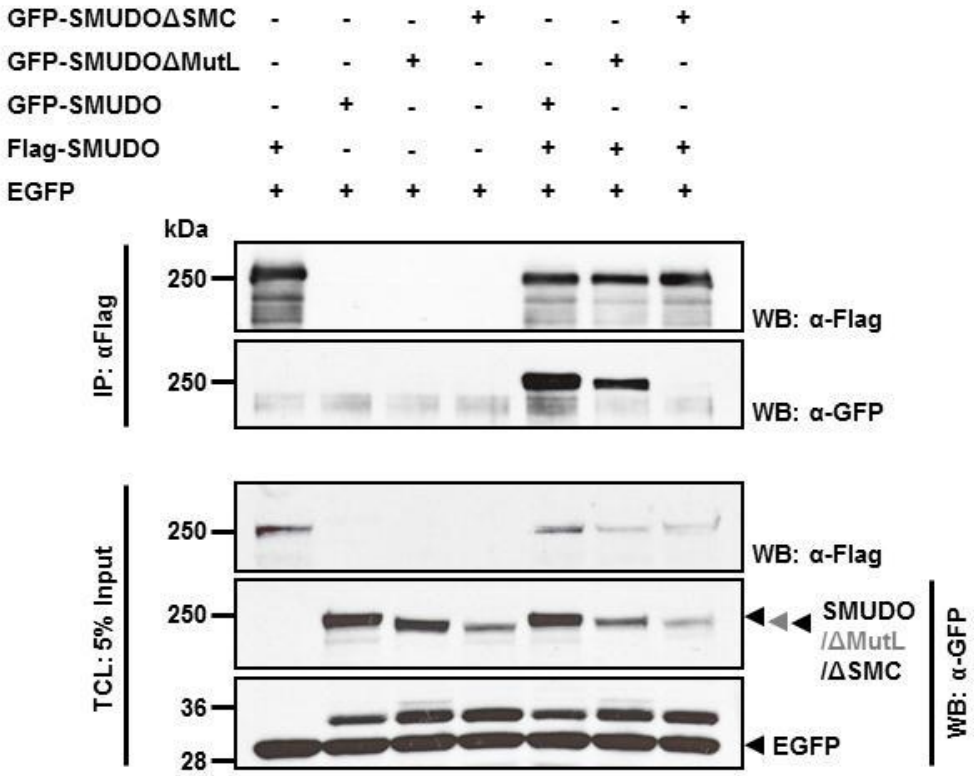

Figure 17: The SMC-hinge domain mediates binding between SMUDO proteins. Experiment resembles experiment shown in Fig. 16 but additionally SMC and MutL deletion constructs of GFP-SMUDO have been included. Missing the SMC hinge disables co-immunoprecipitation of SMUDO (last lane). The band above EGFP is a degradation product of GFP-tagged constructs.

The results of this experiment clearly prove that the SMC-hinge domain of the SMUDO protein is capable and sufficient to mediate dimerization or multimerization, whereas the MutL domain seems to be insufficient to mediate binding (Fig. 17). SMUDO-SMUDO co-immunoprecipitation protocol included a sonication procedure. Without this immunoprecipitation of SMUDO protein was difficult since almost always a smear appeared on Western blot after incubation with anti-SMUDO antibodies indicating association of the protein with chromatin or another insoluble fraction. DNase digestion prior precipitation did not solve the problem and using sonication is the only working method for SMUDO-SMUDO co-immunoprecipitation so far. The interaction mediated by the SMC-hinge domains

of SMUDO seems to be strong enough to withstand sonication or to achieve reassembling afterwards. However, other potential interaction partner of SMUDO might have a less strong affinity to the protein and sonication could terminate interaction permanently. Unfortunately, neither SMUDO interaction with HIPK2 nor with any other tested protein, such as SMC proteins or TDG, could be demonstrated with the exception of SMUDO itself. For that reason alternative SMUDO interaction assays will be discussed. Several SMC proteins, which share related hinge domains with SMUDO, have been tested, but could not be precipitated in interaction assays under diverse conditions. Since dimerization of SMC proteins is restricted to form distinct heterodimers and not miscellaneous dimers with all proteins exhibiting a SMC hinge domain, SMUDO might not be able to form dimers with SMC proteins even though the proteins have a homolog hinge domain in common.

5.10 SMUDO protein is primarily localized in the nucleus

One of the first experimental attempts to characterize SMUDO protein has been overexpression of GFP-tagged constructs in U2OS cells and following microscopic analysis. The most notable observation was that the major part of the protein population seems to accumulate in the nucleus, while a smaller fraction remains in cytoplasm (Fig. 18A). Furthermore, in many cases irregularly shaped dots were observed in the nuclei of transfected cells.

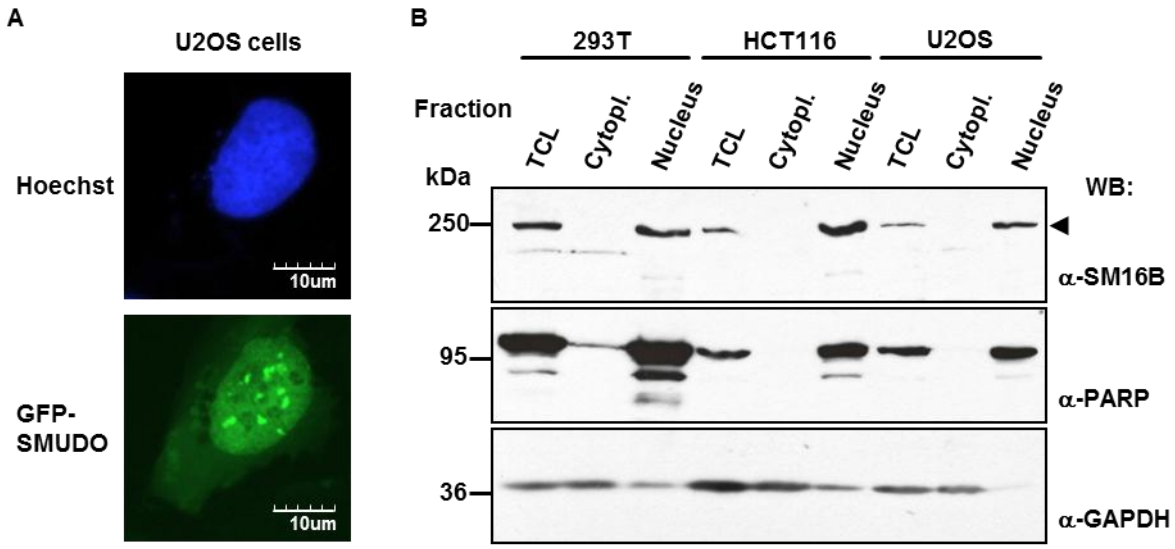

Figure 18: Nuclear localization of SMUDO. (A) GFP-SMUDO has been overexpressed in U2OS cells and showed a primarily nuclear localization and partially formation of dot like structures inside the nucleus. Pictures were taken with a classical fluorescence microscope. **(B)** Cellular compartment fractions have been analyzed by Western blot. PARP was used as indicator the nuclear fraction and GAPDH for the cytosolic fraction.

To validate the indication of a nuclear localization of SMUDO, cellular compartment fractions of non-transfected cells have been prepared for Western blot analysis. As shown in Fig. 18B, the strongest endogenous SMUDO signals appeared in the nuclear fractions. Total cell lysates displayed weaker signals and in cytoplasmic fractions the signal was undetectable. These results confirmed a primarily nuclear localization of SMUDO protein.

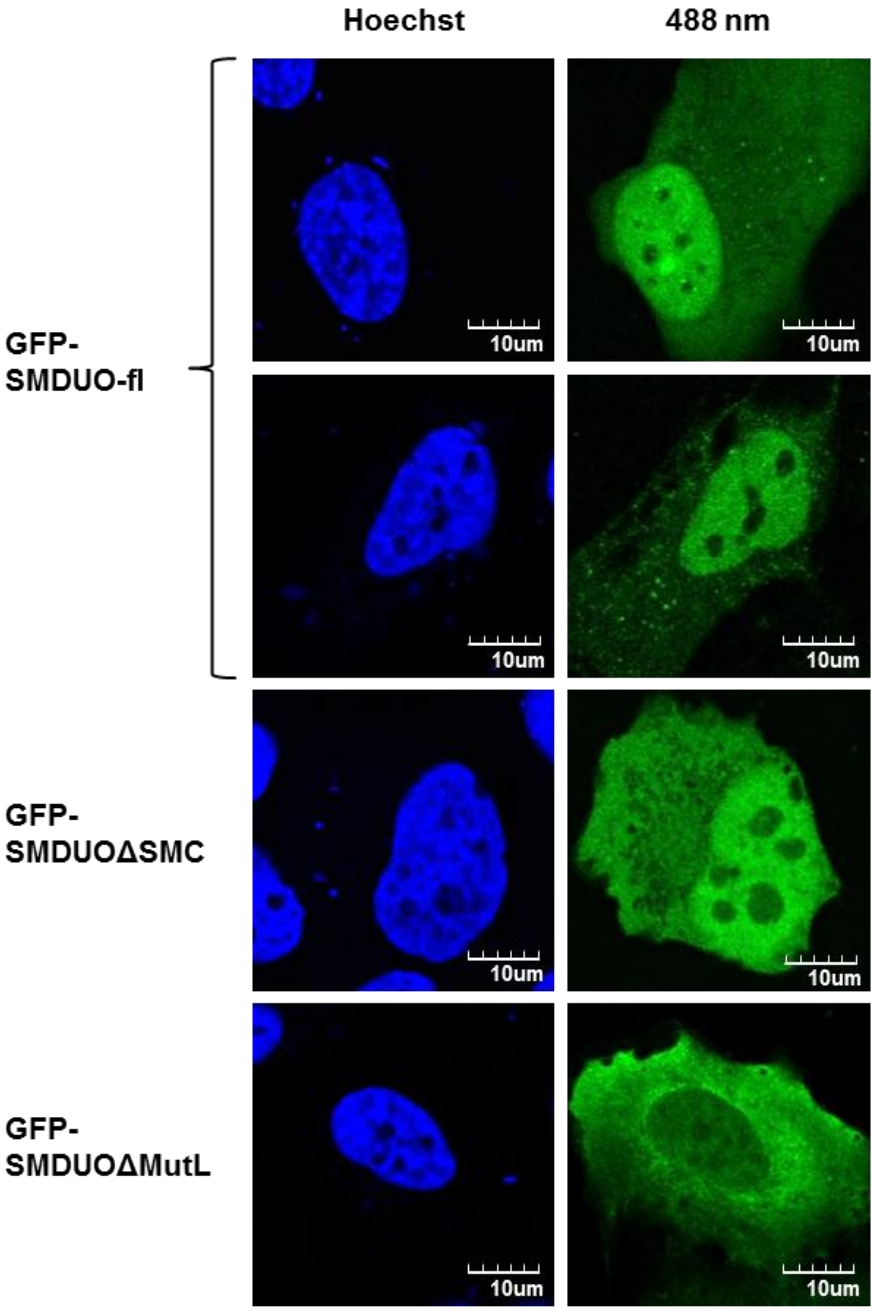

Figure 19: Localization of the different SMUDO constructs. GFP-tagged SMUDO constructs have been overexpressed in U2OS cells and fluorescence pictures have been taken with a confocal microscope (pinhole diameter: 90 nm). Pictures display the predominant phenotypes caused by overexpression of the different constructs. GFP-SMUDO-full-length: As shown before, predominantly nuclear localization and, in some cases, formation of irregularly shaped dots. GFP-SMUDOΔSMC: Similar phenotypes to full-length SMUDO, but no formation of nuclear dots have been observed. GFP-SMUDOΔMutL: Distribution has been reversed and protein was more concentrated in the cytosol. Images have been taken with a confocal microscope.

U2OS cells and other cells lines tested seemed to be affected by a kind of cytotoxic effect of ectopic SMUDO overexpression. A striking number of cells, whose remains showed strong GFP-SMUDO expression, died. In total the transfection efficiency was low which might also at least in part due to the large plasmid size. Since GFP-SMUDO expression could be detected on the Western blot level, it is to assume that low level GFP-SMUDO overexpression is not toxic and not detectable in fluorescence as well, whereas high overexpression makes a detectable signal and somehow mediates cytotoxicity.

Once GFP-tagged SMUDO deletion constructs for the MutL and SMC hinge domain had been cloned, they have been expressed in U2OS cells and resulting phenotypes have been compared with cells expressing full-length GFP-SMUDO. GFP-SMUDOΔSMC expressing cells resembled the described GFP-SMUDO-full-length phenotype, with the difference of not forming dots inside the nucleus (Fig. 19). In case of the GFP-SMUDOΔMutL signal was stronger in the cytosolic compartment rather than in the nucleus (Fig. 19). Neither the single nuclear localization signal (NLS) nor the two nuclear export signals (NES) inside SMUDOs amino acid sequence had been compromised by deletion of the concerned domains. Nevertheless, absence of the MutL domain seems to alter the distribution of overexpressed SMUDO protein and suggest that this domain supports localization within the nucleus. The reason for the lack of nuclear dot formation is highly speculative since the dots could be a result of protein aggregation upon overexpression and MutL and SMC deletion constructs had shown a slightly lower expression level where still only few cells exhibited detectable signal.

Since immunofluorescence experiments on endogenous SMUDO protein turned out to be difficult because of background staining produced by the anti-SMUDO antibodies, experiments on overexpressed tagged SMUDO had to be used for further localization and mobility studies. To gain further information on SMUDO behavior in living cells, GFP-tagged SMUDO was over expressed in U2OS cells which then were used for fluorescence recovery after photobleaching (FRAP) experiments. One set of experiments comprised nuclear point bleaches applied by a laser beam at 488 nm. The other set included bleaching of either the cytosolic compartment or the nucleus. In both cases pictures have been taken over a time course and subsequently analyzed to determine the rate of recovery.

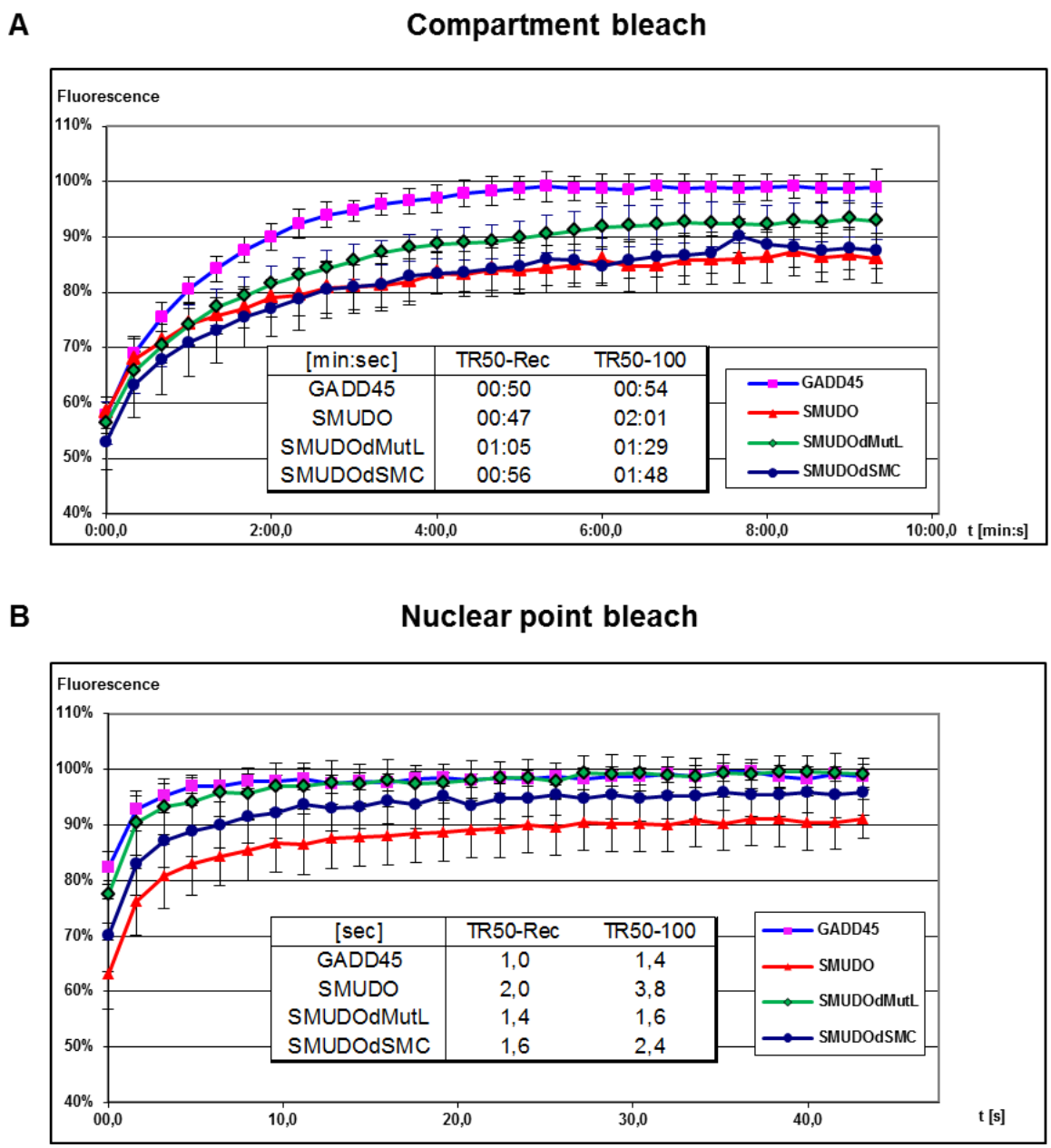

Figure 20: SMUDO FRAP experiments. (A) Compartment bleach experiments. Whole compartments, namely either the nucleus or the cytosolic compartment, have been bleached. Intensity of fluorescence is given in relation to whole cell. **(B)** Nuclear point bleach experiments. Laser emission of 488 nm was used to bleach GFP-SMUDO protein at a limited area inside the nucleus of U2OS cells. Intensity of fluorescence is given in relation to the whole nucleus. Curves start at different fluorescence levels because of fast recovery prior the first frame of documentation. **(A)+(B)** Pictures have been taken at indicated time points. TR50-100 = time for recovery of 50% of fluorescence level before bleaching. TR50-Rec = time for recovery of 50% of fluorescence level at end of measurement. GADD45 protein is known to shuttle between nucleus and cytoplasm and was used as control (Carrier et al, 1994; Kearsey et al, 1995). Experiments and analysis performed with support of Dr. Eva Krieghoff-Henning.

Analysis of the compartment bleach experiments (Fig. 20A) displayed a distinct recovery of GFP-SMUDO fluorescence in the bleached areas, indicating shuttling of the tagged protein between nucleus and cytosol at a rate substantially slower compared to the GADD45 control. This effect might be explained with a conclusion from the nuclear point bleach experiments which also showed a clear recovery for GFP-SMUDO, but in contrast to the GFP-GADD45 control it plateaued clearly beneath 100% fluorescence (Fig. 20B) within the measurement time. Since fluorescence intensity of bleached points was evaluated in relation to the whole nuclei, this result suggests the existence of an immobile fraction of GFP-SMUDO that cannot quickly diffuse into a bleached area. Besides, no significant accumulation of GFP-SMUDO at the site of laser induced DNA damage has been documented over an imaging time of about three hours (not shown).

Additional FRAP experiments including deletion constructs (Fig. 20B) revealed an increase of fluorescence recovery rate for SMC hinge deletion constructs upon nuclear point bleaches. For ΔMutL constructs the increase was even stronger and very close to the rate of the GADD45 control. In compartment FRAP experiments GFP-SMUDOΔSMC displayed a recovery rate similar to the full-length construct, GFP-SMUDOΔMutL in contrast showed an elevated rate at intermediate level between GFP-SMUDO-full-length and GADD45 control (Fig. 20A). Together the IF and FRAP data suggest that the MutL domain may anchor SMUDO at immobile structures within the nucleus, for instance on chromatin, whereas the SMC hinge domain only slightly affects SMUDO nuclear localization and mobility within the nucleus.

6 Discussion

6.1 Discovery of an unknown protein

HIPK2 functions as an important switching element in the cellular DNA damage response. Dependent on the extent of damage the kinase promotes apoptosis or induces growth arrest to prevent proliferation and heredity of corrupted genetic information (D'Orazi et al, 2002; Dauth et al, 2007; Di Stefano et al, 2005). Over the last years many studies concerning HIPK2 were conducted, most of them focusing on HIPK2 regulation and its role in the induction of p53-dependent and p53-independent apoptosis. A number of interaction partners of HIPK2 involved in DNA damage response or other processes have been found and investigated (Calzado et al, 2007; Puca et al, 2010; Rinaldo et al, 2007b; Sombroek&Hofmann, 2009).

Within this thesis SMUDO, a novel HIPK interaction partner, which had been unknown at the beginning of the work, was studied and characterized. Initially SMUDO was found to be a potential binding partner of HIPK2 in a yeast two-hybrid screen. Two times overlapping parts of a not yet described protein came up as prey and based on these fragments a construct of the protein coding sequence could be cloned from cDNA libraries.

Upon production of a full-length construct first software analyses based on the amino acid sequence have been performed and revealed some remarkable features of the protein. One characteristic of the protein is its size of almost two thousand amino acids and a calculated molecular weight of about 230kDa that exceeds even that of the large SMC proteins, such as the human SMC1A, which consists of 1233 amino acids and has a mass of 143 kDa (www.uniprot.org; accession: Q14683).

Most importantly, the amino acid structure of SMUDO compromises two domains related to known protein classes. One domain shows homology with the mentioned SMC protein family, while the second domain seems to be related to the MutL proteins. Together the protein classes gave the reason to name the newly found protein SMC-hinge and MutL-homology domain protein, SMUDO. The members of the SMC protein family are involved in diverse cellular functions, especially their roles in chromosome metabolism and DNA repair mechanisms are prominent and in the focus of research (Cortes-Ledesma et al, 2007; Losada&Hirano, 2005). MutL proteins are known for their participation in DNA mismatch repair as well as in mitotic and meiotic recombination (Polosina&Cupples, 2010a). The extent of homology to the referring protein classes differ between the MutL and the SMC-

hinge domain. While the SMC-hinge domain is relatively highly homologous to SMC proteins, the MutL domain shows only a low homology to the MutL protein family (NCBI, Conserved Domains server). As a consequence it is very unlikely that the SMUDO MutL domain exhibits ATPase activity similar to the corresponding region of MutL proteins, since three of four motifs important for ATP binding which are stated in the literature (Ban&Yang, 1998; Guarne et al, 2001) are not conserved.

Additionally, two classical nuclear export signals, a classical nuclear localization signal, a couple of potential HIPK2 phosphorylation motifs, several ATM/ATM phosphorylation motifs and more than ten high potential SUMOylation sites have been found in the primary protein structure.

It was decided to investigate the unknown SMUDO protein and its potential connection to HIPK2 more in detail, where the circumstances of its discovery and its structural features predetermined the focus of work to be on DNA damage response.

First, SMUDO mRNA expression in several human cell lines of different backgrounds as well as in different human tissues was checked and verified. All tested cell lines showed SMUDO mRNA expression in semi-quantitative RT-PCR and at least one isoforms of SMUDO mRNA could be detected in every single tissue analyzed by Northern blot (chapter 5.2). These results strongly suggest the ubiquitously expression of SMUDO protein in human tissues and functions that are not tissue restricted.

The UniProtKB protein knowledge base lists three potential protein isoforms for the human SMUDO/SMCHD1 protein. The first and longest one is 2005 amino acids in size, the second displays a length of 1917 amino acids and the third consists of 726 amino acids (www.uniprot.org; accession: A6NHR9). Only the longest isoform has been confirmed on protein level so far and has been stated to be the canonical one. Besides of seven additional amino acids at the C-terminus, this isoform resembles the SMUDO-full-length construct which was used within this thesis. In addition, the ratios of the isoforms stated at the UniProtKB database match the mRNA isoforms found in the Northern blot experiment: The biggest and the second biggest isoform are similar in size, while the third isoform is distinctly smaller.

Consisting of 2005 amino acids the first protein isoform has to be translated from an mRNA with a coding region of 6015 base pairs followed by a stop codon. However, the largest mRNA isoform found in the Northern blot experiment is approximately 8-9 kilobases in size

which can be explained by the untranslated regions contained in eukaryotic mRNA, namely the 5' untranslated region (5'-UTR), the 3' untranslated region (3'-UTR) and the poly-A tail.

It has to take into account that only the first isoform has been confirmed at protein level whereas the other two isoform are predictions primarily based on large scale RNA screenings. Whether these isoforms exist on protein level remains unclear, even in the experiments presented in this work no confirmation of their existence was given. Neither comparisons of SMUDO Western blot signals of knockdown cells and control cells nor the usage of different anti-SMUDO antibodies revealed any hints for smaller protein isoforms (5.5). One possible explanation may be protein expression on a very low level undetectable in the used assays. Whether such a small amount of an isoforms could accomplish a biological task by itself is not clear, but cooperation with the attested canonical protein isoform is imaginable. Regulatory mechanisms might be another explanation for the existence of additional SMUDO mRNA isoforms. Several of such RNA silencing mechanisms in plants, animals or other eukaryotes are known, but so far only RNAs significant smaller than the SMUDO isoforms have been shown to be involved (Heard&Colot, 2008; Kanno et al, 2008; Ng et al, 2007).

At the same time first examinations were made, production of tools for further investigations of SMUDO was started. Most important was the production of SMUDO specific antibodies, since antibodies working for Western blot detection were essential perquisite for this study and no commercial antibody had been available at that time. Thus a number of polyclonal antibodies, directed against either a 16 peptide or a 17 peptide of the SMUDO amino acid sequence, were generated in rabbit. The value of the antibodies for protein detection in Western Blot as well as for immunoprecipitation of overexpressed or endogenous SMUDO protein has been validated (section 5.4). Several of these antibodies generated clear SMUDO signals in Western blot analysis which have been confirmed by SMUDO protein knockdown (see below). Usually the same antibodies adequate for Western blot were also suitable for immunoprecipitation of SMUDO. Since the antibodies were generated against peptides this might be a clue for a structure of the areas containing the epitopes that is not in a coiled or a compact form what would likely prevent epitope recognition. Immunofluorescence studies have also been conducted, but the outcomes showed far too much background staining at endogenous protein so far. Another aim this study was the establishment of a SMUDO knockdown system to study the effect of a reduced SMUDO level on cellular phenotypes and on markers of the DNA damage response.

6.2 SMUDO in the DNA damage response

As mentioned before, by the time first characterizations had been made on SMUDO protein it has been decided to focus on its potential involvement in DNA damage response. Several facts pointed towards this field as a promising candidate for a cellular system SMUDO is a component of. First, the protein was found in a yeast two-hybrid screen in which a part of HIPK2 was the bait, therefore being a potential interaction partner of the kinase that is known for its role in mediating and integrating the cells response upon genotoxic stress. Second, the most prominent structural features of the protein refer to two different protein classes which have one thing in common, their participation in DNA repair. A third indication was given by an additional yeast two-hybrid screen. This time a part of SMUDO was used as bait and a protein was fished which is also involved in DNA repair, the thymine-DNA glycosylase (TDG). Together these hints were convincing to concentrate investigations onto DNA damage response.

At first it was checked whether SMUDO protein level is changed upon several kinds of DNA damage, but no alterations have been observed (not shown). It was decided to develop a SMUDO knockdown system (section 5.5) to examine possible effects on the DNA damage response using several protein markers as indicators for activated DNA damage signaling. DNA damage has been applied by several means but primarily by UV radiation or Adriamycin (doxorubicin), because these agents are known to activate HIPK2.

One obvious question was if a decrease in SMUDO protein level would influence HIPK2 level and/or activity, since a basic idea of this thesis is a potential interaction between SMUDO and HIPK2 in the context of the DNA damage response. For this, HIPK2 levels of SMUDO knockdown cells and control cells have been compared. As an indicator for HIPK2 activity p53 protein phosphorylated at serine residue 46 (p53Ser46-P) has been used.

The corresponding experiments revealed no significant alterations in HIPK2 levels under steady state conditions as well as upon applied DNA damage. A similar observation was made for p53Ser46-P levels indicating an unchanged HIPK2 activity in case of SMUDO knockdown (Fig. 11, 12A).

Additional markers were analyzed to investigate the effect of SMUDO knockdown on DNA damage response independent of HIPK2. Phosphorylation of Histone H2AX at Ser139 (γ-H2AX) suggested formation of DNA repair foci and p53 phosphorylated at Ser15 reflected activity of Chk1, a central downstream kinase in the DNA damage response. Like in the case

of HIPK2 no noticeable and reproducible changes could be observed in SMUDO knockdown cells compared to control cells (Fig. 11, 12).

Some experiments showed variations in γ-H2AX, p32-Ser15-P (Fig. 12A) or even in SMUDO levels (Fig. 11), but overall they were proven to be not reproducible. Accordingly, these alterations were considered to be results of factors like small differences in the density of a cell population or in its passage counts and not to be provoked by the SMUDO knockdown.

Upon obtaining no hints for an influence of SMUDO knockdown on the examined DNA damage response factors, colony formation assays were performed to check the overall cell survival since possible effects on the cellular response upon genotoxic stress may not have been detectable in the former experiments. Compared to control cells the SMUDO knockdown cells displayed no decrease in cell growth at any extent of applied DNA damage (Fig. 13).

A further attempt to gain information that could give a lead to possible SMUDO functions in the DNA damage response based on the outcome of a yeast two-hybrid screen already mentioned in which a part of SMUDO was the bait. In this screen the thymine-DNA glycosylase (TDG) was found to be a potential interaction partner of SMUDO. This enzyme possesses a G/T mismatch DNA glycosylase activity, with an additional low affinity for C/T and T/T mismatches, as well as a uracil DNA glycosylase (UDG) activity which removes uracil species misincorporated into DNA or generated by deamination. The uracil DNA glycosylase activity has been shown to mediate cytotoxicity of the chemotherapeutic 5-fluorouracil (5-FU), metabolites of the pyrimidine analogue are incorporated into DNA and RNA where they cause genotoxic stress. Human as well as mouse cells deficient in TDG exhibit a strongly increased resistance to 5-FU exposure and heterozygous cells display intermediate sensitivity to the drug.

According to this an influence of SMUDO knockdown on TDG activity and the cytotoxic effect of 5-FU has been tested. In case of SMUDO being involved in the uracil DNA glycosylase function of TDG, a change in the impact of 5-FU exposure on SMUDO knockdown cells compared to control cells should have been the consequence. Colony formation assays have been performed and indicated that a knockdown of SMUDO has no effect on the uracil DNA activity of TDG. No changes in cell viability could be observed (14).

Furthermore, no GFP-SMUDO accumulation at the site of UV-laser applied DNA damage has been observed within a period of three hours, when tested in context of FRAP experiments (not shown). Taken together, no indications for an effect of a SMUDO knockdown on the

examined DNA damage pathways have been found. The crucial point to mainly use these agents was their known activating effect on HIPK2, the kinase that had appeared to interact *in vitro* with SMUDO and possibly cooperates with the protein *in vivo*. Since the efficiency of the SMUDO knockdown proved to be very high it seems to be unlikely that the performed experiments could not demonstrate SMUDO involvement in DNA damage response because of too much protein remaining in the cells.

Participation of SMUDO in other pathways of the DNA damage response triggered by different kinds of genotoxic stress remains to be unclear and is point to be checked in further studies about SMUDO. Many types of DNA damage and the responsible repair pathways have been covered in the performed experiments. In most of the referring experiments DNA damage has been applied by UV or Adriamycin (doxorubicin), but also by 5-fluorouracil, agents causing the formation of bulky adducts, replication fork stalling, single-strand damage, double strand breaks and U/G mismatches.

Several types of base mismatches, G/T, T/T or C/T mismatches for instance, remain to be investigated in respect of TDG and the DNA mismatch repair in general. Direct lesion reversal of alkylated bases such as 6-O-methylguanine or the repair of DNA lesions like 8-oxoguanine caused by reactive oxygen species could also be investigated. Hydrolytic chemicals (for G/T mismatches), alkalyting agents such as ethylnitrosurea (for 6-O-methylguanine) or oxidative chemicals (for 8-oxoguanine) could be used to generate the corresponding kind of DNA damage for colony formation assays similar to these shown in this work which were used to examine a potential effect of a strongly reduction in SMUDO level.

Despite the found connection to HIPK2, SMUDO could be part of DNA damage pathways the kinase is not involved in or its involvement is not known yet. Moreover, cooperation is also possible in HIPK2 pathways apart from DNA damage repair and will be discussed in the last chapter.

6.3 SMUDO interactions and alternative functions

Besides fundamentally characterizing SMUDO, in the course of this thesis potential functions of the protein were supposed to be identified. In part this was done by protein interaction assays. Given that the SMUDO project started with a yeast two-hybrid screen suggesting an interaction with HIPK2, a part of the experiments were dedicated to pursue this link. In the first instance *in vitro* interaction of the two proteins was to be verified. Next, *in vivo* interaction was to be investigated.

The investigations started with pulldown experiments which confirmed the *in vitro* interaction of SMUDO and HIPK2 fragments indicated by the initial yeast two-hybrid screen. A GST-tagged HIPK2 construct matching the same part of the kinase that had been used for yeast two-hybrid screen showed binding to a radioactive labeled SMUDOΔN construct (5.3, Fig.6). Subsequent studies addressing *in vivo* interaction of the proteins were started. Immunoprecipitation experiments with overexpressed as well as with endogenous HIPK2 and SMUDO protein were performed under various conditions, but could not demonstrate HIPK2-SMUDO binding. Mammalian two-hybrid system might be used to proceed with HIPK2-SMUDO interaction studies, since protein binding in mammalian cells better mimics *in vivo* protein interaction and the system might even allow usage of full-length constructs.

Furthermore, *in vitro* assays concerning phosphorylation of SMUDO by HIPK2 could not confirm a functional cooperation of the proteins. This might be due to the usage of SMUDO fragments recombinantly expressed in bacteria without eukaryotic post-translational modifications. GST-protein expression in yeast could improve experimental conditions by allowing those modifications.

Other proteins than HIPK2 were also candidates for SMUDO interaction studies. Especially SMUDO itself was predestinated for autointeraction testing due to the fact that dimerization via SMC-hinge domains is well known from the SMC protein family. Two differently tagged SMUDO constructs were used for co-immunoprecipitation assays which showed that SMUDO autointeraction occurs indeed (section 5.9, Fig. 16). In further experiments the role of SMUDO's SMC hinge domain in mediating the interaction has been examined, because binding between SMUDO proteins could have be achieved by the remaining parts of its structure, like the MutL domain.

GFP-SMUDO constructs either lacking the SMC hinge domain or the MutL domain have been used together with a Flag-tagged full-length construct for regarding tests. In the absence of

the MutL domain the concerning construct could still be co-precipitated, whereas the construct lacking the SMC hinge domain was lost (5.9, Fig. 17).

These results clearly demonstrated that the SMC-hinge domain contained in the SMUDO amino acid structure is capable and essential for mediating binding between SMUDO proteins under the given experimental conditions. Concurrent the MutL domain has been proved to be insufficient to mediate binding. In view of the SMC protein family, whose members form heterodimers, it is likely that SMUDO proteins act similarly and also make up dimers *in vivo*. In this case they would be homodimers. However, other ways for linking SMUDO proteins different from the SMC protein mechanism are not very likely but still possible (Fig. 21). One or more unknown factors could be required for mediating dimerization or even multimerization of SMUDO. And, of course, multimerization could also occur without an additional mediator. To test this pulldown assays could be performed using recombinant expressed SMUDO fragments containing the SMC-hinge domain. One fragment would be tagged by GST, a second one by a different tag what allows detection and differentiation after pulldown.

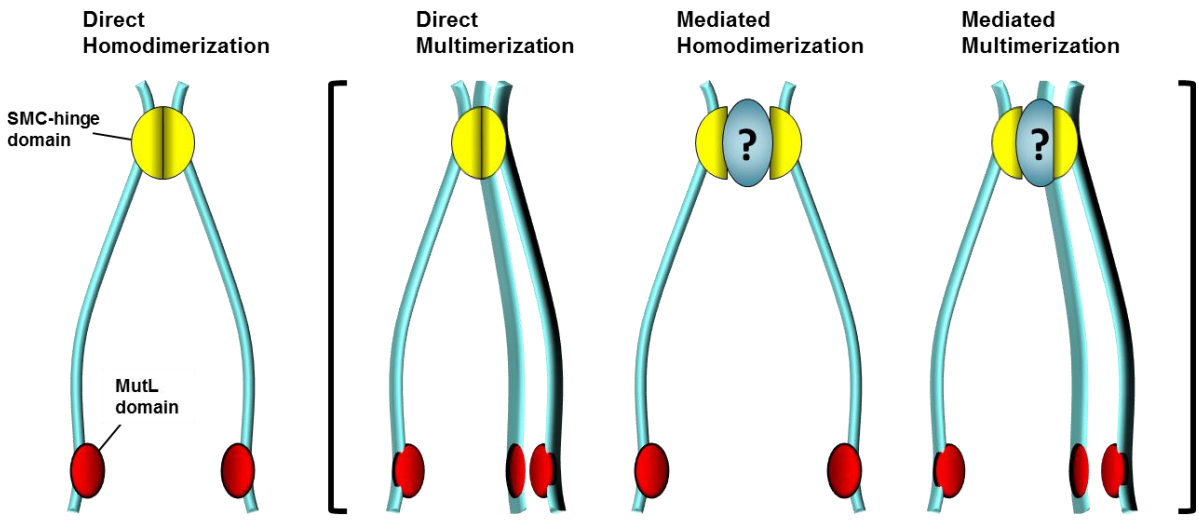

Figure 21: Models for SMUDO-SMUDO interaction. Binding could be directly achieved by the SMC hinge domain or mediated by an unknown factor. Formation of dimers as well as of complexes consisting of more than two SMUDO proteins is conceivable. In consideration of mechanisms known from SMC proteins, direct formation of dimers is the most likely option. The spatial structural of the protein is unknown and areas others than the SMC-hinge and MutL domain have been illustrated as curved arms due to impressions from SMC complexes (Losada&Hirano, 2005).

In addition to HIPK2 and SMUDO a couple of other proteins have been tested in co-immunoprecipitation assays for interaction with SMUDO. The thymine DNA glycosylase (TDG) and several SMC proteins had been other obvious candidates, since they were found in yeast two-hybrid screen as a potential SMUDO interaction partner or share a related hinge domain, respectively. Similar to the previously described HIPK2-SMUDO interaction experiments none of these proteins was found to bind to SMUDO.

The tested proteins may not interact with SMUDO, but another reason could be inappropriate experimental protocols. Early on, SMUDO immunoprecipitation assays had proven to be difficult. When lysis buffer containing mild detergents that spare the nuclear membrane were used, the yield of SMUDO protein was very low. Later immunofluorescence studies showed a primarily nuclear localization of the protein, thus only a small cytosolic fraction was extracted from cellular lysates. Buffers breaking down nuclear membranes provided increased yield, but smear disturbed SMUDO signal on Western blot after incubation with anti-SMUDO antibodies, suggesting the association of the protein with an insoluble fraction like chromatin. Efforts to solve this problem by DNase digestion prior precipitation or usage of alternative buffers have not been successful. So far, sonication of cellular lysates is the only working method found to make at least SMUDO-SMUDO co-immunoprecipitation possible.

It has been demonstrated that the SMC-hinge domain mediates interaction between SMUDO proteins. Their affinity seems to be strong enough not to be dissolved by sonication or to accomplish reassembling after dissolution. The other tested proteins might have a lower affinity to SMUDO in a way that a potential interaction is permanently destroyed by the sonication procedure. For further interaction studies intermolecular crosslinking could be integrated into precipitation protocols to stabilize fragile bonds between SMUDO and other proteins before sonication is applied. Crosslinking SMUDO to binding partners and subsequent immunoprecipitation followed by SDS-PAGE and Western blot analysis could be used to detect suspected proteins. Additionally, it would be possible to cut bands of proteins crosslinked and co-precipitated with SMUDO out of the blotting membrane for analysis by mass spectrometry. This method would allow identifying new proteins which interact with SMUDO in a transient or stable way.

Another strategy to investigate SMUDO protein and its interactions was to use fluorescence as well as immunofluorescence microscopy techniques. One goal was to overexpress tagged SMUDO protein together with a potential binding partner, HIPK2 for instance, and to

analyze intracellular localization of the proteins particularly with regard to co-localization. Further experiments should have included immunostaining of endogenous proteins to validate possible findings. Unfortunately two big problems emerged in the context of these studies.

First, a part of the cells in which SMUDO was overexpressed to high levels suffered a sort of cytotoxic effect, especially when HIPK2 was co-expressed. Together with very low transfection efficiency this was the reason why co-expression experiments and subsequent microscopic analysis could not be performed. Since SMUDO overexpression was frequently applied in other experiments and signal of ectopic SMUDO could be detected in Western blot, low level overexpression is apparently not toxic but also not detectable in fluorescence as well.

Second, the generated anti-SMUDO antibodies have been tested for immunofluorescence applications, but proved to produce a high amount of cellular background signal which prevented their usage in experiments involving the staining of endogenous SMUDO protein. Thus, microscopy examinations were restricted to tagged SMUDO overexpressed in the few cells that had not died by the treatment.

When GFP-SMUDO overexpressing cells were observed under a microscope, the dominant phenotypes suggested a predominantly nuclear localization of the protein (chapter 5.10, Fig. 18), thereby strengthening the indications from co-immunoprecipitation assays. To confirm a primarily nuclear localization of SMUDO cellular fractions were prepared and analyzed by Western blot. The results demonstrated that the biggest fraction of endogenous SMUDO is indeed localized in nucleus of a cell, while only a minor fraction remains inside the cytosolic compartment (5.10, Fig. 19).

Most observed cells expressing tagged SMUDO full-length (GFP-SMUDO-fl) construct displayed a pan-nuclear staining often manifold stronger than the signal from the cytosol. Moreover, many of these cells showed formation of irregular shaped dots inside the nucleus (section 5.10, Fig. 18). This could be due to regular localization of SMUDO protein and might be cell cycle dependent or due to an artificial protein aggregation caused by overexpression.

Deletion constructs lacking either the SMC-hinge domain (GFP-SMUDOΔSMC) or the MutL domain (GFP-SMUDOΔMutL) have been cloned and expressed in cells to compare the resulting phenotypes with cells expressing the full-length construct. In case of overexpressing GFP-SMUDOΔSMC the phenotypes was similar to that of full-length SMUDO featuring a higher protein concentration in the nucleus than in the cytosol (Fig. 19).

Nevertheless, one remarkable difference was observed, since dot formation did not occur in even one examined cell, which could imply that the SMC-hinge domain might be responsible for SMUDO recruitment to the dots or protein aggregation.

When the GFP-SMUDOΔMutL construct was overexpressed, the distribution of SMUDO protein was changed. Fluorescence signal was now stronger in the cytosolic compartment and distinctly weaker in the nucleus (Fig. 19). By deleting the MutL or the SMC-hinge domain, neither the predicted nuclear export signals nor the nuclear localization signal had been destroyed, suggesting that the domains themselves cause the described phenotypes.

Fluorescence recovery after photobleaching (FRAP) techniques were used to gather more information about SMUDO localization and mobility. In one series of experiments either the nucleus or the cytosolic compartment of cells expressing different GFP-SMUDO constructs was bleached by a laser beam to measure the rate of fluorescence over time.

Upon bleaching the concerned compartments, recovery of GFP-SMUDO fluorescence suggested that the protein shuttles between cytosol and nucleus (section 5.10, Fig. 20A). The rate of recovery was substantially lower compared to the used control. In a second experimental series, in which a restricted nuclear area had been bleached (nuclear point bleach), GFP-SMUDO-fl signal recovered, but in contrast to the control it reached a plateau clear beneath 100% fluorescence (Fig. 20B). Taken together these results give a hint to the existence of an immobile GFP-SMUDO fraction which is not able to diffuse quickly into bleached areas.

GFP-SMUDOΔSMC displayed a recovery rate similar to that of GFP-SMUDO-fl upon compartment bleach, whereas the MutL deletion construct displayed a distinctly elevated recovery rate (Fig. 20A). In nuclear point bleach FRAP experiments GFP-SMUDOΔSMC showed a higher recovery rate compared to full-length GFP-SMUDO. GFP-SMUDOΔMutL displayed an even faster recovery that was almost as fast as the used control (Fig. 20B).

Considering all data from immunofluorescence microscopy studies and FRAP experiments, the MutL domain might be responsible for the nuclear localization of SMUDO and act as an anchor to the immobile phase of the nucleus such as chromatin. The SMC-hinge domain in contrast seems to influence only SMUDO mobility and localization within the nucleus to some extent by supporting the binding to the immobile phase (Fig. 22).

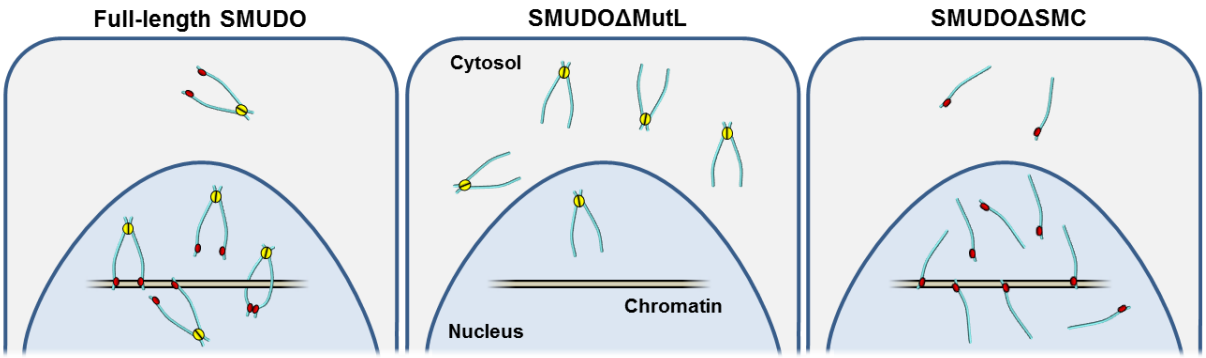

Figure 22: Impact of SMUDO domains on protein localization. SMUDO is primarily nuclear localized and likely binds to chromatin in an unknown way. The MutL domain seems to be required for SMUDO localization into the nucleus. In its absence most protein is present in the cytosolic compartment and its mobility within the nucleus is remarkably increased. The SMC-hinge domain supports binding to the immobile nuclear fraction.

The possibility of SMUDO binding to DNA or chromatin should be investigated in further experiments, since hinge domains of dimerized SMC proteins are known to directly interact with chromatin (Chiu et al, 2004). In addition, the region of MutL protein related to the SMUDO MutL domain also binds DNA, where it has to take into account that the homology is rather low (Polosina&Cupples, 2010b). The idea of chromatin binding is also supported by data from a study on SmcHD1, a SMUDO mouse ortholog, in which the protein is shown to localize to inactivated X chromosomes (Blewitt et al, 2008). This work also shows that SmcHD1 is important for the maintenance of X inactivation and the hypermethylation of CpG islands in the course of X inactivation in female mice, where some of the hypermethylated genes are upregulated in knockout mice. Together with the hints found during this thesis, chromatin binding of SMUDO seems to be very likely.

Since no indications were given for an involvement of SMUDO in the DNA damage response, a role in epigenetic regulation similar to that of SmcHD1, and a possible involvement of HIPK2 in these processes might be promising to explore. SMC proteins are known to participate in dosage compensation in *C.elegans* XX hermaphrodites, mammalian condensin interacts with Dnmt3b and mammalian cohesin associates with Snf2h, a chromatin remodeling enzyme (Geiman et al, 2004; Hakimi et al, 2002; Lieb et al, 1996). Thus, examples for a function of mammalian SMC complexes in epigenetic regulation exist in the literature, although the number of studies in this context is small compared to studies about SMC protein involvement in the DDR and chromatin remodeling during regular meiosis and

mitosis. The same is true for HIPK2, since some studies suggest a role of the kinase in epigenetic processes, for instance by modulating and regulating the methylation-dependent transcriptional repressors ZBTB4 or MeCP2 (Bracaglia et al, 2009; Yamada et al, 2009). Therefore, the chance is given that the function of SMUDO and its connection to HIPK2 is to be found within the field of epigenetic rather than in DNA damage response. However, a function restricted to X dosage compensation is unlikely since SMUDO has been found to be expressed in several male cell lines (e.g. HCT116, HepG2).

Gel mobility shift experiments should be performed for first general analysis of a potential SMUDO-DNA interaction. In case of confirmed binding ChIP-on-chip assays or ChIP-sequencing could be used to map the binding sites of the protein and to obtain indications for the functional relevance of the protein-DNA interaction.

In the course of this work, it could be shown that SMUDO is a primarily nuclear localized protein which likely forms homodimers via its SMC-hinge domain and binds to chromatin through its MutL domain. Although hints were given, an involvement of SMUDO in the DNA damage response, its interaction with TDG or HIPK2 in living cells and a possible impact of SMUDO on cell survival could not be demonstrated. Hence, alternative pathways of the DNA damage response should be investigated. Additionally, a putative connection of SMUDO and HIPK2 in epigenetic silencing presents another interesting direction of research that should be followed.

7 List of Abbreviations

293T	human embryonic kidney 293T cells (HEK293T)
5-FU	5-fluorouracil
53BP1	p53-binding protein 1
γ-H2AX	histone H2AX phosphorylated at Ser139
µg	microgram
AB	antibody
AID	auto inhibitory domain
AML1	acute myeloid leukemia 1
Amp	ampicillin
Asp	aspartic acid
ATM	ataxia-telangiectasia mutated
ATP	adenosine triphosphate
ATR	ataxia-telangiectasia and Rad3 related
ATRIP	ATR interacting protein
BER	base excision repair
BsSMC	Bacillus subtilis SMC
bp	base pair
BP	basic patch
BSA	bovine serum albumin
C/T	cytosine/thymine mismatch
CBP	CREB Binding Protein
CDC25	cell division cycle 25
cDNA	complementary DNA
CDS	coding sequence
ChIP	chromatin immunoprecipitation
CHK1	checkpoint kinase 1
CHK2	checkpoint kinase 2
CIP	calf intestine phosphatase
CtBP	C-terminal binding protein
CTD	C-terminal domain
DAZAP	deleted in azoospermia associated protein

DDR	DNA damage response
DMEM	Dulbecco`s modified Eagle`s medium
DMS3	defective in meristem silencing 3
DMSO	dimethylsulfoxid
DNA	desoxyribonucleic acid
DNA-PK	DNA proteinkinase
dNTP	deoxyribonucleotide phosphate
DSB	DNA-double strand break
dsDNA	double stranded DNA
DTT	dithiotreitol
E. coli	*Escherichia coli*
EDTA	ethylendiamintetraacetic acid
EGFP	enhanced green fluorescent protein
EGTA	ethylene glycol tetraacetic acid
et al.	und andere (et alii)
FCS	fetal calf serum
Fig.	figure
FISH	fluorescence in situ hybridization
For	forward
FRAP	fluorescence recovery after photo bleaching
G/T	guanine/thymine mismatch
Gadd45	frowth arrest and DNA damage inducible protein 45
Gal3	galectin 3
GAPDH	glyceraldehyde 3-phosphate dehydrogenase
GFP	green fluorescent protein
GST	glutathion-S-transferase
h	hour(s)
H2AX	histone H2AX
H3K27me3	histone H3 trimethylated at Lysine 27
HA	hemagglutinin
HCl	hydrogen chloride
HBS	HEPES buffered saline
HDM2	Human Homolog of MDM2
HEK293T	human embryonic kidney 293T cells

HEPES	4-(2-hydroxyethyl)-1-piperazineethanesulfoni acid
HID	homeoprotein interaction domain
HIPK2	homeodomain interacting protein kinase 2
HMGA1	high mobility group AT-hook 1
HNPCC	hereditary nonpolyposis colorectal cancer
HR	homologous recombination
HRP	horseradish peroxidase
IF	immunofluorescence
IgG	immunoglobulin G
IP	immunoprecipitation
IPTG	isopropyl β-D-1-thiogalactopyranoside
IR	ionizing radiation
JNK	Jun N-terminal kinase
Kan	kanamycin
kb	kilo-base pair
KD	kinase domain
kDa	kilo Dalton
LB-medium	Lysogeny broth medium
LTR	long terminal repeats
MBP	myelin basic protein
Mec1	meiosis entry checkpoint 1
MCF7	human mammary adenocarcinoma cells
MDC1	Mediator of DNA-damage Checkpoint 1
MECP2	methyl CpG binding protein 2
MEF	mouse embryonicf
mg	milligramm
min	minute(s)
MMR	mismatch repair
Mre11	meiotic recombination 11 homolog
MRN	Mre11-Rad50-Nbs1 complex
mRNA	messenger RNA
MutH	mutator H
MutL	mutator L
MutS	mutator S

NBS1	Nijmegen breakage syndrome 1
NCBI	center for biotechnology information
ng	nanogramm
NHEJ	non-homologous end joining
NER	nucleotide excision repair
NES	nuclear export signal
NLS	nuclear localization signal
N-terminus	amino-terminus
o/n	over night
p53	protein 53
p53Ser15	p53 phosphorylated at serine 15
p53Ser46	p53 phosphorylated at serine 46
p21	protein 21 or cyclin-dependent kinase inhibitor 1
PAGE	polyacrylamide gel electrophoresis
PARP1	poly ADP ribose polymerase 1
Pax6	paired box 6
PBS	phosphate buffered saline
PcG	polycomb group
PCNA	proliferating cell nuclear antigen
PCR	polymerase chain reaction
PFA	paraformaldehyde
pM	picomolar
PML	promyelocytic leukemia
PMSF	phenylmethylsulfonylfluorid
pol	polymerase
PRC2	polycomb repressor complex 2
PVDF	polyvenylidene difluoride
RdDM	RNA-directed DNA methylation
Rev	reverse
RNA	ribonucleic acid
RNAi	RNA interference
ROS	reactive oxygen species
RPA	replication protein A
rpm	rounds per minute

RT	Reverse Transkription
s	second(s)
Scc	sister chromatid cohesion
SDS	sodium dodecylsulfate
shRNA	small hairpin RNA
Siah	Seven in absentia homolog
SIP	Siah Interacting Protein
siRNS	small interfering RNS
SMC	structural maintenance of chromosomes
SMUDO	SMC-hinge and MutL-homology domain
SmcHD1	structural maintenance of chromosomes hinge domain containing 1
SP/TP	serine-prolien/threonine-proline motif
SQ/TQ	serine-glutamine/threonine-glutamine motif
SRS	Speckle Retention Signal
SSB	single-strand break
SUMO	small ubiquitin-related modifier
SUMOylation	modification by covalent SUMO binding
T/T	thymine/thymine mismatch
Tab.	Table
TAE	tris/acetate/EDTA
TBS	tris-buffered saline
TCL	total cell lysate
TDG	thymine DNA glycosylase
TEMED	tetramethylethylendiamine
TGFβ	transforming growth factor ß
Tris	tri(hydroxymethyl)aminomethane
U	unit
U2OS	human osteosarcoma cells
UDG	uracil DNA glycosylase
UV	ultraviolet
V	Volt
vol/vol	volume/volume
vol/wt	volume/weight
VSV-g	vesicular stomatitis virus glycoprotein G

WB	Western blot
WDTC	well-differentiated thyroid carcinoma
WSB1	WD40 repeat/SOCS box protein 1
WT	wild type
ZBTB4	zinc finger and BTB domain containing 4

8 References

Aikawa Y, Nguyen LA, Isono K, Takakura N, Tagata Y, Schmitz ML, Koseki H, Kitabayashi I (2006) Roles of HIPK1 and HIPK2 in AML1- and p300-dependent transcription, hematopoiesis and blood vessel formation. *The EMBO journal* **25:** 3955-3965

Al-Beiti MA, Lu X (2008) Expression of HIPK2 in cervical cancer: correlation with clinicopathology and prognosis. *Aust N Z J Obstet Gynaecol* **48:** 329-336

Arai S, Matsushita A, Du K, Yagi K, Okazaki Y, Kurokawa R (2007) Novel homeodomain-interacting protein kinase family member, HIPK4, phosphorylates human p53 at serine 9. *FEBS letters* **581:** 5649-5657

Ban C, Yang W (1998) Crystal structure and ATPase activity of MutL: implications for DNA repair and mutagenesis. *Cell* **95:** 541-552

Bar EE, Lin A, Tihan T, Burger PC, Eberhart CG (2008) Frequent gains at chromosome 7q34 involving BRAF in pilocytic astrocytoma. *J Neuropathol Exp Neurol* **67:** 878-887

Bartek J, Bartkova J, Lukas J (2007) DNA damage signalling guards against activated oncogenes and tumour progression. *Oncogene* **26:** 7773-7779

Bartkova J, Horejsi Z, Koed K, Kramer A, Tort F, Zieger K, Guldberg P, Sehested M, Nesland JM, Lukas C, Orntoft T, Lukas J, Bartek J (2005) DNA damage response as a candidate anti-cancer barrier in early human tumorigenesis. *Nature* **434:** 864-870

Bitomsky N, Hofmann TG (2009) Apoptosis and autophagy: Regulation of apoptosis by DNA damage signalling - roles of p53, p73 and HIPK2. *FEBS J* **276:** 6074-6083

Blewitt ME, Gendrel AV, Pang Z, Sparrow DB, Whitelaw N, Craig JM, Apedaile A, Hilton DJ, Dunwoodie SL, Brockdorff N, Kay GF, Whitelaw E (2008) SmcHD1, containing a structural-maintenance-of-chromosomes hinge domain, has a critical role in X inactivation. *Nat Genet* **40:** 663-669

Blewitt ME, Vickaryous NK, Hemley SJ, Ashe A, Bruxner TJ, Preis JI, Arkell R, Whitelaw E (2005) An N-ethyl-N-nitrosourea screen for genes involved in variegation in the mouse. *Proceedings of the National Academy of Sciences of the United States of America* **102:** 7629-7634

Bracaglia G, Conca B, Bergo A, Rusconi L, Zhou Z, Greenberg ME, Landsberger N, Soddu S, Kilstrup-Nielsen C (2009) Methyl-CpG-binding protein 2 is phosphorylated by homeodomain-interacting protein kinase 2 and contributes to apoptosis. *EMBO Rep* **10:** 1327-1333

Buscemi G, Perego P, Carenini N, Nakanishi M, Chessa L, Chen J, Khanna K, Delia D (2004) Activation of ATM and Chk2 kinases in relation to the amount of DNA strand breaks. *Oncogene* **23:** 7691-7700

Calzado MA, de la Vega L, Munoz E, Schmitz ML (2009) Autoregulatory control of the p53 response by Siah-1L-mediated HIPK2 degradation. *Biol Chem* **390:** 1079-1083

Calzado MA, Renner F, Roscic A, Schmitz ML (2007) HIPK2: a versatile switchboard regulating the transcription machinery and cell death. *Cell Cycle* **6:** 139-143

Campisi J, d'Adda di Fagagna F (2007) Cellular senescence: when bad things happen to good cells. *Nat Rev Mol Cell Biol* **8:** 729-740

Cannavo E, Gerrits B, Marra G, Schlapbach R, Jiricny J (2007) Characterization of the interactome of the human MutL homologues MLH1, PMS1, and PMS2. *The Journal of biological chemistry* **282:** 2976-2986

Carrier F, Smith ML, Bae I, Kilpatrick KE, Lansing TJ, Chen CY, Engelstein M, Friend SH, Henner WD, Gilmer TM, et al. (1994) Characterization of human Gadd45, a p53-regulated protein. *The Journal of biological chemistry* **269:** 32672-32677

Cejka P, Stojic L, Mojas N, Russell AM, Heinimann K, Cannavo E, di Pietro M, Marra G, Jiricny J (2003) Methylation-induced G(2)/M arrest requires a full complement of the mismatch repair protein hMLH1. *The EMBO journal* **22:** 2245-2254

Chahrour M, Zoghbi HY (2007) The story of Rett syndrome: from clinic to neurobiology. *Neuron* **56:** 422-437

Chiu A, Revenkova E, Jessberger R (2004) DNA interaction and dimerization of eukaryotic SMC hinge domains. *J Biol Chem* **279:** 26233-26242

Choi DW, Seo YM, Kim EA, Sung KS, Ahn JW, Park SJ, Lee SR, Choi CY (2008) Ubiquitination and degradation of homeodomain-interacting protein kinase 2 by WD40 repeat/SOCS box protein WSB-1. *The Journal of biological chemistry* **283:** 4682-4689

Chuang PT, Albertson DG, Meyer BJ (1994) DPY-27:a chromosome condensation protein homolog that regulates C. elegans dosage compensation through association with the X chromosome. *Cell* **79:** 459-474

Ciccia A, Elledge SJ (2010) The DNA damage response: making it safe to play with knives. *Mol Cell* **40:** 179-204

Cortazar D, Kunz C, Saito Y, Steinacher R, Schar P (2007) The enigmatic thymine DNA glycosylase. *DNA Repair (Amst)* **6:** 489-504

Cortes-Ledesma F, de Piccoli G, Haber JE, Aragon L, Aguilera A (2007) SMC proteins, new players in the maintenance of genomic stability. *Cell Cycle* **6:** 914-918

Cortez D, Guntuku S, Qin J, Elledge SJ (2001) ATR and ATRIP: partners in checkpoint signaling. *Science* **294:** 1713-1716

D'Orazi G, Cecchinelli B, Bruno T, Manni I, Higashimoto Y, Saito S, Gostissa M, Coen S, Marchetti A, Del Sal G, Piaggio G, Fanciulli M, Appella E, Soddu S (2002) Homeodomain-interacting protein kinase-2 phosphorylates p53 at Ser 46 and mediates apoptosis. *Nature cell biology* **4:** 11-19

Dauth I, Kruger J, Hofmann TG (2007) Homeodomain-interacting protein kinase 2 is the ionizing radiation-activated p53 serine 46 kinase and is regulated by ATM. *Cancer Res* **67:** 2274-2279

David SS, O'Shea VL, Kundu S (2007) Base-excision repair of oxidative DNA damage. *Nature* **447:** 941-950

De Piccoli G, Cortes-Ledesma F, Ira G, Torres-Rosell J, Uhle S, Farmer S, Hwang JY, Machin F, Ceschia A, McAleenan A, Cordon-Preciado V, Clemente-Blanco A, Vilella-Mitjana F, Ullal P, Jarmuz A, Leitao B, Bressan D, Dotiwala F, Papusha A, Zhao X, Myung K, Haber JE, Aguilera A, Aragon L (2006) Smc5-Smc6 mediate DNA double-strand-break repair by promoting sister-chromatid recombination. *Nat Cell Biol* **8:** 1032-1034

Deshmukh H, Yeh TH, Yu J, Sharma MK, Perry A, Leonard JR, Watson MA, Gutmann DH, Nagarajan R (2008) High-resolution, dual-platform aCGH analysis reveals frequent HIPK2 amplification and increased expression in pilocytic astrocytomas. *Oncogene* **27:** 4745-4751

Di Stefano V, Soddu S, Sacchi A, D'Orazi G (2005) HIPK2 contributes to PCAF-mediated p53 acetylation and selective transactivation of p21Waf1 after nonapoptotic DNA damage. *Oncogene* **24:** 5431-5442

Friedberg EC (2001) How nucleotide excision repair protects against cancer. *Nat Rev Cancer* **1:** 22-33

Geiman TM, Sankpal UT, Robertson AK, Chen Y, Mazumdar M, Heale JT, Schmiesing JA, Kim W, Yokomori K, Zhao Y, Robertson KD (2004) Isolation and characterization of a novel DNA methyltransferase complex linking DNMT3B with components of the mitotic chromosome condensation machinery. *Nucleic acids research* **32:** 2716-2729

Gorgoulis VG, Vassiliou LV, Karakaidos P, Zacharatos P, Kotsinas A, Liloglou T, Venere M, Ditullio RA, Jr., Kastrinakis NG, Levy B, Kletsas D, Yoneta A, Herlyn M, Kittas C, Halazonetis TD (2005) Activation of the DNA damage checkpoint and genomic instability in human precancerous lesions. *Nature* **434:** 907-913

Gresko E, Moller A, Roscic A, Schmitz ML (2005) Covalent modification of human homeodomain interacting protein kinase 2 by SUMO-1 at lysine 25 affects its stability. *Biochem Biophys Res Commun* **329:** 1293-1299

Gresko E, Roscic A, Ritterhoff S, Vichalkovski A, del Sal G, Schmitz ML (2006) Autoregulatory control of the p53 response by caspase-mediated processing of HIPK2. *The EMBO journal* **25:** 1883-1894

Grilley M, Welsh KM, Su SS, Modrich P (1989) Isolation and characterization of the Escherichia coli mutL gene product. *The Journal of biological chemistry* **264:** 1000-1004

Guarne A, Junop MS, Yang W (2001) Structure and function of the N-terminal 40 kDa fragment of human PMS2: a monomeric GHL ATPase. *The EMBO journal* **20:** 5521-5531

Haering CH, Lowe J, Hochwagen A, Nasmyth K (2002) Molecular architecture of SMC proteins and the yeast cohesin complex. *Molecular cell* **9:** 773-788

Haering CH, Nasmyth K (2003) Building and breaking bridges between sister chromatids. *BioEssays : news and reviews in molecular, cellular and developmental biology* **25:** 1178-1191

Hakimi MA, Speicher DW, Shiekhattar R (2002) The motor protein kinesin-1 links neurofibromin and merlin in a common cellular pathway of neurofibromatosis. *The Journal of biological chemistry* **277:** 36909-36912

Hanahan D, Weinberg RA (2000) The hallmarks of cancer. *Cell* **100:** 57-70

Harper JW, Elledge SJ (2007) The DNA damage response: ten years after. *Mol Cell* **28:** 739-745

Harvey SH, Sheedy DM, Cuddihy AR, O'Connell MJ (2004) Coordination of DNA damage responses via the Smc5/Smc6 complex. *Molecular and cellular biology* **24:** 662-674

Heard E, Colot V (2008) Chromosome structural proteins and RNA-mediated epigenetic silencing. *Dev Cell* **14:** 813-814

Hirano M, Anderson DE, Erickson HP, Hirano T (2001) Bimodal activation of SMC ATPase by intra- and inter-molecular interactions. *EMBO J* **20:** 3238-3250

Hirano M, Hirano T (2002) Hinge-mediated dimerization of SMC protein is essential for its dynamic interaction with DNA. *EMBO J* **21:** 5733-5744

Hirano M, Hirano T (2006) Opening closed arms: long-distance activation of SMC ATPase by hinge-DNA interactions. *Mol Cell* **21:** 175-186

Hirano T (2005) Condensins: organizing and segregating the genome. *Current biology : CB* **15:** R265-275

Hirano T (2006) At the heart of the chromosome: SMC proteins in action. *Nature reviews Molecular cell biology* **7:** 311-322

Hoeijmakers JH (2001) Genome maintenance mechanisms for preventing cancer. *Nature* **411:** 366-374

Hoeijmakers JH (2009) DNA damage, aging, and cancer. *N Engl J Med* **361:** 1475-1485

Hofmann TG, Jaffray E, Stollberg N, Hay RT, Will H (2005) Regulation of homeodomain-interacting protein kinase 2 (HIPK2) effector function through dynamic small ubiquitin-related modifier-1 (SUMO-1) modification. *J Biol Chem* **280:** 29224-29232

Hofmann TG, Moller A, Sirma H, Zentgraf H, Taya Y, Droge W, Will H, Schmitz ML (2002) Regulation of p53 activity by its interaction with homeodomain-interacting protein kinase-2. *Nat Cell Biol* **4:** 1-10

Hofmann TG, Stollberg N, Schmitz ML, Will H (2003) HIPK2 regulates transforming growth factor-beta-induced c-Jun NH(2)-terminal kinase activation and apoptosis in human hepatoma cells. *Cancer Res* **63:** 8271-8277

Hopfner KP, Craig L, Moncalian G, Zinkel RA, Usui T, Owen BA, Karcher A, Henderson B, Bodmer JL, McMurray CT, Carney JP, Petrini JH, Tainer JA (2002) The Rad50 zinc-hook is a structure joining Mre11 complexes in DNA recombination and repair. *Nature* **418:** 562-566

Huettel B, Kanno T, Daxinger L, Bucher E, van der Winden J, Matzke AJ, Matzke M (2007) RNA-directed DNA methylation mediated by DRD1 and Pol IVb: a versatile pathway for transcriptional gene silencing in plants. *Biochimica et biophysica acta* **1769:** 358-374

Isono K, Nemoto K, Li Y, Takada Y, Suzuki R, Katsuki M, Nakagawara A, Koseki H (2006) Overlapping roles for homeodomain-interacting protein kinases hipk1 and hipk2 in the mediation of cell growth in response to morphogenetic and genotoxic signals. *Molecular and cellular biology* **26:** 2758-2771

Iyer RR, Pluciennik A, Burdett V, Modrich PL (2006) DNA mismatch repair: functions and mechanisms. *Chem Rev* **106:** 302-323

Jackson SP, Bartek J (2009) The DNA-damage response in human biology and disease. *Nature* **461:** 1071-1078

Jans J, Gladden JM, Ralston EJ, Pickle CS, Michel AH, Pferdehirt RR, Eisen MB, Meyer BJ (2009) A condensin-like dosage compensation complex acts at a distance to control expression throughout the genome. *Genes & development* **23:** 602-618

Kanei-Ishii C, Ninomiya-Tsuji J, Tanikawa J, Nomura T, Ishitani T, Kishida S, Kokura K, Kurahashi T, Ichikawa-Iwata E, Kim Y, Matsumoto K, Ishii S (2004) Wnt-1 signal induces phosphorylation and degradation of c-Myb protein via TAK1, HIPK2, and NLK. *Genes & development* **18:** 816-829

Kanno T, Bucher E, Daxinger L, Huettel B, Bohmdorfer G, Gregor W, Kreil DP, Matzke M, Matzke AJ (2008) A structural-maintenance-of-chromosomes hinge domain-containing protein is required for RNA-directed DNA methylation. *Nat Genet* **40:** 670-675

Kastan MB, Bartek J (2004) Cell-cycle checkpoints and cancer. *Nature* **432:** 316-323

Kearsey JM, Coates PJ, Prescott AR, Warbrick E, Hall PA (1995) Gadd45 is a nuclear cell cycle regulated protein which interacts with p21Cip1. *Oncogene* **11:** 1675-1683

Kim EA, Noh YT, Ryu MJ, Kim HT, Lee SE, Kim CH, Lee C, Kim YH, Choi CY (2006) Phosphorylation and transactivation of Pax6 by homeodomain-interacting protein kinase 2. *The Journal of biological chemistry* **281:** 7489-7497

Kim ST, Xu B, Kastan MB (2002) Involvement of the cohesin protein, Smc1, in Atm-dependent and independent responses to DNA damage. *Genes & development* **16:** 560-570

Kim YH, Choi CY, Lee SJ, Conti MA, Kim Y (1998) Homeodomain-interacting protein kinases, a novel family of co-repressors for homeodomain transcription factors. *The Journal of biological chemistry* **273:** 25875-25879

Kitagawa R, Bakkenist CJ, McKinnon PJ, Kastan MB (2004) Phosphorylation of SMC1 is a critical downstream event in the ATM-NBS1-BRCA1 pathway. *Genes & development* **18:** 1423-1438

Kumagai A, Lee J, Yoo HY, Dunphy WG (2006) TopBP1 activates the ATR-ATRIP complex. *Cell* **124:** 943-955

Kunz C, Focke F, Saito Y, Schuermann D, Lettieri T, Selfridge J, Schar P (2009) Base excision by thymine DNA glycosylase mediates DNA-directed cytotoxicity of 5-fluorouracil. *PLoS Biol* **7:** e91

Lacks SA, Dunn JJ, Greenberg B (1982) Identification of base mismatches recognized by the heteroduplex-DNA-repair system of Streptococcus pneumoniae. *Cell* **31:** 327-336

Lammens A, Schele A, Hopfner KP (2004) Structural biochemistry of ATP-driven dimerization and DNA-stimulated activation of SMC ATPases. *Current biology : CB* **14:** 1778-1782

Lavra L, Rinaldo C, Ulivieri A, Luciani E, Fidanza P, Giacomelli L, Bellotti C, Ricci A, Trovato M, Soddu S, Bartolazzi A, Sciacchitano S (2011) The Loss of the p53 Activator HIPK2 Is Responsible for Galectin-3 Overexpression in Well Differentiated Thyroid Carcinomas. *PLoS One* **6:** e20665

Lee KM, O'Connell MJ (2006) A new SUMO ligase in the DNA damage response. *DNA Repair* **5:** 138-141

Lehmann AR (2005) The role of SMC proteins in the responses to DNA damage. *DNA Repair (Amst)* **4:** 309-314

Lehmann AR, Walicka M, Griffiths DJ, Murray JM, Watts FZ, McCready S, Carr AM (1995) The rad18 gene of Schizosaccharomyces pombe defines a new subgroup of the SMC superfamily involved in DNA repair. *Mol Cell Biol* **15:** 7067-7080

Li GM (2008) Mechanisms and functions of DNA mismatch repair. *Cell Res* **18:** 85-98

Lieb JD, Capowski EE, Meneely P, Meyer BJ (1996) DPY-26, a link between dosage compensation and meiotic chromosome segregation in the nematode. *Science* **274:** 1732-1736

Losada A, Hirano T (2005) Dynamic molecular linkers of the genome: the first decade of SMC proteins. *Genes Dev* **19:** 1269-1287

Mailand N, Falck J, Lukas C, Syljuasen RG, Welcker M, Bartek J, Lukas J (2000) Rapid destruction of human Cdc25A in response to DNA damage. *Science* **288:** 1425-1429

Mao JH, Wu D, Kim IJ, Kang HC, Wei G, Climent J, Kumar A, Pelorosso FG, Delrosario R, Huang EJ, Balmain A (2011) Hipk2 cooperates with p53 to suppress gamma-ray radiation-induced mouse thymic lymphoma. *Oncogene*

Matoba K, Yamazoe M, Mayanagi K, Morikawa K, Hiraga S (2005) Comparison of MukB homodimer versus MukBEF complex molecular architectures by electron microscopy reveals a higher-order multimerization. *Biochem Biophys Res Commun* **333:** 694-702

Matsuoka S, Ballif BA, Smogorzewska A, McDonald ER, 3rd, Hurov KE, Luo J, Bakalarski CE, Zhao Z, Solimini N, Lerenthal Y, Shiloh Y, Gygi SP, Elledge SJ (2007) ATM and ATR substrate analysis reveals extensive protein networks responsive to DNA damage. *Science* **316:** 1160-1166

Melby TE, Ciampaglio CN, Briscoe G, Erickson HP (1998) The symmetrical structure of structural maintenance of chromosomes (SMC) and MukB proteins: long, antiparallel coiled coils, folded at a flexible hinge. *The Journal of cell biology* **142:** 1595-1604

Negrini S, Gorgoulis VG, Halazonetis TD (2010) Genomic instability--an evolving hallmark of cancer. *Nat Rev Mol Cell Biol* **11:** 220-228

Ng K, Pullirsch D, Leeb M, Wutz A (2007) Xist and the order of silencing. *EMBO Rep* **8:** 34-39

Peltomaki P (2005) Lynch syndrome genes. *Fam Cancer* **4:** 227-232

Pierantoni GM, Bulfone A, Pentimalli F, Fedele M, Iuliano R, Santoro M, Chiariotti L, Ballabio A, Fusco A (2002) The homeodomain-interacting protein kinase 2 gene is expressed late in embryogenesis and preferentially in retina, muscle, and neural tissues. *Biochem Biophys Res Commun* **290:** 942-947

Pierantoni GM, Rinaldo C, Mottolese M, Di Benedetto A, Esposito F, Soddu S, Fusco A (2007) High-mobility group A1 inhibits p53 by cytoplasmic relocalization of its proapoptotic activator HIPK2. *J Clin Invest* **117:** 693-702

Polosina YY, Cupples CG (2010a) MutL: conducting the cell's response to mismatched and misaligned DNA. *Bioessays* **32:** 51-59

Polosina YY, Cupples CG (2010b) Wot the 'L-Does MutL do? *Mutation research* **705:** 228-238

Potts PR, Porteus MH, Yu H (2006) Human SMC5/6 complex promotes sister chromatid homologous recombination by recruiting the SMC1/3 cohesin complex to double-strand breaks. *EMBO J* **25:** 3377-3388

Puca R, Nardinocchi L, Givol D, D'Orazi G (2010) Regulation of p53 activity by HIPK2: molecular mechanisms and therapeutical implications in human cancer cells. *Oncogene* **29:** 4378-4387

Rinaldo C, Prodosmo A, Mancini F, Iacovelli S, Sacchi A, Moretti F, Soddu S (2007a) MDM2-regulated degradation of HIPK2 prevents p53Ser46 phosphorylation and DNA damage-induced apoptosis. *Molecular cell* **25:** 739-750

Rinaldo C, Prodosmo A, Siepi F, Soddu S (2007b) HIPK2: a multitalented partner for transcription factors in DNA damage response and development. *Biochemistry and cell biology = Biochimie et biologie cellulaire* **85:** 411-418

Roscic A, Moller A, Calzado MA, Renner F, Wimmer VC, Gresko E, Ludi KS, Schmitz ML (2006) Phosphorylation-dependent control of Pc2 SUMO E3 ligase activity by its substrate protein HIPK2. *Molecular cell* **24:** 77-89

Rui Y, Xu Z, Lin S, Li Q, Rui H, Luo W, Zhou HM, Cheung PY, Wu Z, Ye Z, Li P, Han J, Lin SC (2004) Axin stimulates p53 functions by activation of HIPK2 kinase through multimeric complex formation. *The EMBO journal* **23:** 4583-4594

Sjogren C, Nasmyth K (2001) Sister chromatid cohesion is required for postreplicative double-strand break repair in Saccharomyces cerevisiae. *Current biology : CB* **11:** 991-995

Sombroek D, Hofmann TG (2009) How cells switch HIPK2 on and off. *Cell Death Differ* **16:** 187-194

Sonoda E, Matsusaka T, Morrison C, Vagnarelli P, Hoshi O, Ushiki T, Nojima K, Fukagawa T, Waizenegger IC, Peters JM, Earnshaw WC, Takeda S (2001) Scc1/Rad21/Mcd1 is required for sister chromatid cohesion and kinetochore function in vertebrate cells. *Developmental cell* **1:** 759-770

Spampinato C, Modrich P (2000) The MutL ATPase is required for mismatch repair. *The Journal of biological chemistry* **275:** 9863-9869

Strom L, Lindroos HB, Shirahige K, Sjogren C (2004) Postreplicative recruitment of cohesin to double-strand breaks is required for DNA repair. *Molecular cell* **16:** 1003-1015

Strunnikov AV, Hogan E, Koshland D (1995) SMC2, a Saccharomyces cerevisiae gene essential for chromosome segregation and condensation, defines a subgroup within the SMC family. *Genes Dev* **9:** 587-599

Taylor EM, Moghraby JS, Lees JH, Smit B, Moens PB, Lehmann AR (2001) Characterization of a novel human SMC heterodimer homologous to the Schizosaccharomyces pombe Rad18/Spr18 complex. *Mol Biol Cell* **12:** 1583-1594

Unal E, Arbel-Eden A, Sattler U, Shroff R, Lichten M, Haber JE, Koshland D (2004) DNA damage response pathway uses histone modification to assemble a double-strand break-specific cohesin domain. *Molecular cell* **16:** 991-1002

van Attikum H, Gasser SM (2009) Crosstalk between histone modifications during the DNA damage response. *Trends Cell Biol* **19:** 207-217

Weber A, Marquardt J, Elzi D, Forster N, Starke S, Glaum A, Yamada D, Defossez PA, Delrow J, Eisenman RN, Christiansen H, Eilers M (2008) Zbtb4 represses transcription of P21CIP1 and controls the cellular response to p53 activation. *The EMBO journal* **27:** 1563-1574

Wei G, Ku S, Ma GK, Saito S, Tang AA, Zhang J, Mao JH, Appella E, Balmain A, Huang EJ (2007) HIPK2 represses beta-catenin-mediated transcription, epidermal stem cell expansion, and skin tumorigenesis. *Proceedings of the National Academy of Sciences of the United States of America* **104:** 13040-13045

Weiss RS, Matsuoka S, Elledge SJ, Leder P (2002) Hus1 acts upstream of chk1 in a mammalian DNA damage response pathway. *Current biology : CB* **12:** 73-77

Winter M, Sombroek D, Dauth I, Moehlenbrink J, Scheuermann K, Crone J, Hofmann TG (2008) Control of HIPK2 stability by ubiquitin ligase Siah-1 and checkpoint kinases ATM and ATR. *Nat Cell Biol* **10:** 812-824

Yamada D, Perez-Torrado R, Filion G, Caly M, Jammart B, Devignot V, Sasai N, Ravassard P, Mallet J, Sastre-Garau X, Schmitz ML, Defossez PA (2009) The human protein kinase HIPK2 phosphorylates and downregulates the methyl-binding transcription factor ZBTB4. *Oncogene* **28:** 2535-2544

Yang W (2000) Structure and function of mismatch repair proteins. *Mutation research* **460:** 245-256

Yang W (2007) Human MutL alpha: The jack of all trades in MMR is also an endonuclease. *DNA Repair* **6:** 135-139

Yoshida H, Kitabayashi I (2008) Chromatin regulation by AML1 complex. *Int J Hematol* **87:** 19-24

Zhang Q, Yoshimatsu Y, Hildebrand J, Frisch SM, Goodman RH (2003) Homeodomain interacting protein kinase 2 promotes apoptosis by downregulating the transcriptional corepressor CtBP. *Cell* **115:** 177-186

Zhou BB, Elledge SJ (2000) The DNA damage response: putting checkpoints in perspective. *Nature* **408:** 433-439

Die vorliegende Arbeit wurde am Deutschen Krebsforschungszentrum Heidelberg in der Zeit von Juli 2007 bis Februar 2011 unter Anleitung von Dr. Thomas G. Hofmann in der Arbeitsgruppe „Zelluläre Seneszenz“ angefertigt.

9 Danksagungen

Hier möchte ich mich bei den Menschen bedanken, die durch ihre fachliche und persönliche Unterstützung zum Gelingen dieser Arbeit beigetragen haben.

Herrn Dr. Thomas G. Hofmann möchte ich für die Möglichkeit danken, diese Arbeit in seiner Abteilung anfertigen zu können, sowie für die wissenschaftliche Betreuung.

Prof. Dr. Rainer Zawatzky danke ich für die freundliche Übernahme des Erstgutachtens und kritische Anmerkungen.

Den Mitarbeitern der Arbeitsgruppe „Zelluläre Seneszenz“ danke ich für ihre immerwährende Hilfsbereitschaft, die geleistete Unterstützung und eine angenehme Arbeitsatmosphäre.

Ganz besonders bedanke ich mich bei Eva Krieghoff-Henning für viel praktische Unterstützung, unzählige Ratschläge und geduldiges Korrekturlesen.

Ich danke Dorothea Muschik für moralischen Aufbau und notwendige Zerstreuung.

Meinen Eltern danke ich für die liebevolle Unterstützung und Hilfe auf meinem Weg.

Hiermit erkläre ich an Eides statt, dass ich die vorliegende Arbeit selbstständig und ohne unerlaubte Hilfsmittel durchgeführt habe.

Heidelberg, den 30.08.2011